

MICHe: CASE STUDY UNIBO-MODENA CATHEDRAL

INDICE

MICHE: CASE STUDY UNIBO-MODENA CATHEDRAL	1
Introduction	5
PART 1: GUIDELINES	7
1 Introduction	7
1 Guidelines for the integrated knowledge of cultural heritage assets	9
2 Guidelines for Multi- Analysis Integrated Assessment and weaknesses identification	10
3 Atlas of structural solutions for the conservation of cultural heritage buildings	11
PART 2: CASE STUDY- THE MODENA CATHEDRAL	12
CATHEDRAL OF MODENA: THE INTEGRATED KNOWLEDGE	12
1 THE CATHEDRAL OF MODENA	12
1.1 The actual state of the Cathedral	13
1.1.1 The construction phases and the main interventions	13
1.1.2 The reconstruction of the geometric configuration through laser scanner and the geotechnical investigations	16
1.1.3 Material properties	18
1.1.4 The actual state of degradation	19
1.2 Seismic Hazard analyses	22
1.2.1 Historical Deterministic Seismic Hazard Analysis (HDSHA)	23
1.2.2 Maximum Historical Earthquake Analysis (MHEA)	25
1.3 The 2012 Emilia's earthquake	26
1.4 Conclusions	28
MULTI-ANALYSES ASSESSMENT OF THE MODENA CATHEDRAL	29
2 GLOBAL STRUCTURAL BEHAVIOUR	29
2.1 Introduction	29
2.2 The models and the simulations	29
2.3 Static analyses	30
2.3.1 The applied loads/actions	30
2.3.2 Structural analysis with simple models	31

2.3.3	Structural analysis with 3D finite element models	36
2.4	Seismic Vulnerability analyses	41
2.4.1	Natural frequency analysis	41
2.4.2	Global seismic response	42
2.4.3	Time history analyses: input the main shock recorded by the station of Modena	47
2.5	The main vulnerabilities and conclusions	49
3	LOCAL STRUCTURAL ANALYSES	50
3.1	Introduction	50
3.2	The models and the simulation	50
3.3	Local collapse mechanisms	50
3.4	The vault	55
3.4.1	3D FE models of the vaults	55
3.5	Conclusions	59
4	STRUCTURAL ANALYSES VIA DISCRETE ELEMENT METHOD	61
4.1.1	The model and the analyses	61
4.1.2	The modelling parameters of the three numerical models	63
4.1.3	The results	67
4.2	Conclusion	69
5	RESULTS OBTAINED FROM THE STATIC STRUCTURAL HEALTH MONITORING OF THE CATHEDRAL OF MODENA	70
5.1	Introduction	70
5.2	Approach for a critical interpretation of the data acquired by a Static SHM system	70
5.2.1	Reference quantities	72
5.3	Types and location of instruments	76
5.4	Reference quantities	80
5.4.1	Invar deformeter	80
5.4.2	Joint meter	82
5.4.3	Inclinometer	90
5.4.4	Conclusions	92

STRENGTHENING INTERVENTIONS PERFORMED ON THE CATHEDRAL	93
6 THE MAIN VULNERABILITY	93
7 SOLUTION STRATEGIES TO REDUCE THE MAIN VULNERABILITIES	94
PART 3: PRELIMINARY FLOOD RISK ASSESSMENT	99
BIBLIOGRAPHY	107

Introduction

Cultural heritage buildings represent inestimable values and not removable resources of most of European countries, which have to be preserved for future generations in order to transmit their history, culture, art. The correct management of cultural heritage buildings is a crucial issue: on one side, the conservative restoration requires compatible and limited intervention techniques in order to preserve the integrity of the monuments, and on the other side, this implies a profound knowledge of the structural behaviour, often difficult to understand and to predict for these complex buildings.

The most widespread construction material used, especially in Italy, for the monumental buildings is the masonry that is characterized by a quite complex mechanical behaviour due to composite nature resulting from the interaction of bricks and mortar (both characterized by significantly different behaviour under tension and compression) thus leading to specific issues to be faced when analysing and modelling these constructions. Moreover, historical monuments are built and modified during the centuries by using various construction techniques, workmanships of different expertise, with the result of a complex fabric, characterized by a high degree of uncertainties, quite far from our modern buildings. In most cases, their actual configuration and the state of conservation are not only the result of the natural degradation due to aging effects, but also the consequence of the impact of past extreme natural events (such as earthquakes, floods, groundwater changes), which may sometime have caused partial or total collapses. The inherent complexity of historical buildings (due to the articulated geometrical configuration, the use of different construction techniques, different materials, the level of the connections between orthogonal walls), together with the natural material decay and the effects of natural hazards, makes the assessment the "structural health" extremely challenging. Furthermore, all the uncertainties due to this complexity render each monument a "unique". This means that there is no baseline directly applicable in order to obtain useful information concerning the "health" of the structure and the approach commonly used for the assessment of modern steel and concrete building (largely based on the use of computer software and well-established guidelines or codes) cannot be simply adopted for historical buildings. On the other hand such effects tend to inevitably reduce the level of safety and therefore increases the risks to future extreme events, but the monuments have also to meet the practical test of utility. Therefore, it clearly appears the need of a reliable estimation of the actual level of safety in order to plan effective interventions. In this respect, while for the case of conventional structures, a common strategy to reduce the uncertainties and therefore provide a reliable assessment of the "structural health" is based on the use of extended in situ experimental tests (destructive tests). For the case of cultural heritage sites, the authorities responsible of monuments conservations in the spite of preserving the original integrity often prohibit this strategy.

An alternative approach to reduce the uncertainties in the knowledge of historical sites should be based on the development of a multidisciplinary approach aimed at providing an “integrated knowledge” through the mutual exchanging of expertise and capabilities offered by different fields. In this interdisciplinary knowledge process a fundamental contribution is played by the Structural Health Monitoring (SHM) whose aim is to evaluate the evolution of the structural health through a continuous real-time monitoring.

Hence, the main feature of Structural Health Monitoring strategy for monuments is to be geared towards a long-term evaluation of what is ‘normal’ structural performance or ‘health’. In this regard several studies available in the scientific literature, in fact, reported the main information obtained through structural health monitoring. However, such information are not so easy to compare given that a no unique approach is used for data analysis and interpretation.

Similarly, the assessment methods commonly used for the analyses of the “structural health” and for the evaluations of the effects of extreme events, consisting in the developments of single computer-based model and numerical simulations, do not always appear as appropriate for the case of historical monuments. Generally, only one model of the whole building is not able to capture all the structural peculiarities.

The research work developed by the UNIBO Unit focus on:

- the development of guideline to obtain a reliable integrated knowledge of the cultural heritage buildings;
- the development of a multi analyses method for the assessment of the structural behaviour of the monuments;
- the identification of an atlas of structural solutions for the conservation of cultural heritage buildings
- the application of the knowledge process and the multi analyses methods to the case study (Cathedral of Modena)
- preliminary flood hazard estimation.

.

PART 1: GUIDELINES

1 Introduction

Historical masonry monuments are not only works of art, but also have to meet the practical test of utility and a suitable safety level. The efficient preservation of the structural health of these unique buildings presents several challenges. From a structural point of view, historical monuments are characterized by much larger uncertainties than ordinary buildings and conventional analysis tools may fail in providing a reliable characterization of their structural behaviour. According to the principles of restoration, only with a thorough knowledge it is possible to develop a consistent structural analyses (able to represent the real structural behaviour) and conceive, thus, intervention solutions targeted at preserving the integrity of the historical monuments. The concept of integrity, often, is only interpreted as the requirement of preserving the shape and the appearance of the monument. Instead, with reference to historical monuments, the requirement of integrity is not so simple because it also implies historic integrity, by considering the changes of the monument with time, as well as material integrity that means construction techniques, materials and structural scheme. Therefore, preserving integrity requires, beside an interdisciplinary approach, the development of a holistic approach in the monuments conservation. A possible approach to reduce the uncertainties in the knowledge of historical buildings and obtain the necessary information to evaluate its structural health should be based on the development of a multi-disciplinary research aimed at providing an "integrated knowledge" through the mutual exchange of expertise and capabilities of different disciplines and a real-time monitoring of the state of the buildings [1]. Moreover, as already briefly mentioned, approaches and tools commonly used in structural analysis of ordinary buildings, extensively based on numerical models, do not always seem to be appropriate for historical masonry monuments of unique features and are generally not able to provide convenient material models to describe highly nonlinear behaviour and masonry orthotropic. To conceive a unique tool valid to describe all possible structural responses of the historical masonry monuments is therefore complex, and most likely impossible. Quite often, more reliable results can be obtained by employing a multi-analysis method that integrates different approaches (from simple but more reliable limit schematizations, to more complex but, usually more sensible, finite element models, [2]. Figure 1 display an overview of the presented Multi-Disciplinary Multi Analyses approach for a proper assessment of the structural health of historical monuments.

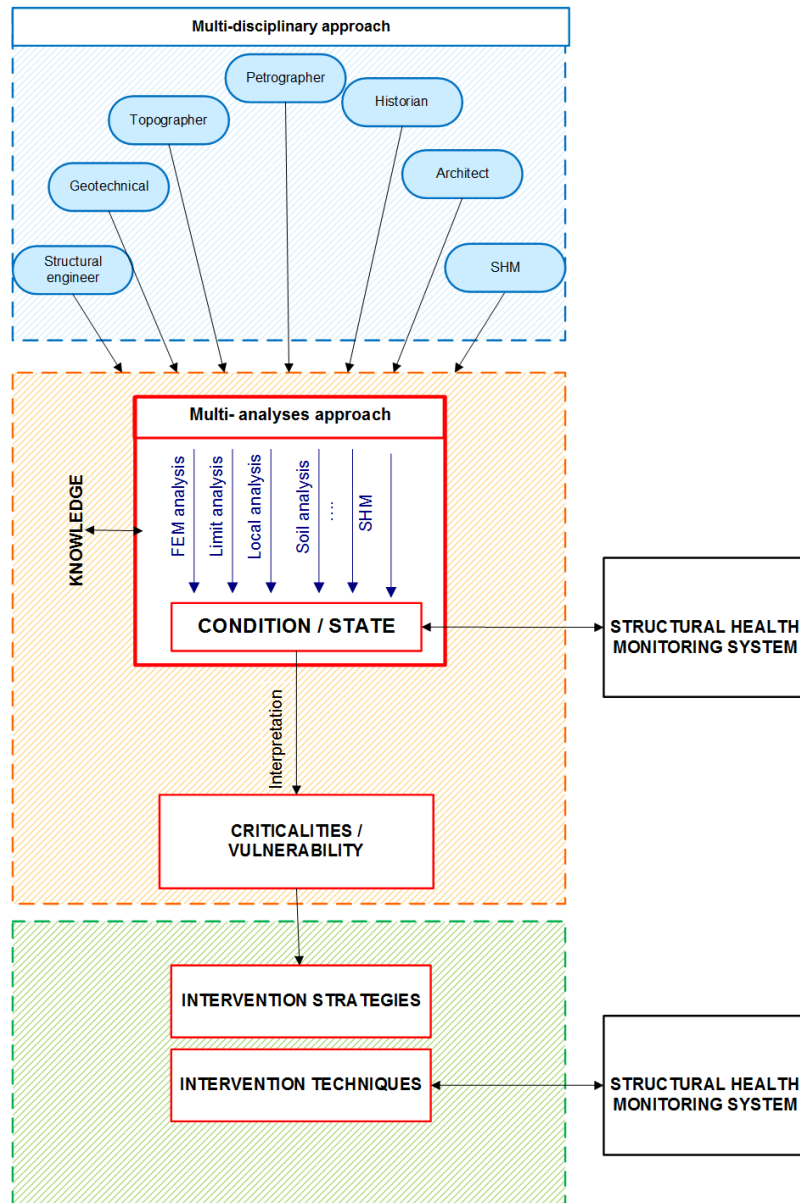


Figure 1-Overview of the MDMA approach

1 Guidelines for the integrated knowledge of cultural heritage assets

The current standard requirements recommend an interdisciplinary approach that thanks to an investigating team that incorporates a range of skills appropriate allows discovering phenomena involving structural behaviour of the monuments. [1], [3]. A correct and complete analysis of an historical building have to be based on the historical, geometrical, material and structural knowledge of the structure in order to design structural interventions not only to guarantee safety, but also to respect the context, which surrounds them. Knowledge of the structure requires information on its conception, on its constructional techniques, on the processes of decay and damage, on changes that have been made and finally on its present state. The following steps can usually reach this knowledge [4]:

- definition, description and understanding of the historic and cultural significance of the buildings;
- a description of the original building materials and construction techniques;
- historical research covering the entire life of the structure including both changes to its form and any previous structural interventions;
- description of the structure in its present state including identification of damage, decay and possible progressive phenomena, using appropriate types of test;
- description of the actions involved, structural behaviour and types of materials;
- implementation of a SHM system.

The purpose of the historical investigation is to understand the conception and the significance of the building, the techniques and the skills used in its construction, the subsequent changes in both the structure and its environment and any events that may have caused damage (such as past earthquakes..). Knowledge of what has occurred in the past can help to forecast future behaviour and can be a useful indication of the level of safety provided by the current state of the structure. The direct observation and the survey of the structure is essential phase in order to identify decay and damage, geometric irregularities which can be the result of previous deformations (it can indicate the junction between different building phases or alterations to the fabric) and to determining whether or not the phenomena have stabilised. The identification of the mechanical characteristics of the materials should be investigated through non-destructive tests to avoid any alterations to a structure [4]. In addition to these remarks, it must be outlined the role of the monitoring, as an essential component of the integrated studies when exploring the long-term performances. SHM system can be very useful to acquire information of possible progressive phenomena, but also during and after

the implementation of strengthening intervention in order to evaluate their effectiveness. Figure 2 shows a schematic representation of the multi-disciplinary approach to obtain an integrated knowledge of the monuments.

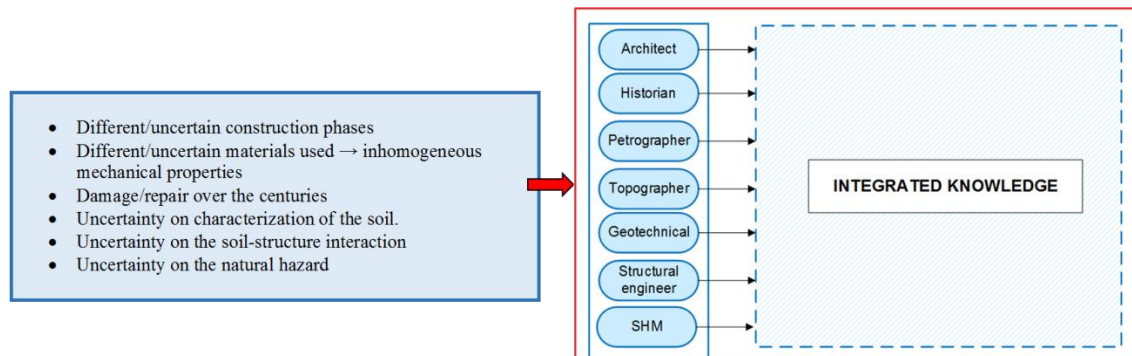


Figure 2- Schematic representation of the multi-disciplinary approach to obtain an integrated knowledge of the monuments

2 Guidelines for Multi- Analysis Integrated Assessment and weaknesses identification

The amount of data collected by the multi disciplinary approach are used to develop reliable structural analyses in order to evaluate the safety levels of the monument. The structural behaviour of a monument is usually very complex and influenced by many factors. Therefore, only one model of the whole building generally is not able to capture all the structural peculiarities. The monument should be represented by different simplified 'structural scheme', (i.e. an idealisation of the building) with different complexity and different degrees of approximation to reality. Moreover, the model used has to take into account any alterations and weakening, such as cracks, disconnections, leanings, ..., whose effect may significantly influence the structural behaviour. Structural analyses of ancient masonry structures is very far from the modelling of ordinary buildings, and the most widespread tools generally based on Finite Element methods are affected by several limitations, that may be related to the material behaviour, the actual effectiveness of the connections, the effectiveness of the chains, the restraints provided by the soil. In addition, the dynamic properties of global models in terms of fundamental frequencies and modal shapes may be are very far from the real ones, provided that they are based on linear elastic analysis, whilst the masonry material is characterized by a highly non-linear response [5]. All these problems point to the need to develop a multiple analyses approach which integrating the potential of various methods of analyses, from simple but more robust ones, to more accurate but generally more sensible complex numerical simulations allows to assess the

“structural health” of the monuments. The schematic representation of the concept of the multi analyses approach is shown in Figure 3

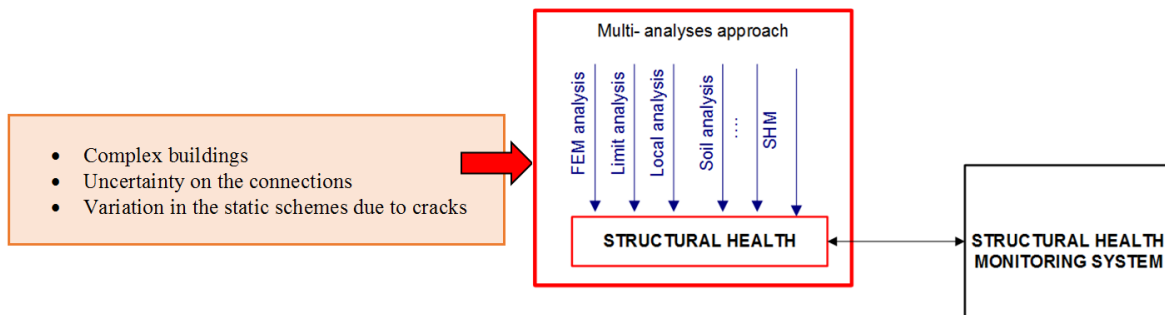


Figure 3: Schematic representation of the multi-analyses approach to evaluate the “structural health” of the monuments

3 Atlas of structural solutions for the conservation of cultural heritage buildings

To be completed based on the results of ongoing research and studies.

PART 2: CASE STUDY- THE MODENA CATHEDRAL

Cathedral of Modena: the integrated knowledge

1 The Cathedral of Modena

The Cathedral of Modena and the adjacent Ghirlandina Tower are part of the UNESCO site of Piazza Grande, since 1997. The Cathedral is a masterpiece of Romanesque architecture and sculpture of northern Italy (Figure 4). Its construction was realized between 1099 (the date of its foundation is marked on a stone on its façade) and 1319, when the construction of the Ghirlandina was completed. Inscriptions on the façade and on the central apse celebrate respectively the sculptor Wiligelmo and the architect Lanfranco. As it will be better explained later (§1.1.1), the actual Cathedral rise up on the ruins of three previous Cathedrals [6], the first one containing the tomb of St. Geminianus (the Modena city's patron). The in-plan geometry is approximately 25 m wide, in the transversal direction, and 66 m long, in the longitudinal direction, for an area of roughly 1650 m². The maximum roof height is approximately 24 m (Figure 5). The Cathedral has a Latin cross plant with three naves, a false transept and the chancel (the area of the liturgical altar) in an elevated position, due to the presence of a crypt containing the corpse of the city's patron, Saint Geminianus.



(a)



(b)

Figure 4: Photographs of Cathedral of Modena: (a) view of the apses and (b) view of the facade.

The structural configuration consists of heavy masonry walls, sturdy masonry and stone piers supporting the weight of impressive thin masonry vaults, added in the XV century. Both the central

nave and the side aisles have four spans. The vaults of the central nave have double length span with respect to the length span of the vaults of the aisles. The maximum height of the vaults of the central nave is around 20 m, while that of the side aisles is approximately 13 m. Next to the Cathedral, there is the Ghirlandina Tower, a high tower of roughly 88 m high whose construction proceeded in parallel with that of the Cathedral up to the fourth level. The upper part of the Tower was built later, between 1261 and 1319 [7].

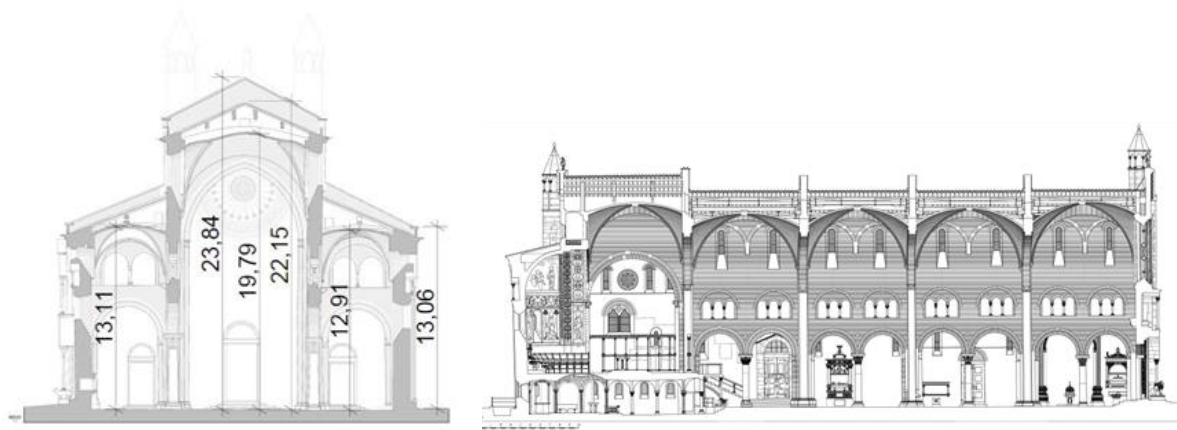


Figure 5: Cross-section of the Cathedral of Modena

1.1 The actual state of the Cathedral

1.1.1 The construction phases and the main interventions

The current configuration of the Cathedral is the result of various transformations and interventions that occurred on the fabric during centuries. These changes did not only affect the architecture of the Cathedral, but also influenced significantly its structural behavior. In the light of this, it is of fundamental importance to have a clear view of the most significant construction phases. Before the present Cathedral, three ones were built on the necropolis containing the tomb of St. Geminianus (the founder of the church of Modena) which is the only remaining evidence of the first one. A second Cathedral was erected in the same place around the VIII-IX century. The archaeological remains indicate that this church had a length of around 32 m and width of 18 m. The presence of polylobate piers [8], discovered during past excavations, allow to suppose the existence of another Cathedral, presumably built around the XI century (Figure 6) [9].

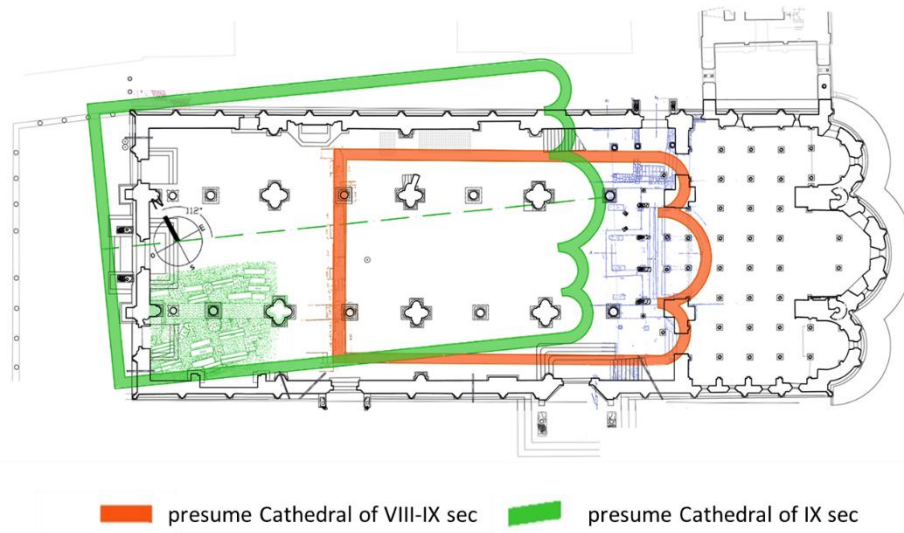


Figure 6: The pre-existing Cathedrals

There is an open debate about the construction phases leading to the actual fabric [10], [11], [12], [13],[14]. According to the hypothesis of Porter [15], confirmed later by other researchers, the construction began in 1099, almost in parallel, from the apses and, just few years later, from the main façade. At 1130, the complex knew the construction of the clerestory and the joining of the lateral naves where, according to Peroni (1989 and 1999) and Lomartire (1989), the initial construction was interrupted in order to maintain the portions of the pre-existing Cathedral. More recent historical studies [14] suggest that the construction of the outer perimeter did not proceed in parallel from the two sides, specifically the main façade and the apses, but started from the apses (phases A) to end with the main façade (phases B), (Figure 7: The construction phases). In light of this alternative hypothesis, the phase C was remarked by the repair of some damages due to early soil settlements manifested during the first two phases. This reconstruction may be further supported by the analysis of the cracking pattern. Figure 7 graphically represents the three construction phases according to this last hypothesis.

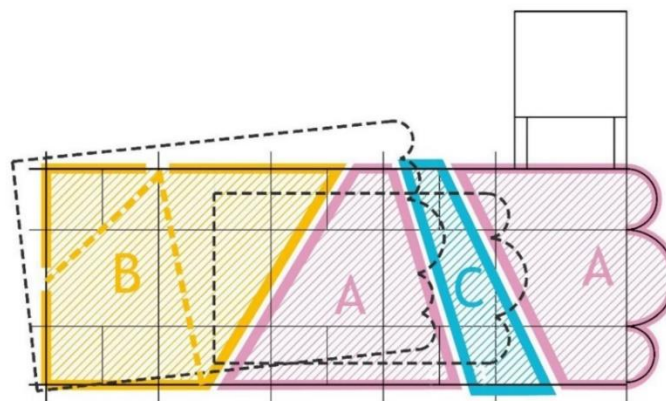


Figure 7: The construction phases

After the end of the construction, several interventions were carried out during the years. The elevation of the Tower in the following years caused the lowering and slight rotation of the apses due to differential soil settlements. The presbytery appeared so slanted that it was necessary to realize many reparations and reconstructions according to a new verticality and horizontality. This was one of the principal intents of the architectural renovation applied by the Campionesi masters at the Cathedral of Modena during the years 1180-1220. In the light of the studies on the construction phases, the 3D laser scanner survey was able to measure the different inclinations of the masonry walls belonging to the different phases, thus dating the successive increases of the foundation settlements along the centuries. According to several historians, the original roof system, made of timber trusses (“capriate”) arranged in the transversal direction, was rebuilt after 1413. The orientation of the principal beams was changed when the vaults of the naves were constructed. Probably during this phase, the original timber beams were replaced causing deformations of the longitudinal walls. Later on, other interventions proved to be necessary after the earthquake events occurred in the 1501, 1505 1671 and 1832. The main interventions affected the vaults, the arches, the façade and the portions of walls adjacent to the Ghirlandina Tower [16]. In the following years, additional strengthening interventions were performed, such as refilling the main cracks, repairing the roof (new wood structures connected to the masonry wall by iron chains) and connecting the walls through iron chains in the naves at different heights (Figure 8). At the beginning of the XX century, all the constructions built next and into the Cathedral during the years (rectory, cluster, sacristy and internal chapels) were demolished in order to restore the original Romanesque aspect. In 1975, Modena and its Cathedral were affected by the soil subsidence. During the recent years, starting from the 2006, a restoration campaign has interested the external stone facade, until the earthquakes of the 2012 shifted the attention to the damages of the interior, principally the vaults, as it will be better explained in § 3.4.

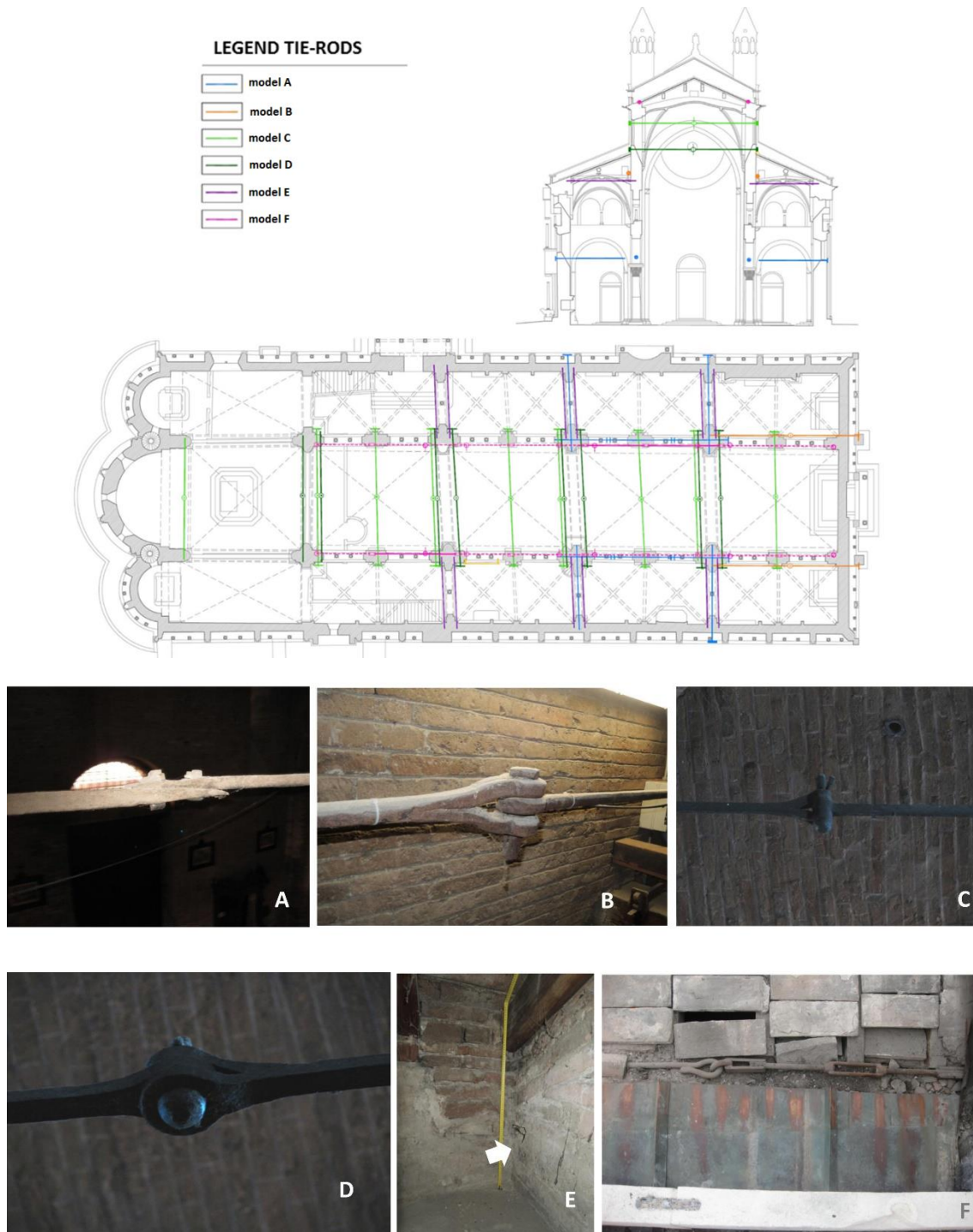


Figure 8: Survey of the tie-rods installed on the Cathedral during the years and respective photographers.

1.1.2 The reconstruction of the geometric configuration through laser scanner and the geotechnical investigations

A 3D laser scanner of the Cathedral was carried out to identify with accuracy walls dimensions and deviation from verticality [17]. Figure 9 displays the inclinations of the external wall and internal pillars as obtained from the 3D laser scanner. In general, excluding the area of the South transept, the

walls are inclined towards the outside. As already clear by simple visual inspection, the overhanging increases moving closer to the Ghirlandina Tower, thus indicating a strong interaction between the Tower and the Cathedral. Notably, this interaction caused so important damages to the two masonry arches connecting the Tower with the Cathedral, at the point that they were completely reconstructed at the beginning of the last century.

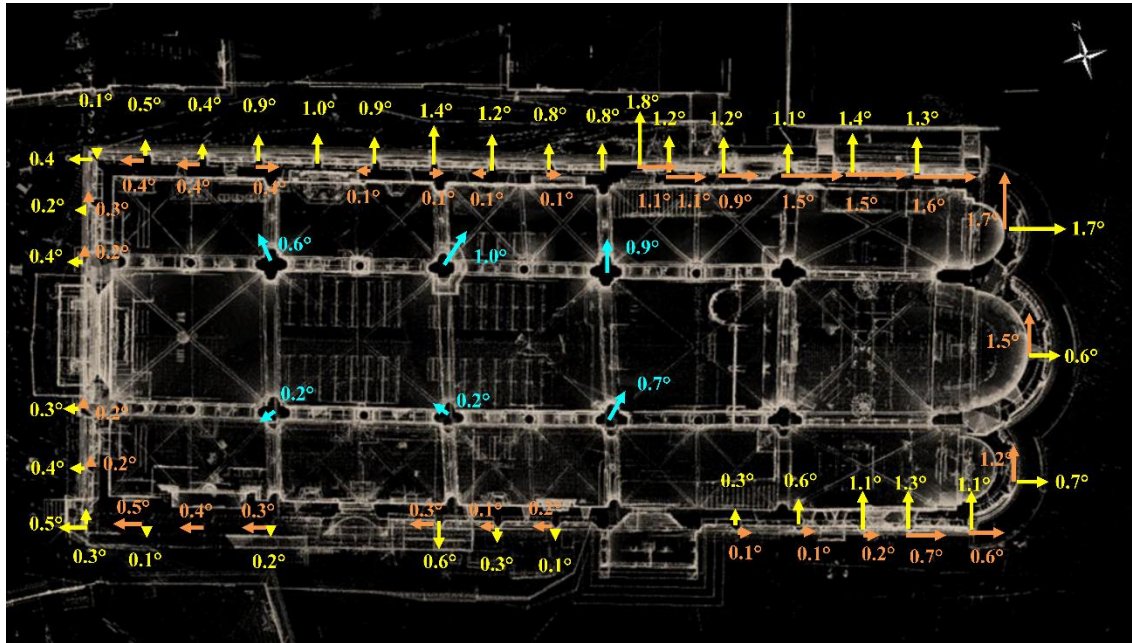


Figure 9: The inclinations of the external walls and internal pillars as obtained from the 3D laser scanner.

In addition to the differential settlements induced by the interaction between the Tower and the Cathedral, also a discontinuity in the soil stiffness due to the presence of the ruins in only one portion of the plan (see Figure 6), could have significantly contributed to the walls deformation. Since that soil has “memory” of its previous loading history [18], due to loading-unloading (as consequence of sequences of construction and demolitions), the soil response of these portions would be much stiffer than those parts that never experienced any previous loading-unloading. Therefore, this loading history could contribute to explain why the Cathedral suffered uneven settlements not only moving from South towards North (due to the presence of the Tower, as before explained), but also moving from East towards West. These differential settlements were also more pronounced due to the nature of the foundation soil. The soil profile was investigated up to a depth of 80 m resulting in a sequence of recently deposited alluvial horizons. The first horizon is made of medium to high-plasticity inorganic clays with a number of millimeter-thick laminas of sands and peats. The upper portion of this horizon, which has a thickness of about 5 m to 7 m, is known as the Modena unit and it is linked to flooding events (of post-Roman era) produced by minor streams. Geological and geotechnical studies [19],[20],[21] have shown events of exposition during deposition and generate layers that therefore were slightly over consolidated by desiccation. From these geotechnical investigations, also

the soil mechanical properties useful for the structural analysis have been obtained. For instance, two different values of the Winkler constant may be assumed to account for the presence of a portion of more consolidated soil (see Figure 10).

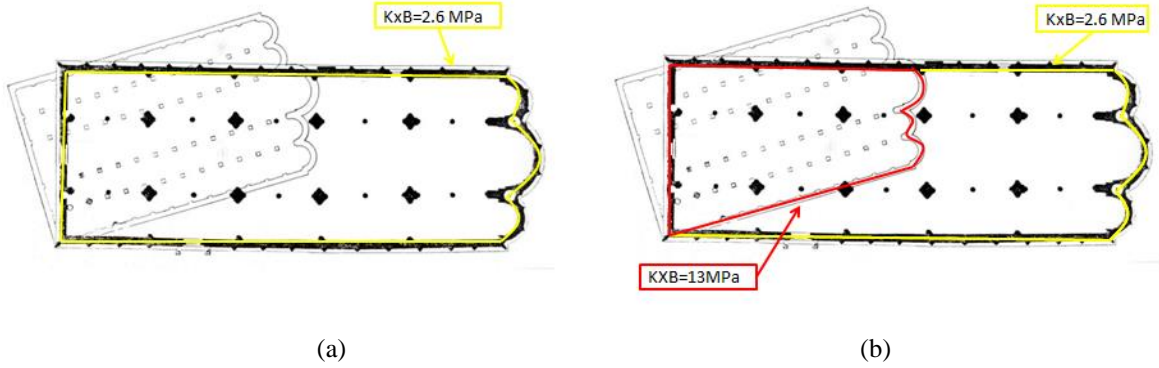


Figure 10: (a) Uniform distribution of Winkler's constant (W1) and (b) Non Uniform distribution of Winkler's constant (W2).

1.1.3 Material properties

It is a matter of well consolidated knowledge that the assessment of material properties of historical masonries is a rather challenging problem. Extensive destructive and non-destructive tests are typically used to evaluate material properties of ordinary existing buildings. Nonetheless, for important monuments, only limited tests are usually allowed by the local authorities in charge of the conservation of the monument. Moreover, the mechanical parameters as obtained from few non-destructive tests provide only partial and local information. This means that these few data must be critically analyzed in terms of their reliability. Therefore, experimental data have to be compared not only with values suggested by the codes or literature but as well as with values based on material models. This approach was already successfully applied to the ancient masonry "Asinelli" Tower in Bologna [22] and has been also used in the present case. The results of video-endoscopic investigations on the facade and sonic and radar tests on the remaining walls and piers, were integrated and validated with the values suggested by the scientific literature [23],[24] or by codes (Circ. n. 617, 2009) leading to masonry and stone Young's modulus equal to $E_m = 1800\text{-}4000 \text{ MPa}$, and $E_s = 25000 \text{ MPa}$, respectively. For the timber beams, considering aging effects, the lower bounds mechanical properties have been used as suggested by the document CNR-DT 206 [25]: Young's modulus $E = 600 \text{ MPa}$, compression strength $f_m = 14 \text{ MPa}$ and mean density $\rho_m = 350 \text{ Kg/m}^3$.

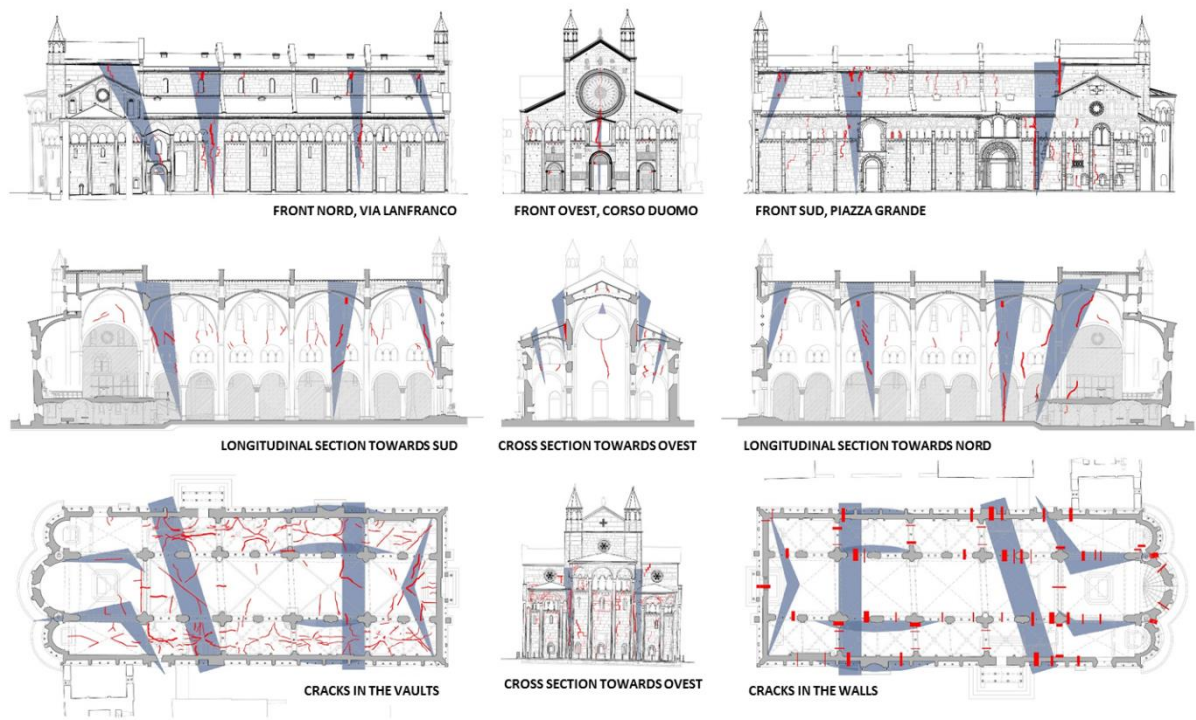
1.1.4 The actual state of degradation

A first detailed survey of the cracking pattern was carried out in the 2010. After the 2012 Emilia Earthquakes, the Cathedral suffered minor damages, mainly localized in the vaults. Therefore, a second survey was carried out to detect in detail the damages caused by the earthquake sequence. After this detailed survey, a strengthening intervention has been planned and the design is actually under development.

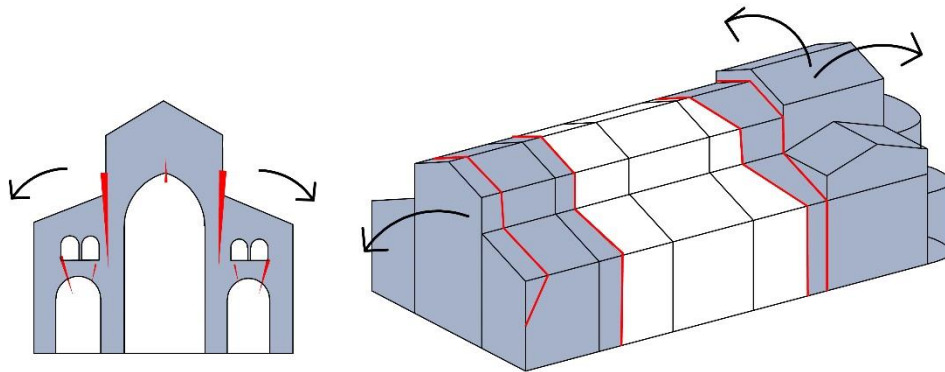
The initial crack pattern (2010) has been studied not only to monitor the state of the main cracks but also to correlate their location within the construction phases and main interventions. The analyses of past studies also helped in the classification of the cracks. In particular, the correlation between the damage and the past interventions allow to identify the probable causes and distinguish between stable cracks and still evolutionary situation. The major cracks are displayed in Figure 11. The main cracks are indicated in red, while grey areas indicates the zones of diffused cracks with potential high vulnerabilities. It can be noted that:

- a large vertical crack is located in the main facade, just below the big rose window;
- a concentration of cracks has been identified in the connection between the walls, all along the portion of the building constructed during the phase C, in the fourth span from the west;
- another cracks concentration appears near the main facade, along a line parallel to the façade, in the second span from the west;
- vertical cracks along the main transversal walls and arches separate the central naves from the lateral naves.

The grey areas are mainly located in the portion of the Cathedral coinciding with the location of the old Cathedrals. During the survey after the 2012 Emilia Earthquakes, new cracks appeared in the intrados of the main vaults. Moreover, an evolution of some existing cracks has been also observed (Figure 12).



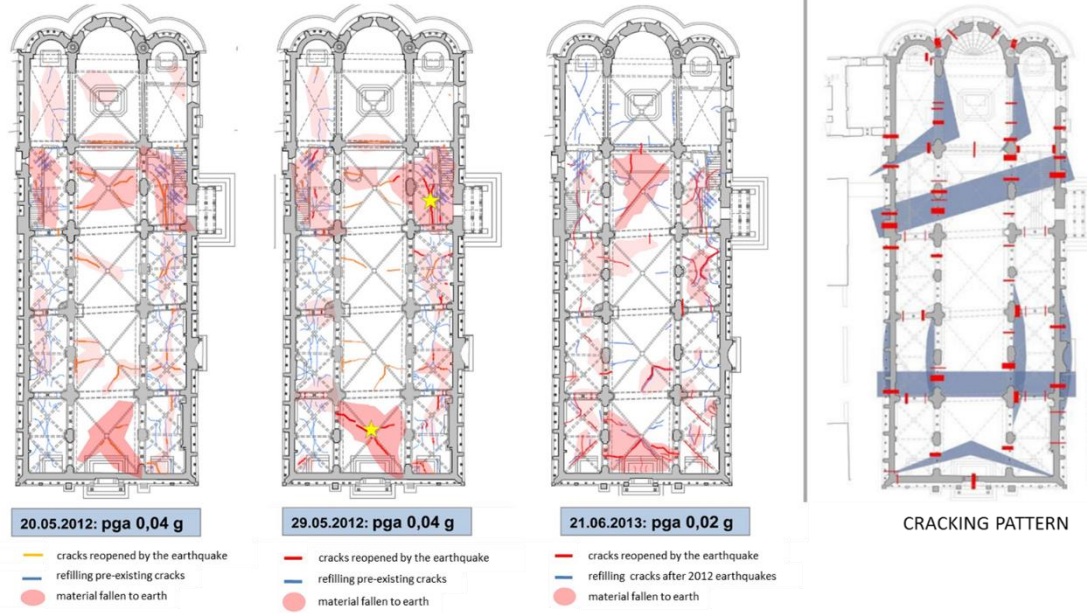
a)



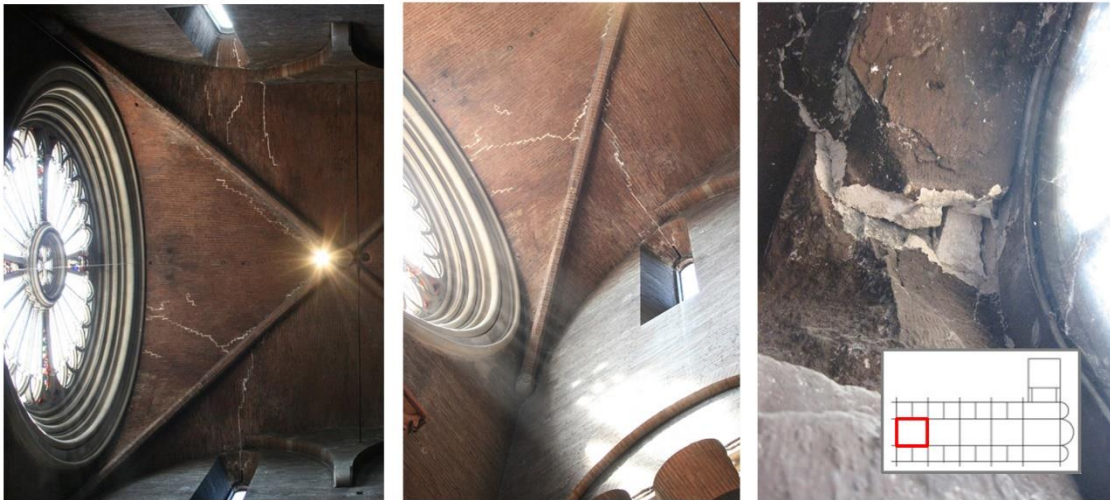
b)

Figure 11: (a) Crack pattern of the Cathedral of Modena and (b) main failure mechanisms of the Cathedral on the longitudinal and transverse direction

MAPS OF THE CRAKS DETECTED ON THE VAULTS-earthquakes of the 20, 29 may 2012 and 21 June 2013



a)



b)

Figure 12: (a) Maps of the cracks detected on the vaults after the earthquakes of the 20 and 29 May 2012 and 21 June 2013 and comparison with the crack pattern and (b) photographs on the damage caused by recent earthquakes.

1.2 Seismic Hazard analyses

The objective of the seismic hazard analysis is to compute, for a given site over a given observation time, the probability of exceeding any particular value of a specified ground motion parameter (commonly the Peak Ground Acceleration, PGA). In the case of monumental buildings, seismic hazard analysis does not allow only to predict the characteristics of possible future earthquakes, but also to obtain information on the characteristics of already occurred past earthquakes. The past seismic input has been studied through the reconstruction and the position of the historical earthquakes that have affected the Cathedral. This analysis allows to collect information useful for the identification of the historical periods of specific cracks and failures or interventions and for the reconstruction of the history of the building. The possible future seismic input has been studied through probabilistic and deterministic seismic hazard in order to identify the most probable earthquake scenarios which can shake the site of the monuments. Typical probabilistic seismic hazard analysis (as performed according to the approach suggested by Cornell) [26] assume that, in each point of the seismic zone area, the probability of occurrence of an earthquake is uniform. Thus, this approach is suitable for designing new buildings and for regional planning. However, it is not adequate for the identification of the seismic input to be adopted in the studies of monumental buildings, where the consequences of failure are intolerable and protection is needed against the worst that can be reasonably expected to occur. In these cases, the deterministic method is strongly recommended [27]. Two kinds of deterministic seismic hazard analyses have been performed for the site of the Cathedral of Modena:

- Historical Deterministic Seismic Hazard Analysis (HDSHA);
- Maximum Historical Earthquake Analysis (MHEA);

These analyses have been based on the following data: the ZS9 zoning (subdivision of the Italian Territory):

- the Cathedral of Modena is located in the zone 912 (<http://zonesismiche.mi.ingv.it/>);
- the CPTI04 earthquake catalogue (<http://emidius.mi.ingv.it/CPTI04/>);
- the Sabetta-Pugliese attenuation law [28];
- the Gutenberg-Richter recurrence law [29].

1.2.1 Historical Deterministic Seismic Hazard Analysis (HDSHA)

HDHSA has the objective to reconstruct the intensity of historical earthquakes that have actually affected the Cathedral of Modena in the past centuries. Significant historical earthquakes have been selected from the CPTI04 earthquake catalogue, through the following criteria:

- earthquakes that occurred within 20 km from the Cathedral;
- earthquakes characterised by the greater magnitude that occurred in the ZS9 seismogenetic zones near to the site of the Cathedral;
- significant earthquakes in relation to the historical information.

Table 1 shows these significant earthquakes of the past and the reconstruction of their Peak Ground Accelerations, in correspondence of the site of the Cathedral, as obtained using the Sabetta-Pugliese attenuation law. Based on the five past earthquakes with epicentre in Modena (4 earthquakes with epicentre in Modena respectively in the years 1249, 1474, 1660, 1850 and the earthquake of the Appennino Modenese of 1501), it can be stated that the cathedral might have been hit by accelerations around 0.15 g. The earthquake of 1249 was the most violent and might have rocked the Cathedral with an acceleration of approximately 0.20 g. **Errore. L'origine riferimento non è stata trovata.** shows the reconstruction of the median of the PGA, obtained considering the epistemic uncertainty associated to the Sabetta-Pugliese ground motion prediction model, for all earthquakes of the CPTI04 earthquake catalogue. Inspection of Figure 13 indicates that, looking at the past, the earthquake with acceleration between 0.15 g and 0.20 g is characterized by a return period of about 200-250 years.

Table 1- Reconstruction of peak Ground Acceleration (PGA) in correspondence of the site of the Cathedral of Modena for the selected earthquakes

Selection criteria	N.	Year	Location Name	Seismogenetic zone (ZS9)	R [Km] (distance)	Msp (magnitude)	PGA mode	PGA median	PGA mean value	PGA percentile 80%
Earthquakes that occurred within 20 km from the Cathedral	53	1249	Modena	912	0.65	4.80	0.200	0.245	0.270	0.360
	171	1474	Modena	912	0.12	4.61	0.170	0.211	0.232	0.310
	195	1501	Appennino	913	16.37	5.82	0.140	0.170	0.187	0.250
	279	1586	Spilamberto	913	10.86	4.53	0.070	0.083	0.091	0.120
	362	1660	Modena	912	0.12	4.25	0.130	0.156	0.172	0.230
	374	1671	Rubiera	912	14.26	5.23	0.100	0.117	0.129	0.170
	720	1811	Sassuolo	913	23.49	5.09	0.050	0.066	0.072	0.100
	871	1850	Modena	912	5.66	4.53	0.110	0.131	0.144	0.190
	984	1873	Reggiano	913	25.29	4.93	0.040	0.053	0.059	0.080
	1739	1923	Formigine	913	15.20	5.05	0.080	0.095	0.105	0.140
	1808	1928	Carpi	912	17.83	4.54	0.040	0.054	0.059	0.080
	1859	1931	Modenese	913	15.80	4.54	0.050	0.060	0.066	0.090
	1897	1934	Vignola	913	19.38	4.06	0.030	0.033	0.037	0.060
	2237	1967	Formigine	913	9.21	4.09	0.050	0.065	0.072	0.100
Earthquakes characterised by the greater magnitude that occurred in the ZS9 seismogenetic zones near to the site of the Cathedral	393	1688	Romagna	912	116.68	5.85	0.020	0.025	0.028	0.390
	30	1117	Veronese	906	82.03	6.49	0.050	0.062	0.068	0.090
	776	1828	Valle dello	911	209.68	5.55	0.010	0.011	0.012	0.050
	195	1501	Appennino	913	16.37	5.82	0.140	0.170	0.187	0.250
	278	1584	Appennino	914	147.54	5.99	0.020	0.023	0.025	0.230
	1708	1920	Garfagnana	915	88.64	6.48	0.050	0.057	0.062	0.090
	988	1873	Liguria	916	73.43	5.47	0.020	0.029	0.032	0.060
Significant earthquakes in relation to the historical information	47	1222	Basso	906	96.77	6.05	0.030	0.036	0.040	0.060
	202	1505	Bologna	913	40.57	5.41	0.040	0.050	0.055	0.080
	1499	1909	Bassa Padana	912	85.20	5.48	0.020	0.026	0.028	0.400
	1684	1919	Mugello	915	99.06	6.18	0.030	0.040	0.043	0.060
	2509	1996	Correggio	912	30.95	5.26	0.050	0.058	0.064	0.090
		2012	Finale Emilia	912	43.42	5.90	0.060	0.071	0.078	0.110
		2012	Medolla (MO)	912	28.97	5.80	0.080	0.097	0.107	0.150

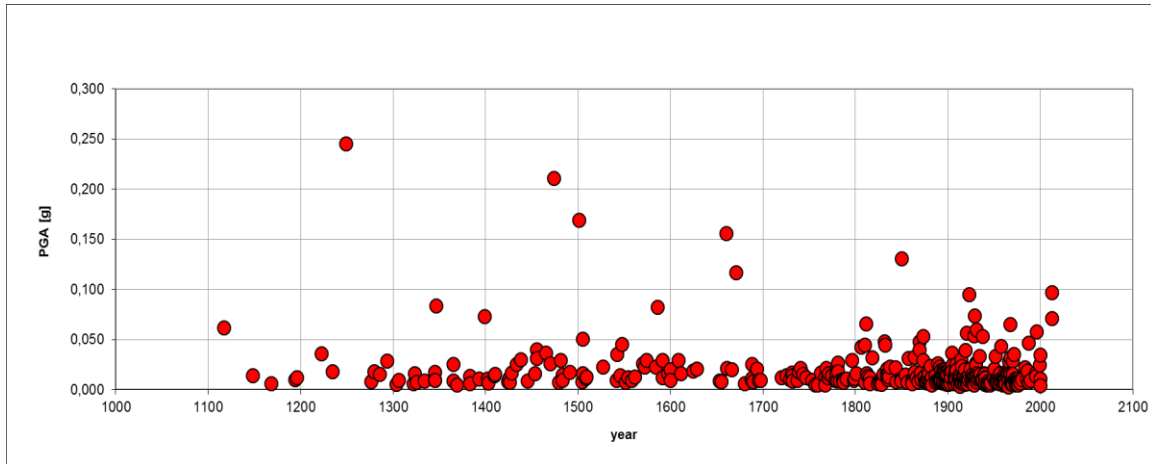


Figure 13: Reconstruction of the median of the PGA, obtained considering the epistemic uncertainty associated to the Sabetta-Pugliese ground motion prediction model, for all earthquakes of the CPTI04 earthquake catalogue.

1.2.2 Maximum Historical Earthquake Analysis (MHEA)

The MHEA is aimed at estimating the most violent earthquake that could occur in the future on the specific site of the Cathedral. The PGA recorded in a specific site during an earthquake depends on two factors: the magnitude and the distance between the epicentre and the site. Therefore, the worst seismic scenario for a specific site occurs with the combination of the high magnitude and null epicentre-site distance. The maximum magnitudes recorded in the past in the seismic zone (912) of the Cathedral and in the adjacent zones (913, 914, 915, 916, 911 and 906) were obtained from the earthquake catalogue. Then, it is assumed that earthquakes of such magnitudes could occur at zero distance from the Cathedral, and the intensity of the earthquake worse future is reconstructed considering the epistemic uncertainty associated to the Sabetta-Pugliese ground motion prediction model. Table 2 shows the list of the highest magnitudes occurred in all the considered zones and the reconstructed median, mode, mean values and 80% percentile values of the PGA variable. According to seismic activity of the two areas 912 and 913, it can be stated that a future earthquake with acceleration of about 0.50 g can occur, as shown in the Figure 14.

Table 2- Estimation, through MHEA, of the PGA that can occur in the future in the site of the Cathedral of Modena

ZS zoning	Rmin from Cathedral	Mas max	Msp max	Mode	Median	Mean value	80% percentile
912 (zone of Cathedral)	0.00	5.85	5.85	0.49	0.60	0.65	0.87
913	2.96	5.82	5.82	0.41	0.50	0.55	0.73
914	67.50	5.99	5.99	0.04	0.05	0.05	0.08
915	54.67	6.48	6.48	0.08	0.09	0.10	0.14
916	75.48	5.32	5.47	0.02	0.03	0.03	-
911	99.35	5.55	5.55	0.02	0.02	0.03	-
906	72.12	6.49	6.49	0.06	0.07	0.08	0.11

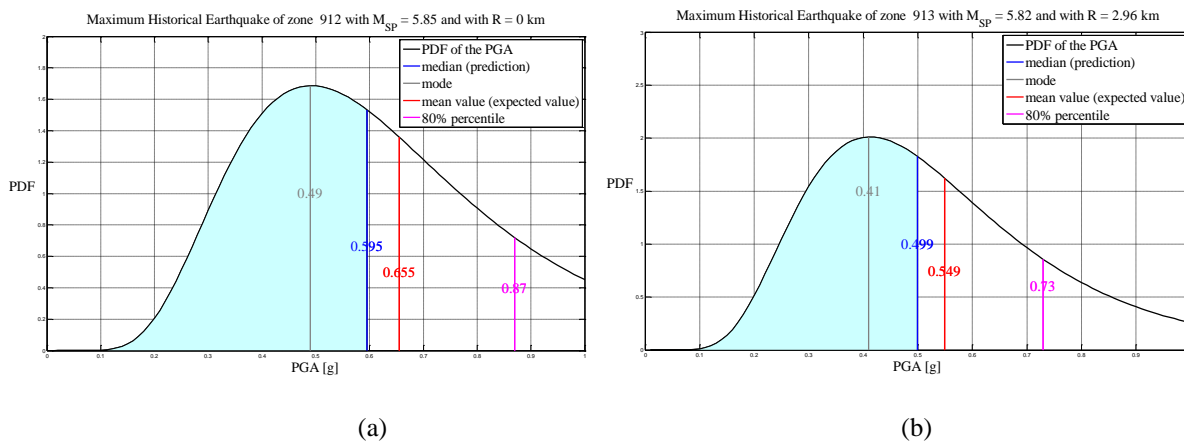
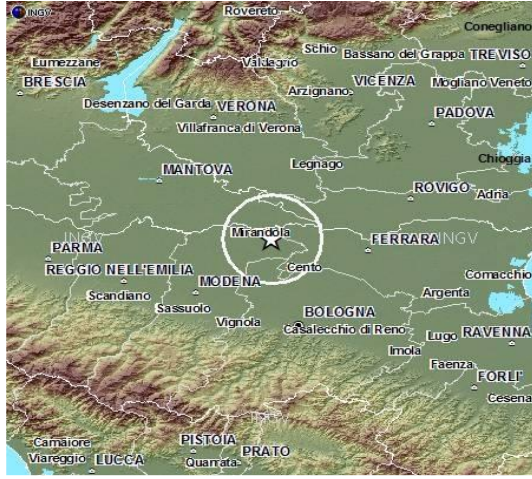


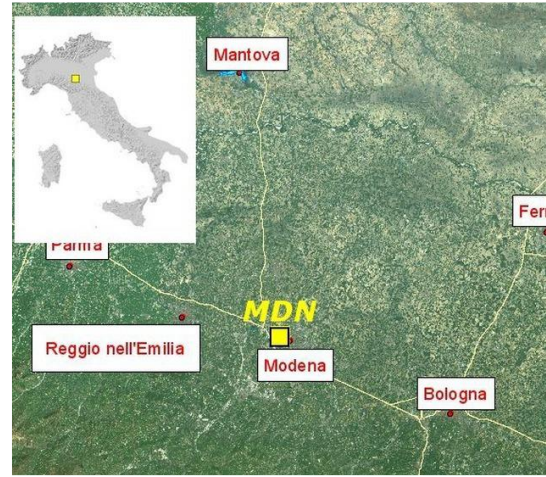
Figure 14: Probability density function (PDF) of the PGA in the site of the Cathedral of Modena as a result of seismic activity of zones: (a) zone 912, (b) zone 913.

1.3 The 2012 Emilia's earthquake

The 20th May 2012, at 02:03:53 (UTC), Emilia Romagna region (Northern Italy) was struck by an earthquake of magnitude $M=5.9$ (latitude 44.890 longitude 11.230). The main shock was preceded by a $M=4.1$ event on 19th May and followed on the 29th May 2012 by a 5.8Mw earthquake with epicentre 15km North West of the former event (**Errore. L'origine riferimento non è stata trovata.**a). Several events with magnitude $4.0 \leq M_I \leq 4.5$, plus several other minor earthquakes, occurred in the same area the following days, as reported in Italian Instrumental and Parametric Data-Base (ISIDe),[30]. As reported, this earthquake sequence has caused a lot of damage / collapse in the monumental building, including the Cathedral of Modena. The cathedral has been considered, first, as a model of itself with the purpose of understanding its intrinsic structural behaviour. For this reason, the strong motions of the main shock recorded by the station of Modena (code MDN) have been used in some of the next analyses developed on the Cathedral. The localization of the recording station MDN is reported in Figure 15.



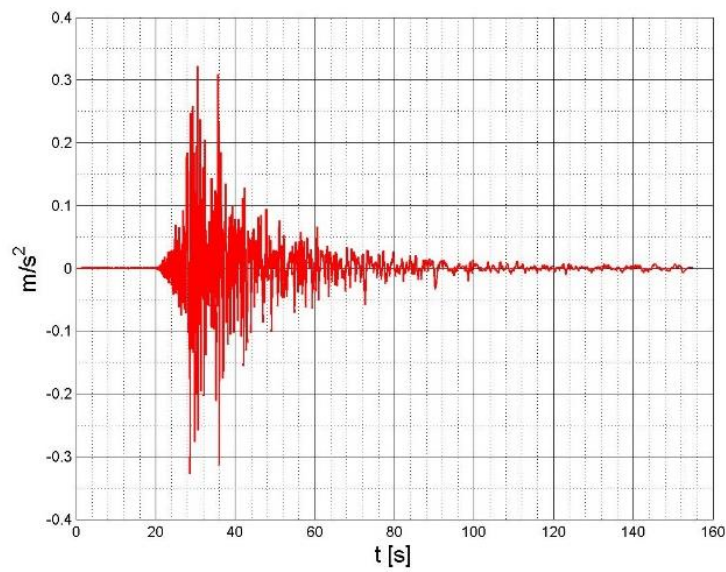
(a)



(b)

Figure 15(a) Location of epicentre of May 29th earthquake (INGV), (b) Localization maps of the recording station in Modena (MND)

Figure 16 display the acceleration as recorded by MDN station during the main shock of 20th May and used in the dynamic analyses of the Cathedral and the corresponding spectral acceleration and the spectral displacement.



(a)

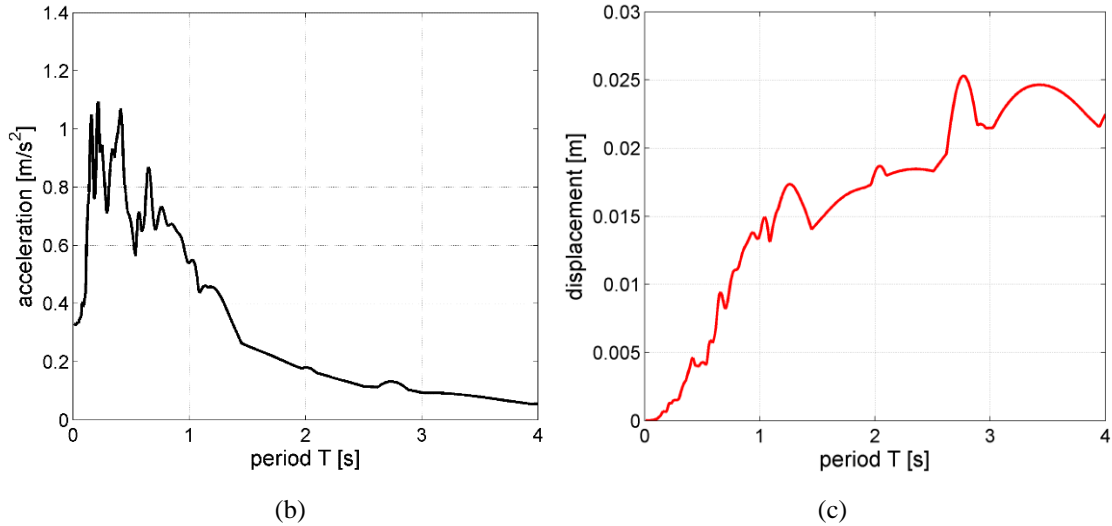


Figure 16: (a) The acceleration recorded by the station MDN during the main shock of 20th May 2012, (b) the corresponding spectral acceleration and (c) the corresponding spectral displacement

1.4 Conclusions

The integrated knowledge of a monument is the first step to develop consistent structural analyses and, thus, to understand correctly its structural health. The knowledge process developed for the cathedral highlighted the important role played by the following three aspects

- the presence of previous Cathedrals that gave rise to uneven settlements of the actual one, due to the influence of soil behaviour as a “material with memory”;
- the construction phases; and
- the interaction with the Ghirlandina Tower.

These aspects strongly influence the structural behaviour of the cathedral and must to be considered in the structural analyses. Moreover, the seismic hazard analyses allowed reconstructing the intensity of the earthquakes that occurred on the cathedral in the past. Historical Deterministic Seismic Hazard Analysis has highlighted that four important earthquakes (peak ground acceleration around 0.15 and 0.25g) and 20 earthquakes of medium intensity (peak ground acceleration around 0.05 g e 0.10) have hit the cathedral during its life. The comparison with the historical evidence revealed that for the important earthquakes the Cathedral has reported consistent damages, which interested particularly the vaults and slender pinnacles. For earthquakes of medium-low intensity (as the 2012 earthquake) slight damages have been detected always mainly on the vaults and slender pinnacles.

Multi-analyses assessment of the Modena Cathedral

2 Global structural behaviour

2.1 Introduction

The information obtained from the integrated knowledge have been used to study the global structural behaviour of the cathedral, i.e. recognize the structural elements and the actual load paths, to identify the materials properties and the appropriate restrain at the base. Different analyses (simple, but more reliable limit schematizations, and more complex, but too much sensitive to uncertainties, computer-based models) have been conducted on the global structure of the masonry fabric in order to identify the main static and seismic vulnerabilities.

2.2 The models and the simulations

The static behaviour of the cathedral has been investigated through simple limit schematizations and Finite Element models of increasing complexity (2D models, 3D models with fixed base, 3D models accounting for the soil-structure interaction). Due to the complexity of the monument and the relevant influence of different factors (such as construction phases, soil properties, existing cracks, interaction with the Tower, as highlighted in §10), instead of a unique 3D FE model in which all factors are simultaneously taken into account, several specific 3D FE models have been performed to separately investigate, the effects of each single factor. The results of the static analyses as obtained from FE models, validated through the simple static analyses performed on the substructures, have been used to interpret the cracking patterns as obtained from in situ surveys and the deformations related to changes in the geometrical configuration as obtained from the topographic surveys§10. In addition, on the 3D FE model able to better represent the static behaviour of the cathedral various seismic analyses have been carried out in order to assess its seismic vulnerabilities. The analyses developed are summarized in **Errore. L'origine riferimento non è stata trovata..**

Table 3- The different analyses developed

Model-Element	Analysis
Hand –made schematization of the roof system	Static analysis
Hand –made schematization of the main vertical elements	Static analysis
2D FEM model of the vertical elements	Static analysis

3D FEM models with different restrain at the base and load cases	Static analysis
3D FEM models	Natural frequency analysis
3D FEM models-input consistent with the SHA§10.4	Response spectrum, time history analysis
3D FEM models-input recorded during the 2012 earthquake§10.5	Time history analysis

2.3 Static analyses

2.3.1 The applied loads/actions

The effect of the gravity loads (also considering thermal effects) have been considered in the structural static analysis. The assessment of the monument against the other possible environmental loads is out of the scope of the present work. The vertical load due to snow has been estimated equal to 1.20 kN/m^2 according to the Italian building code (NTC 2008). In addition to the above described loads also the interaction between the Cathedral and the adjacent Ghirlandina Tower has been accounted for (even if, at this stage, in a rather simple way) by imposing a profile of differential vertical displacements at the base of the Cathedral, as provided by the geotechnical studies mentioned in §10.3.2. In detail, the differential displacements have been imposed in the portion closest to the Ghirlandina Tower (Figure 17), the vertical displacements being equal to 20 cm at corner H, 27 cm at corner G, and 30 cm at corner F. Linear variations of vertical imposed displacements have been assumed between the above mentioned points, as well as moving from the side to the center of the Cathedral.

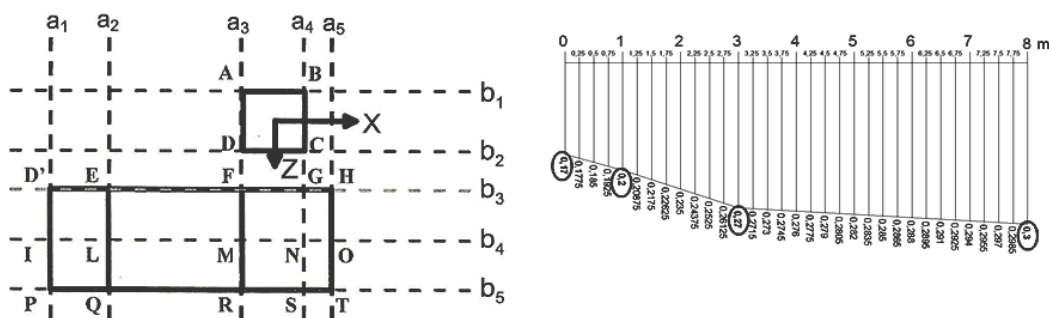


Figure 17: Imposed vertical differential displacements at the base due to the interaction between the Cathedral and the Ghirlandina Tower

2.3.2 Structural analysis with simple models

Simple limit schematizations have been developed for a preliminary structural analysis of the roof system and the main vertical resisting elements (i.e. walls and stone piers). Each substructure is analyzed with the purpose of obtaining the stress state of the main structural elements.

2.3.2.1 The roof system

The roof (Figure 18) is made of timber principal beams arranged in the longitudinal direction (indicated as T_i), which find additional supports on underlying timber beams or timber trusses - “capriate”- (indicated as t_i). The roof system, transferring the gravity loads directly to the masonry walls and stone piers, is covered by thin-masonry non-structural vaults withstanding only their self-weight. It should be noted that the increment of loads (both vertical loads and thrusts) due to the presence of the vaults is negligible.

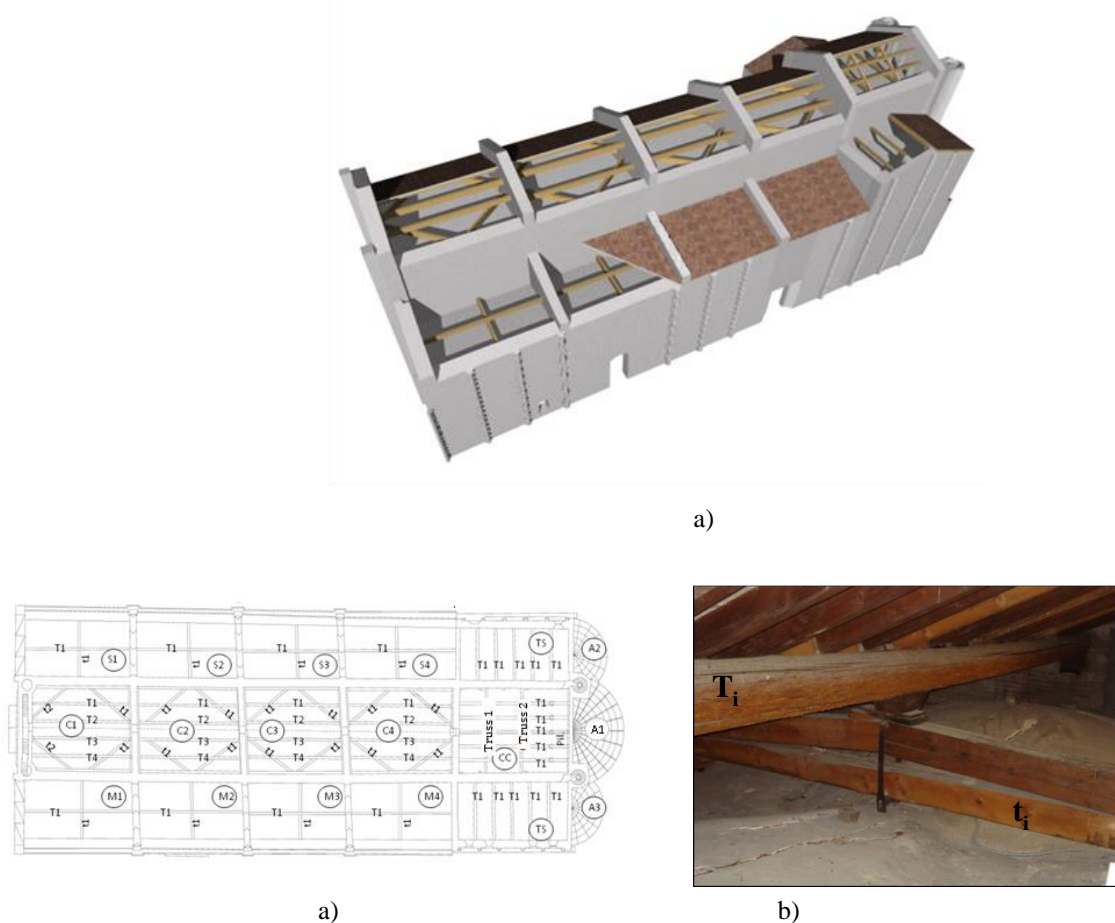


Figure 18: a) A 3D view of the roof system; b) Structural roof elements and c) Main beams (T_i) and trusses system (t_i)

Making use of this geometry, a simple static analysis has been performed of the roof system solely in order to evaluate the stress levels and the reactions at the base of the roof (which are then applied as

loads on the masonry walls). The maximum normal stresses for the main timber beams due to self-weight only are about 5 MPa for the beams of central nave, 8 MPa for the beams in the transept, 10 MPa for the beams of the aisles. The addition of the snow load lead to an increase in the maximum stresses of about 35% leading to stresses close to the material strengths. In detail, Figure 19 shows the stress levels (in a color scale) of the roof beams. The stress levels in the secondary elements (trusses) are about 1 and 1.5 MPa, well below the material strengths. It is worth to note that, due to the absence of specific tests performed on the wood elements, the assumed strength is conservative.

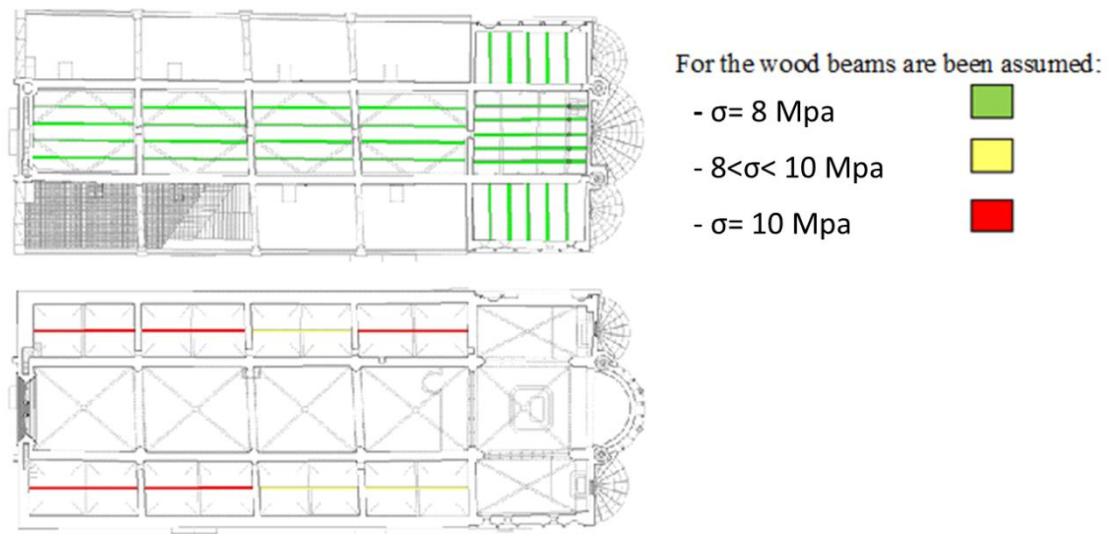


Figure 19: Stress level of the roof elements

2.3.2.2 The vertical resisting elements

The vertical resisting elements of the Cathedral are the masonry walls, the masonry piers and the stone columns. The masonry elements are characterised by non-uniform geometry (variations in thickness) and non-uniform mechanical properties. These discontinuities may lead to significant stress concentrations, and, in order to account for the presence of these geometrical discontinuities, in addition to homogeneous regular hand-made schematization, 2D FE models of each single wall have been also developed, assuming an ideal vertical configuration. These planar models are used to develop in-plane analysis aimed at evaluating the stress levels in the walls.

The hand-made schematizations of the single walls are used to calculate the stresses at the wall base, according to the Navier - de Saint Venant formulation, due to the self-weight, the weight of the vaults and the reactions of the roof system. In detail, the following assumptions have been made: (i) two limiting conditions: full cross-section and hollow cross-section (or “a sacco”, i.e. two exterior masonry layers plus an interior layer composed of chaotic stones and filling materials; in the “a-

sacco" configuration the wall inertia is equal to the inertia of the two exterior layers only); (ii) constant wall thickness equal to the average wall thickness; (iii) the presence of decorative elements has been neglected; (iv) each wall has been subdivided into homogeneous portions (i.e. same cross-section, referred to as a_i , $i=1,\dots,28$) for the evaluation of the normal average stresses at the base, (iv) perfect verticality of the masonry walls. In the limiting case of full cross-section, the normal stresses due to the gravity loads are between 0.3 and 0.8 MPa for exterior walls and between 1 and 1.4 MPa for masonry piers. On the other hand, in the limiting case of hollow cross-section ("a sacco" masonry), the normal stresses due to the gravity loads double both for the external walls and the internal piers. The maximum stress at the base of the stone columns is around 3.2 MPa. The increase due to the snow load is about 2.5% of the stresses due to gravity load. These stresses levels at the walls base obtained from simple hand-made models (Figure 20) have then been compared with those obtained from the 2D FE models, which are reported in terms of contour maps in Figure 21. This comparison indicates a good agreement between the two analyses.

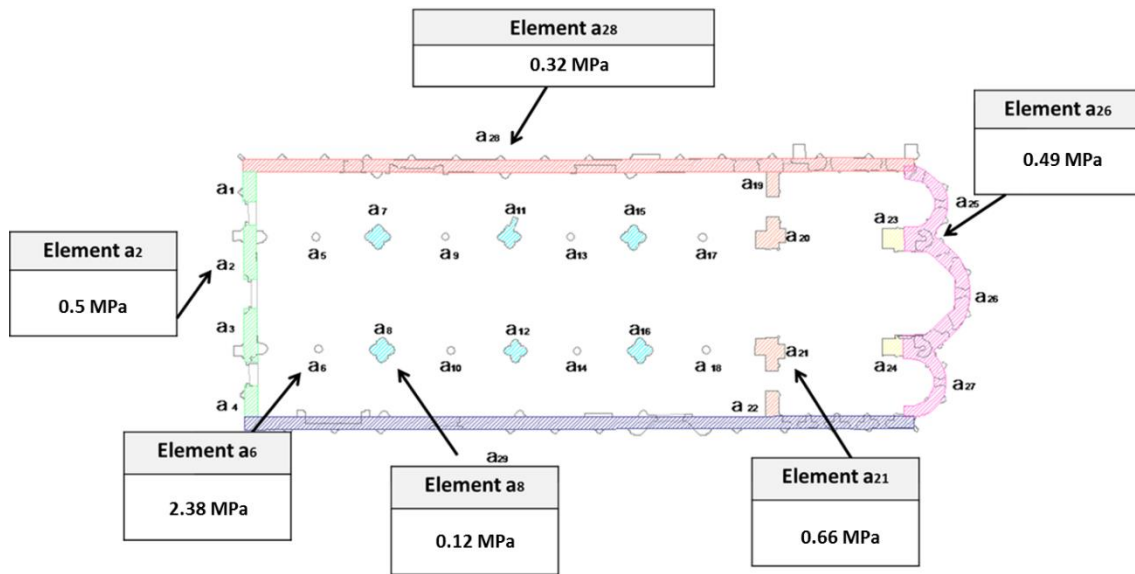


Figure 20: Reference values of the stress level at the base of the principal structural elements.

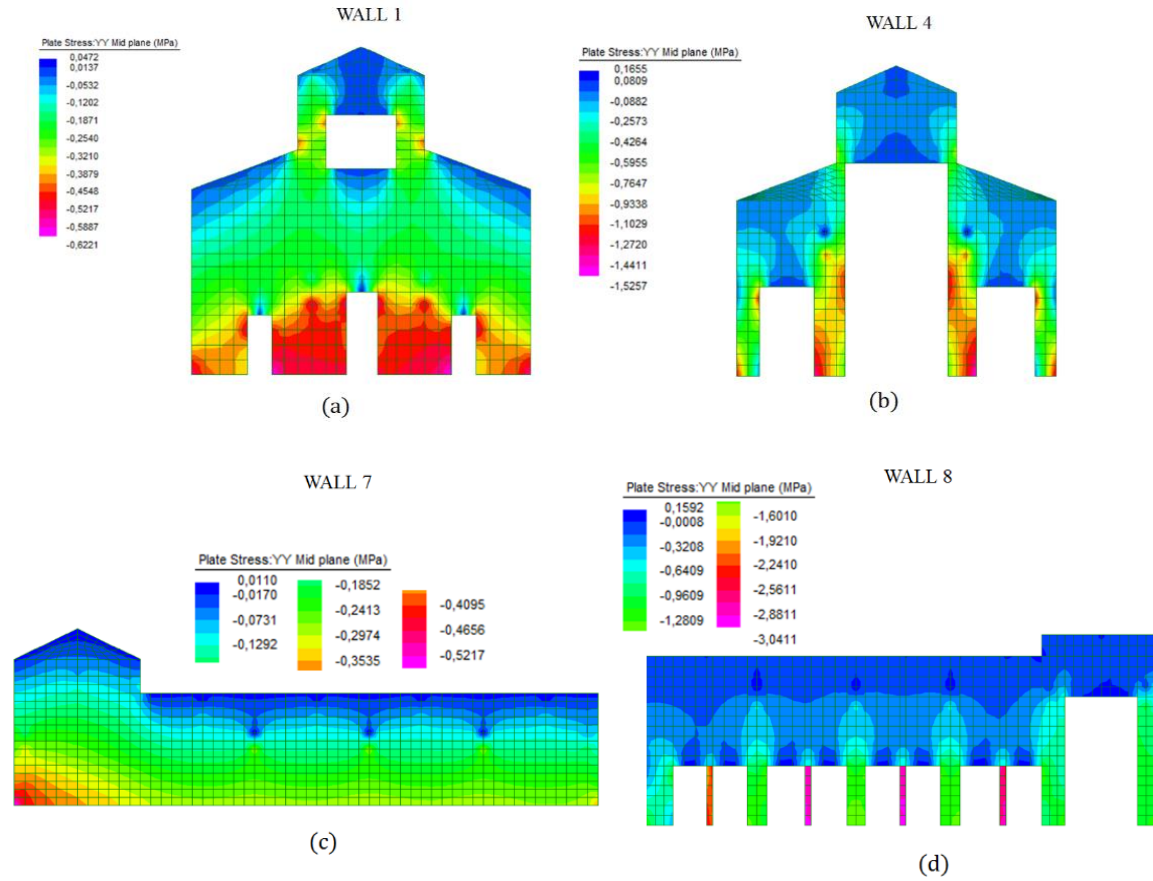


Figure 21: Contour maps of the normal stresses at the base of some walls obtained with two-dimensional FE models: (a) Wall 1; (b) Wall 4; (c) Wall 7; (d) Wall 8;

The 3D laser scanning showed significant inclinations of the longitudinal walls. Consequently, the walls are subjected to additional stresses due to the imperfect verticality. To account for this effect in a rather simplified way, the second order bending moments due to the eccentricity corresponding to the measured overhangs (Figure 22) have been included in the evaluation of the stresses. Figure 23 provides a schematic plan indicating the percentage increment of the normal stresses at the base of the walls and pillars due to their inclination (values are evaluated with reference to the hand-made models). The green color represents increments below 30%, the yellow color represents increments between 30% and 70%, while the red color represents increments larger than 70%. The ranges of the normal stresses at the base of the masonry walls and pillars, including also the effect of walls inclinations, are provided in the plan schematization displayed in Figure 20. Maximum stresses are around 1.5 MPa for the masonry walls and 9 MPa for the stone pillars. All values are well below material strengths.

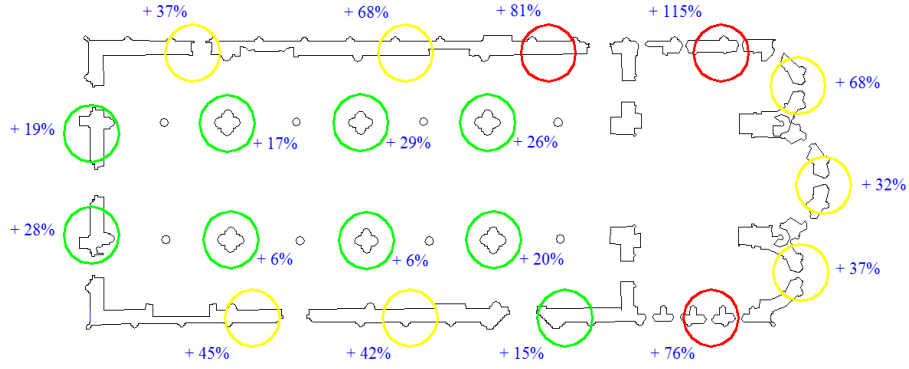


Figure 22: Increments of the stress at the base of the walls due to the inclination of the vertical elements.

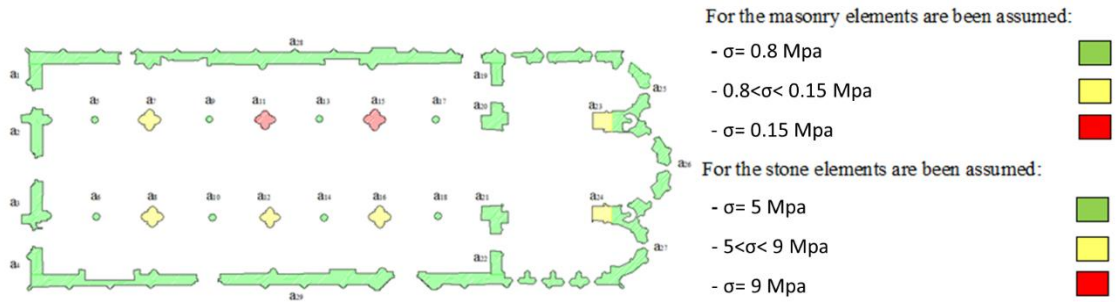


Figure 23: Level of stress at the base of the vertical elements including the effects of the inclinations

To simply evaluate how the presence of the arches in the transversal walls may contribute in the overall inclination of the wall, the thrusts of the arches have been calculated by assuming a simply supported arch schematization subjected to a uniform distributed load (due to the loads transmitted by the roof and the vaults). Then, the lateral forces corresponding to the calculated thrusts have been applied at the top of each corresponding wall in order to evaluate the lateral deflection, assuming a cantilever configuration and a tributary resisting wall width of 1.25 m, and thus neglecting the presence of the chains. The angle of inclination corresponding to the lateral deflection (with reference to the chord) has been compared with the measurements from the 3D laser scanning (Figure 24). It can be noted that the contribution due to the thrusts, in the case of not effective chains, is significant and, in the undisturbed areas (near the façade, where the interaction with the Ghirlandina Tower is weak and the soil is more uniform) is close to the measured one. Larger discrepancies appear in the areas closer to the Ghirlandina Tower where the interaction with the Tower is more relevant or where the chains could be more effective. It has to be noted that the choice of the tributary width significantly affects the estimation of the maximum out-of-plane deformations. A tributary length of 1.00 m can be considered as a lower bound, thus leading to conservative (i.e. reasonably larger) estimations.

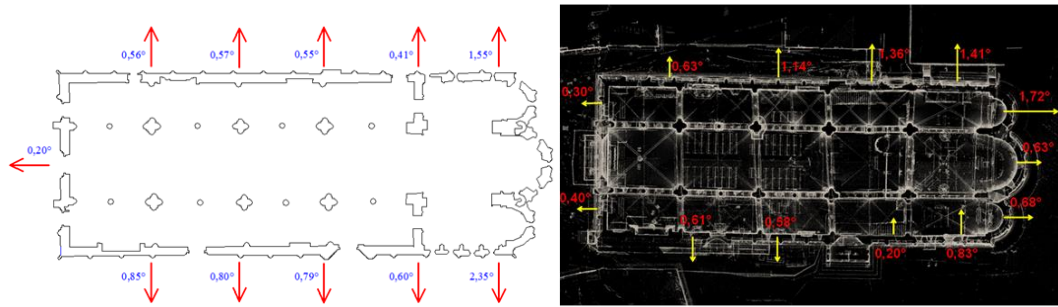


Figure 24: Comparison between the calculated inclinations due to only the lateral thrusts of the arches and those measured by 3D laser scanner

2.3.3 Structural analysis with 3D finite element models

Several 3D FE models have been developed to separately investigate, the effects of each single factor that could be influence the structural response of the cathedral. Once the importance of each single effect has been quantified, a unique 3D FE model has been developed in order to account for the interaction of all effects. All the models have been developed assuming: (i) homogeneous and elastic material characterized by the properties summarized §10.3.3; (ii) full cross-section masonry walls; (ii) average value of the thickness for each wall; (iii) architectural elements are not included in the model; (iv) the roof system and the vaults are not directly modeled and considered only in terms of applied vertical loads (in this respect, note that, on the contrary, the masonry arches both in the longitudinal and in transversal directions have been directly modeled). In more detail, the following types of restraints at the base have been considered to progressively investigate the soil-structure interaction:

- Fixed-base condition (F): the soil is assumed to be infinitely stiff in both vertical and horizontal directions;
- Roller-type base supports (R): the soil is assumed to be rigid in the vertical direction and with negligible lateral stiffness;
- Winkler type 1 base supports (W1): all the foundation soil is assumed to have a unique constant vertical stiffness (i.e. Winkler spring constant equal to $K \times B = 2.6 \text{ MPa}$ as displayed in **Errore. L'origine riferimento non è stata trovata.**(a), with B equal to the wall thickness); the lateral stiffness is assumed to be proportional to the applied axial load up to an horizontal displacement equal to 4 mm (i.e. a non-linear spring characterized by an elastic-perfectly plastic behavior has been assumed, as shown in Figure 25);
- Winkler type 2 base supports (W2): two different vertical stiffness values are used to account for the presence of the ancient Cathedral of the XI century (i.e. Winkler spring constants equal

to $K_{xB}=2.6$ MPa and $K_{xB}=13$ MPa as displayed in **Errore. L'origine riferimento non è stata trovata.**(b); the same non-linear horizontal springs adopted in the W1 type supports have been used.

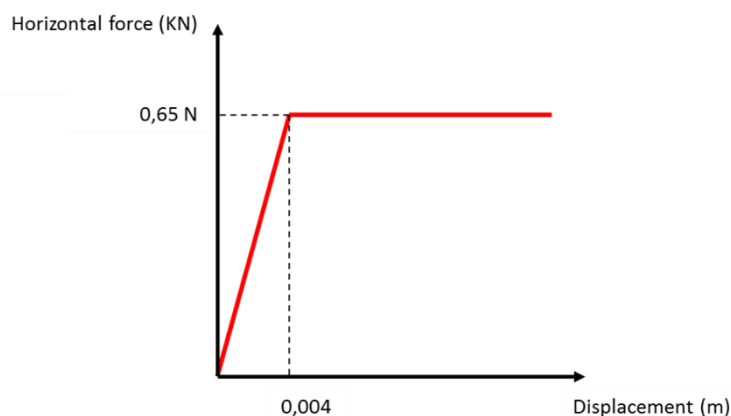


Figure 25: Elastic-perfectly plastic behaviour of the soil

Two geometrical configurations have been developed:

- Undamaged configuration (UD-C);
- Cracked configuration (C-C).

In the C-C configuration, the walls are characterized by discontinuities, which represent the main existing cracks as obtained from the in-situ inspections §1.1.4.

The response to the following single load cases have been evaluated for all models:

- Vertical loads (V);
- Thermal effects (T);
- Imposed differential Displacements (D) at the base representing the interaction between the Cathedral and the Ghirlandina Tower.

As above explained, the separate analyses of each single load case and the successive combination of these elementary contributions allow a more in-depth interpretation of the possible causes of the main cracks. Table 4 summarizes the different models, constraints imposed at the base and the different load cases used to perform the static analyses. For instance, in order to better clarify the nomenclature introduced in Table 4, the response of the undamaged configuration with the fixed based condition subjected to vertical loads will be referred to as UD-C+F+V.

First, a brief overview of the most relevant aspects of the single models is presented. Then, the most relevant results of the more representative models are reported. As expected, the restraints at the base

which better allow to simulate the actual behaviour of the Cathedral (i.e. to provide the most reasonable justification of the main cracks detected with the survey) is the one referred to as W2. In general, the models, which account for the initial presence of the main cracks does not lead to significant discrepancies in terms of maximum stresses. Therefore, in the following the attention will be focused on the W2 restraint and on the UD-C configuration.

Table 4- Summary of the specific models with a specific restraint and a specific load cases provide a specific response developed.

Model and Base Restraints	Model Response			
	Vertical loads (V)	Thermal stresses (T)	Imposed disp. (D)	Combination (C = V+T+D)
UD-C + F	UD-C + F+ V	UD-C + F +T	UD-C + F+ D	UD-C + F+ C
UD-C + R	UD-C + R +V	UD-C + R +T	UD-C + R +D	UD-C + R +C
UD-C + W1	UD-C + W1 +V	UD-C + W1 +T	UD-C + W1 +D	UD-C + W1 +C
UD-C W2	UD-C + W2 +V	UD-C + W2	UD-C + W2 +D	UD-C + W2 +C
C-C + F	C-C + F+ V	C-C + F+ T	C-C + F+ D	C-C + F+ C
C-C + R	C-C + R +V	C-C + R +T	C-C + R +D	C-C + R +C
C-C + W1	C-C + W1 +V	C-C + W1 +T	C-C + W1 +D	C-C + W1 +C
C-C W2	C-C + W2 +V	C-C + W2	C-C + W2 +D	C-C + W2 +C

The stress state for a specific longitudinal wall and transversal wall as obtained from the UD-C + W2 considering all single load cases is summarized in Figure 26 and Figure 27. It can be noted that the locations of the peaks of the tensile stresses are in good agreement with the location of the main cracks.

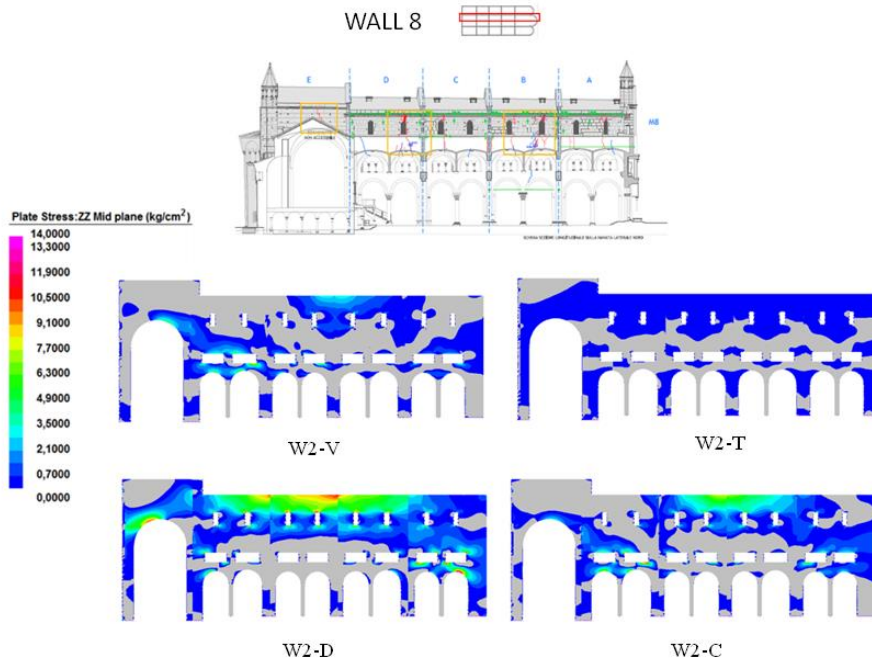


Figure 26: Stress of Wall 8 obtained from the W2 model with the different load cases and compared with the observed cracking patterns.

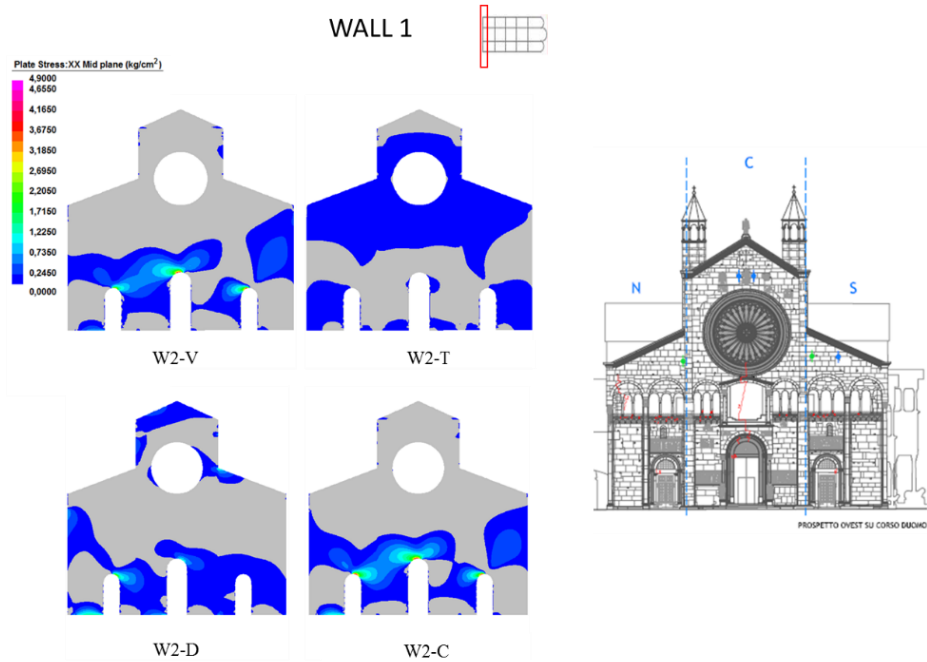


Figure 27: Stress of Wall 1 obtained from the W2 model with the different load cases and compared with the observed cracking patterns.

The in-plane and out-of-plane deformed shapes of a specific longitudinal wall are represented in and compared with the results of the 3D laser scanning. The deformed shapes are qualitatively consistent with the 3D laser scanning indicating that:

- the presence of the ancient ruins of the pre-existing churches reduces the vertical deformations in proximity of the facade (as indicated in Figure 28);
- the interaction between the Cathedral and the Ghirlandina Tower causes significant out-of-plane displacements (Figure 28) of the longitudinal walls, especially for those walls closer to the Tower.

Nonetheless, the maximum out-of-plane wall deformations leads to maximum out-of-plane inclinations of about 0.5° , thus smaller than those obtained from the 3D laser scanner and also from the simple hand calculations (see Figure 24). This can be explained by considering that in the FE models the entire inertia of the global wall as inserted in the whole structural context is considered. In summary, a sketch which schematically shows the main deformations is represented in Figure 29: (a) out-of-plane deformation of the longitudinal walls, (b) global inclination towards the Ghirlandina Tower due to differential soil settlements, which is contrasted by (c) the reactions of the masonry arches which link the Cathedral and the Tower.

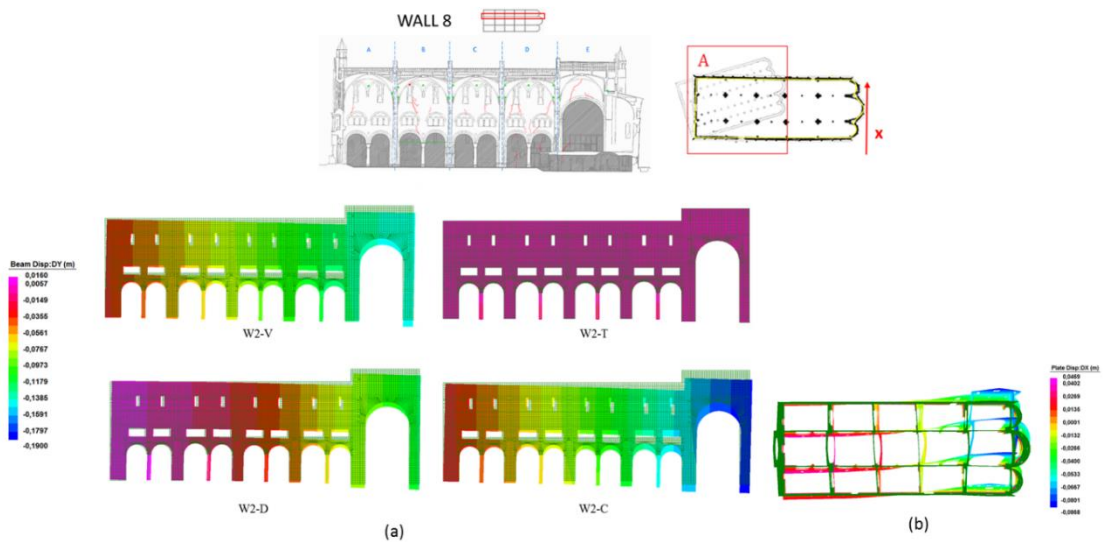


Figure 28: (a) in-plane deformed shape for Wall 8; (b) out-of-plane deformed shape (x direction) for all walls.

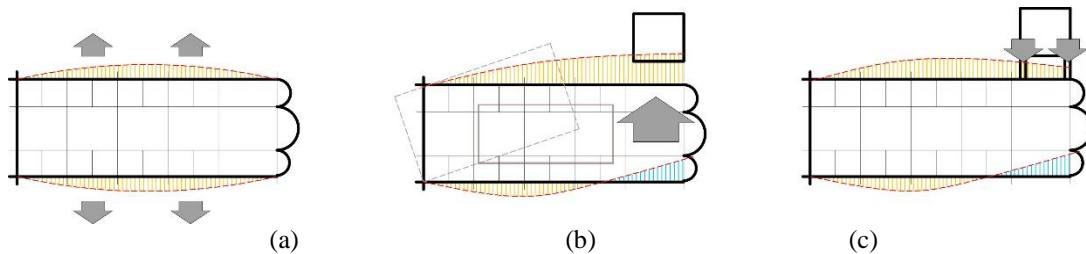


Figure 29: Sketch of the main global movements of the Cathedral as reconstructed by integrating the surveys with the results of the structural analyses.

2.4 Seismic Vulnerability analyses

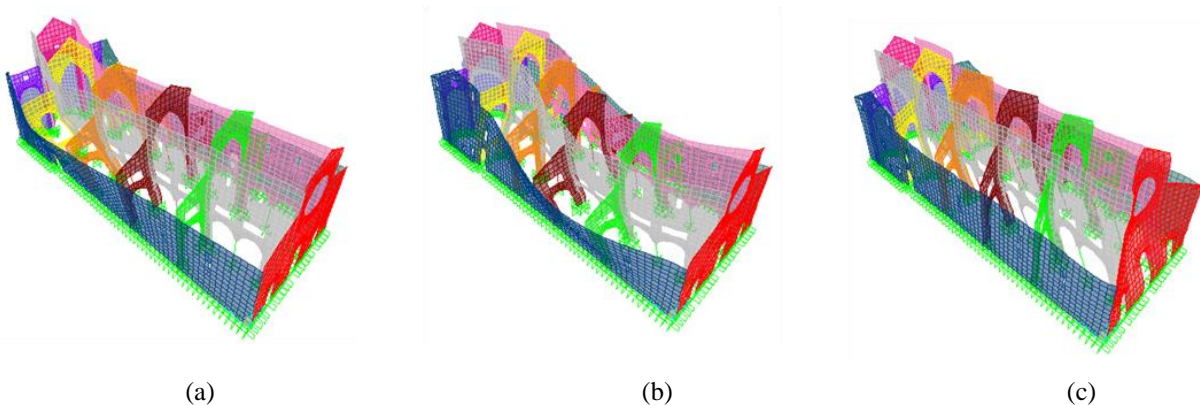
First, the dynamic properties of the monument (natural periods and mode shapes) have been identified through a natural frequency analysis performed on the 3D finite element model which was considered the more representative of the structure, as identified in the previously section. Then, the seismic behaviour of the whole structure have been investigated considering that the seismic response of the cathedral can involve mainly two types of mechanisms:

- in-plane mechanisms and
- out-of-plane mechanisms.

Finally, time history analyses on the 3D finite element models, considering as input the acceleration recorded during the 2012 earthquake §1.3, have been developed to identify the displacements/shearing deformation at the top of the walls and piers (springings of the vaults).

2.4.1 Natural frequency analysis

Since the stress-strain constitutive of masonry structures is yet non-linear for small values of deformation, the reliability of the modes of vibration is to be taken with caution. The common design codes, such as the Italian D.M. 14/01/2008 [31], prescribe that the participating mass must exceed 85%; therefore, in the consecutive seismic analyses 20 mode shapes have been considered in order to satisfy this requirement. The fundamental periods are in the range of 0.25-0.35 s. **Errore. L'origine riferimento non è stata trovata.** shows the first five mode shapes. This analysis shows that the first mode shape is characterized by a translation in the transverse direction of the Cathedral more pronounced in the area of the heavy apses than the area of the nave and the facade. The third mode shape is characterized by a translation along the longitudinal direction.



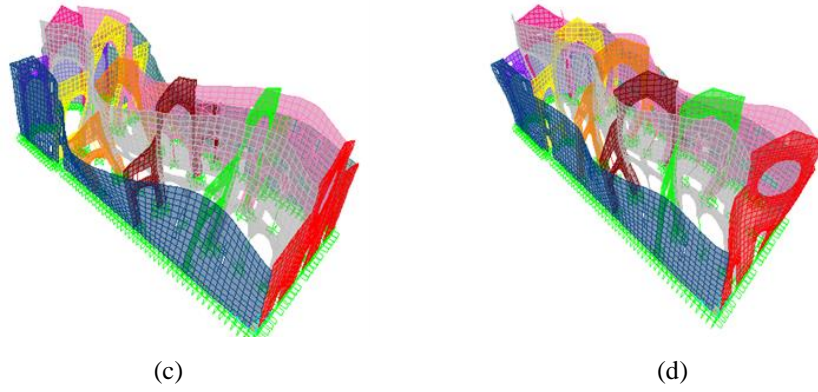


Figure 30 : Mode shapes; (a) T=0.35 sec ;(b) T=0,31sec;(c) T=0,28sec;(d) T=0,28sec; (e) T=0,26sec

2.4.2 Global seismic response

Response spectrum and time history analysis have been performed on the 3D finite element model (called UD-C + W2). The analysis have been devoted to the identification of the criticalities in terms of:

- in-plane mechanisms caused by high shear force (causing possible diagonal cracks or horizontal sliding);
- out-of-plane mechanisms caused by high eccentricity, defined as the ratio between the bending moment and the axial force (causing possible stress concentration at the base or overturning of the wall).

The study of the in-plane mechanisms has been conducted by evaluating the tensile stresses in the walls (diagonal cracking check) and the shear stresses at the base of the walls (sliding check). Figure 31 shows the comparison between the tensile stresses and the cracking patterns for the wall 1 (façade wall). In general, the results obtained from tensile stresses show a high validation with the cracking patterns. The majority of the lesions seems to be caused by the accumulation of damage over time caused by various earthquakes. The sliding check at the base is performed as follows:

$$\tau < \tau_{di} \quad (2.1)$$

where

τ is the tangential mean stress and τ_{di} is the shear strength of the masonry, as evaluated according the two diagonal cracking and (friction) sliding mechanisms:

$$\tau_{di} = \tau_{od} \sqrt{1 + \frac{\sigma_{oi}}{1,5\tau_{od}}} \quad (2.2)$$

$$\tau_{di} = \tau_{od} + 0,4\sigma_{oi} \quad (2.3)$$

where:

τ_{od} = shear strength of the masonry (τ_{od} =1kg/cm²);

σ_{oi} = mean compressive stress.

Figure 32 shows the tangential stresses calculated for wall 1 and Table 5 - Verification of the shear strength for the wall 1 reports the values obtained for the sliding check. Figure 33: Sliding check for all the walls of the cathedral: (a) transversal walls and (b) longitudinal walls summarizes the results obtained for all the walls of the cathedral and highlights that the greatest criticalities are related to the in the internal transversal walls.

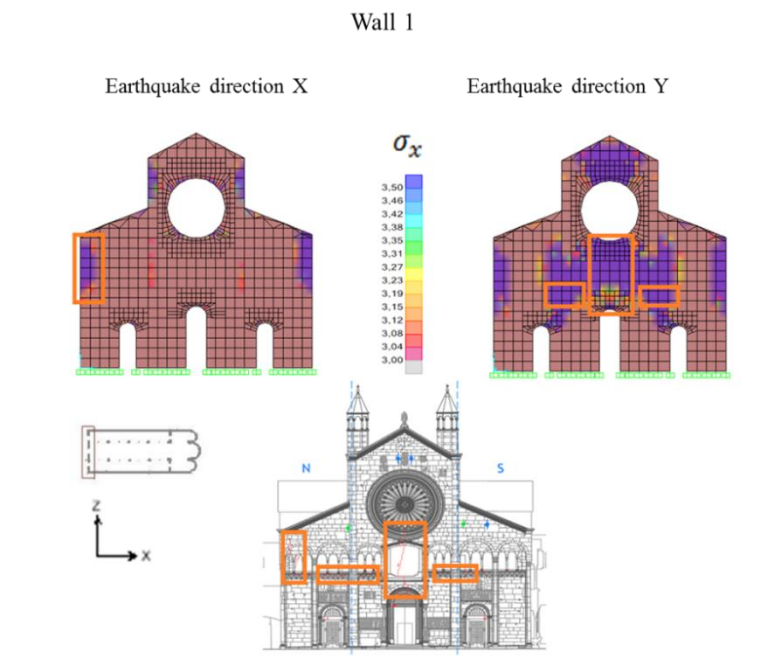


Figure 31: Comparison between tensile stresses and the cracking patterns

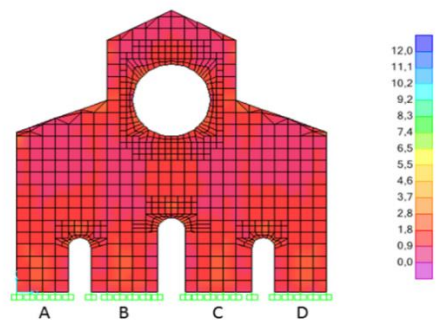


Figure 32: Tangential stresses
Table 5 - Verification of the shear strength for the wall 1

	Compressive mean stress	Shear strength	Shear strength	Tangential mean stress	Demand/ Capacity ratio	Demand/ Capacity ratio
		Eq. (2.2)	Eq. (2.3)	(Demand)	Eq. (2.2)	Eq. (2.3)
	[Kg/cm ²]	[Kg/cm ²]	[Kg/cm ²]	[Kg/cm ²]	[]	[]

Section cut 1A	6.95	2.37	3.78	1.25	0.53	0.33
Section cut 1B	4.66	2.03	2.86	1.36	0.67	0.47
Section cut 1C	4.66	2.03	2.87	1.37	0.68	0.48
Section cut 1D	7.06	2.39	3.82	1.25	0.52	0.33

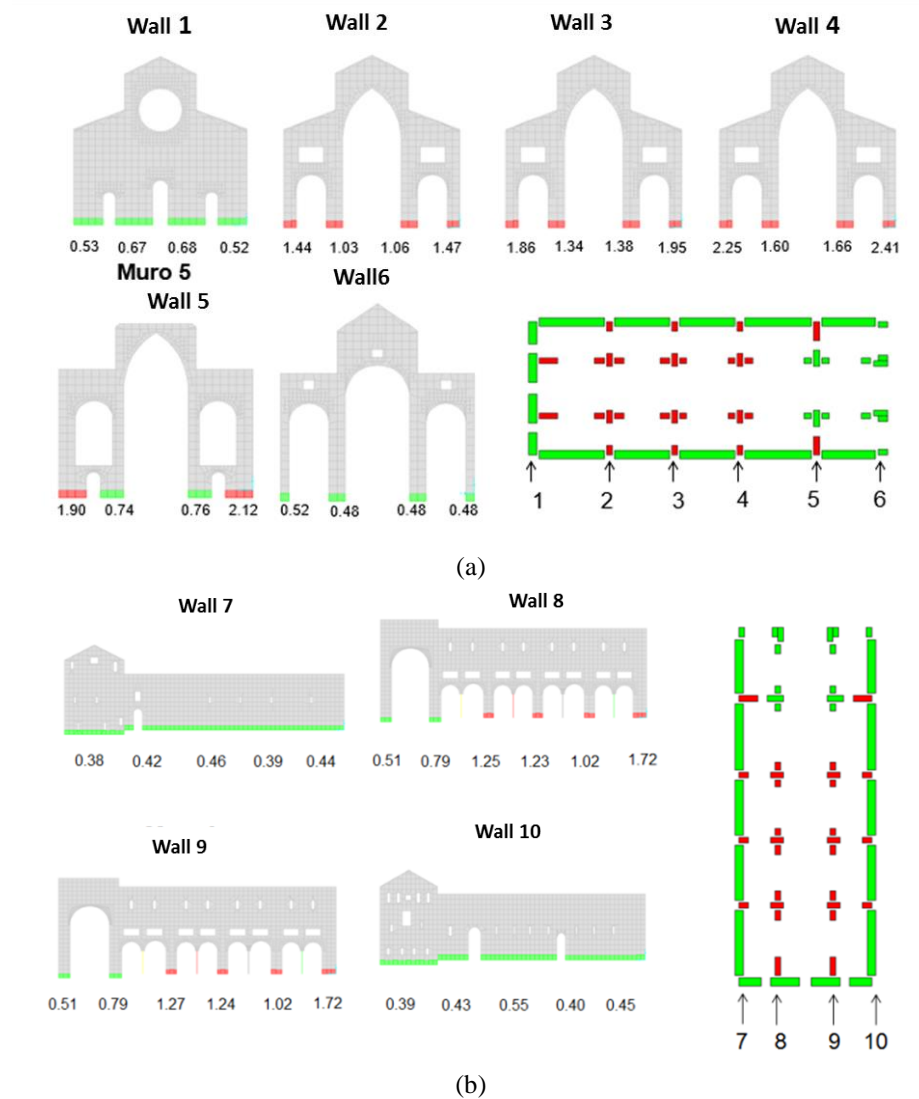


Figure 33: Sliding check for all the walls of the cathedral: (a) transversal walls and (b) longitudinal walls

Out-of-plane mechanisms have been identified by first evaluating the eccentricity at the base of the walls, as defined as the ratio between the bending moment and the axial force in seismic conditions, and then checking that:

- the eccentricity is below the usual reference values $s/6$ and $s/2$ (with s indicating the thickness of the wall) and

- the lateral shear stresses developed on the two vertical lateral sides of the considered wall are below some reference values (i.e. connection capacity).

In detail, the eccentricity at the base of each wall has been calculated by considering both the static loads (self weight and dead loads) and the seismic actions (that, in the case of a dynamic time-history analysis, are function of time) for each section (Figure 34):

$$e(t) = \frac{M_{static} + M_{seismic}(t)}{N_{static} + N_{seismic}(t)} \quad (2.4)$$

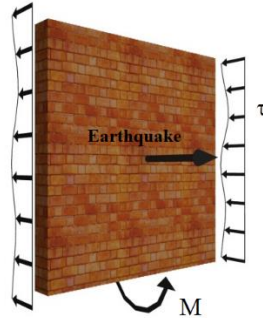
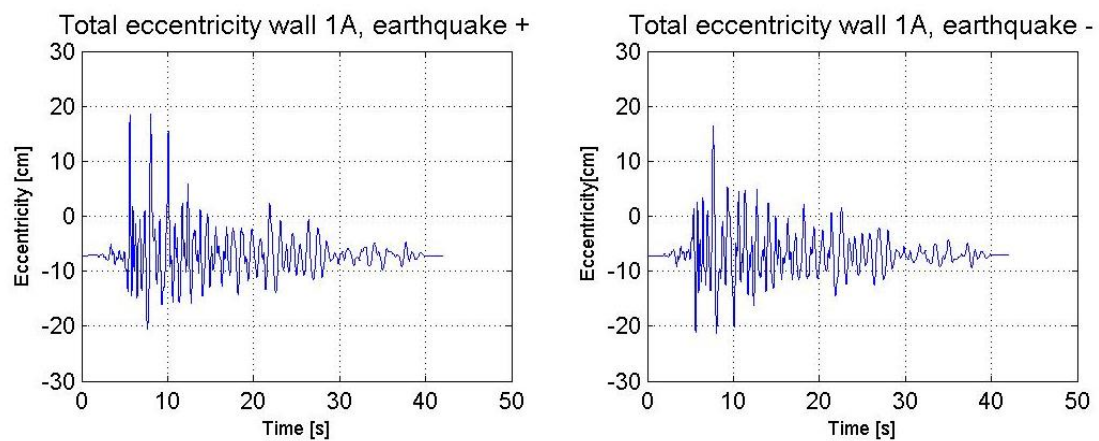


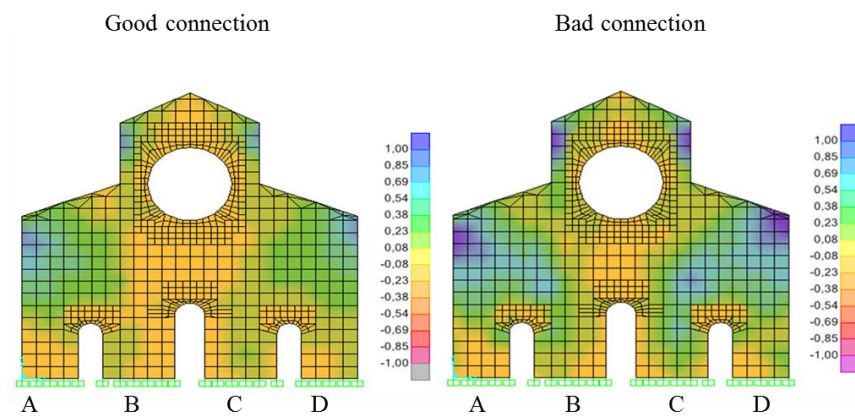
Figure 34: A schematic representation of a single wall with the indication of the out-of-plane seismic action, the base moment and the transversal actions due to the interaction between the orthogonal walls

The time history of the eccentricity has then been evaluated using 9 recorded accelerograms (selected from the P.E.E.R. strong motion database) consistent with the results of the seismic hazard analyses §1.3. Then the maximum absolute eccentricities have been used to check the out of plane stability of the walls. Two limit cases regarding the quality of the connection between orthogonal walls have been considered to compute the eccentricities: good connections (perfect continuity between orthogonal walls) and bad connections (partial continuity between orthogonal walls, modelled by inserting more flexible elements). Figure 35 a shows the time history of the eccentricity for the 1A section of the wall 1 whereas Figure 35 b shows the shear stresses, exchanged between the considered and the adjacent walls, obtained from the time history analysis for the wall 1. Table 6 shows the values of the eccentricity calculated for the various sections of the wall 1 and verify that these values are lower than $s/2$. Figure 36 provides a summary of the results obtained for all the walls of the cathedral. It can be noticed that, the study of the out of plane collapse mechanisms showed criticality in the transversal walls especially in the control sections B-C. However, the values of the shear stresses for each wall suggest that, even leading to cracked conditions at the base of the walls, the connections are able to keep the wall in a stable configuration. In two longitudinal walls, instead, the results indicate both cracked conditions at the base and values of shear stresses greater than the shear strength of the masonry in the absence of vertical loads.



(a)

Wall 1, thickness $s = 145$ cm



(b)

Figure 35: (a) The time history of the eccentricity on the 1A section (b) Tangential stresses for the wall 1

Table 6- Verification of the eccentricity for the wall 1

	Good connection	Bad connection		Good connection	Bad connection	Central core of inertia	$s/2$
	Mean + [cm]	Mean + [cm]		Mean – [cm]	Mean – [cm]	[cm]	[cm]
Section cut 1A	50,10	120,04		-26,15	-51,02	24,17	72,5
Section cut 1B	1183,40	412,82		-28,70	-99,75	24,17	72,5
Section cut 1C	1386,93	470,64		-28,60	-102,97	24,17	72,5
Section cut 1D	57,03	151,55		-26,20	-53,51	24,17	72,5

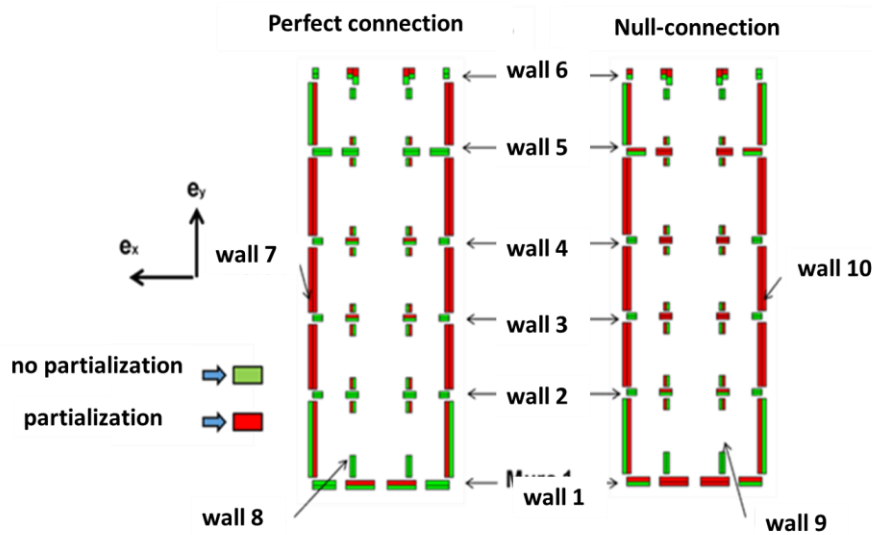


Figure 36: Vulnerability for the out-of-plane mechanisms in the walls

2.4.3 Time history analyses: input the main shock recorded by the station of Modena

Time history analyses on the 3D FEM model of the Cathedral, has been developed to identify the displacements/shearing deformation at the springings of the vaults (top of the walls and piers). The input considered in the analyses is the acceleration recorded by the station close to Modena (MDN) during the 2012 Emilia earthquake (with a pick ground acceleration around 0.04g). The main purpose of these analyses is the assessment of the correlation between the displacements of the springings of the vaults, due to the vibration of the underneath structures, and the damages detected. Figure 37 shows the nomenclature used for the vaults of the cathedral and the displacements that can interest the vaults (shearing displacement referred to VNC1 and widening referred to VNC3). Table 7 and Table 8 collect the displacements (widening and closing) and the shear displacement at the springings of the central and lateral vaults. It can be noticed that during the 2012 Emilia earthquake the springings of the vaults of the cathedral suffered shear imposed displacement lower than 1 cm and negligible widening and closing displacements.

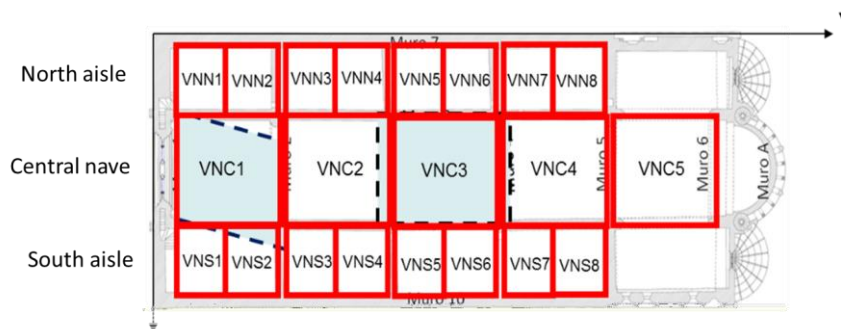


Figure 37: The nomenclature of the vaults of the cathedral

Table 7- The displacement at the springings of the central vaults as obtained from the time history analyses

Central Vault	Displacement [cm]	Shear Displacement[cm]
VNC1	0.014	0.43
VNC2	0.020	0.39
VNC3	0.03	0.39
VNC4	0.03	0.48
VNC5	0.037	0.43

Table 8- The displacement at the springings of the lateral vaults as obtained from the time history analyses

Lateral Vault	Displacement [cm]	Shear Displacement [cm]
VNN1-S1	0.014	0.43
VNN2-S2	0.020	0.39
VNN3-S3	0.03	0.39
VNN4-S4	0.03	0.48
VNN5-S5	0.037	0.43
VNN6-S6	0.014	0.43
VNN7-S7	0.020	0.39
VNN8-S8	0.03	0.39

The results obtained in terms of shear displacement are compared with the survey of the damage observed after the 2012 earthquakes (Figure 38). It can be noticed that generally the vaults mainly damaged correspond at the vaults that suffered the major shear displacement at the springings due to the vibration of the underneath walls and piers.

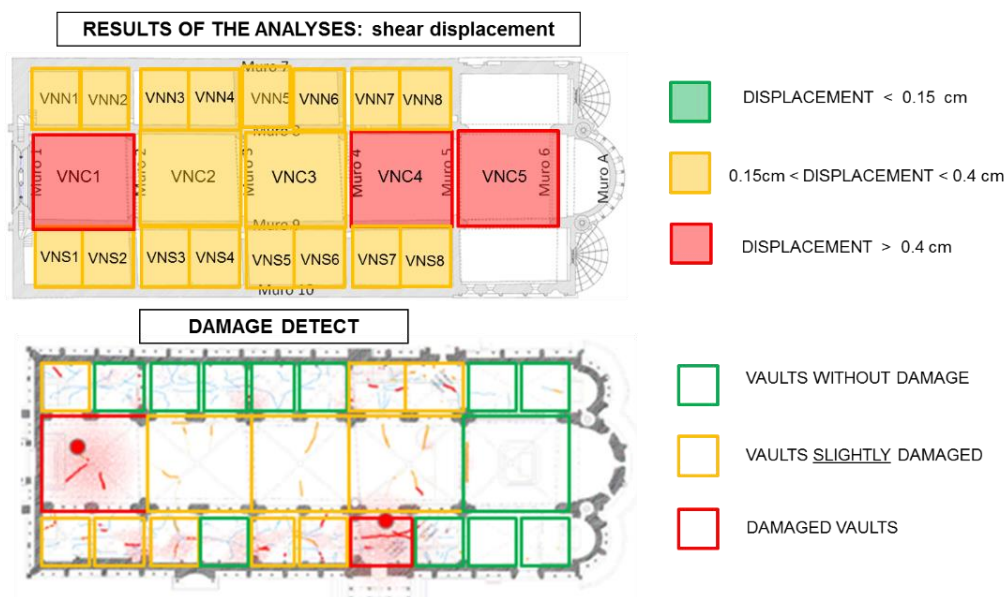


Figure 38: The comparison between the shear displacements and the damage detected on the vaults after the 2012 earthquake

2.5 The main vulnerabilities and conclusions

Starting from the knowledge acquired by the multi-disciplinary approach, the structural behaviour of the Cathedral has been investigated in order to identify the more vulnerable elements of the building. The multi-analyses method which aims at integrate the results obtained by different models, (characterized by different level of accuracy according to typology of problems to be investigated) appears fundamental in order to obtain a consistent assessment of the structural behaviour of the monuments.

The results of the static analyses reveals that the different soil stiffness at the base of the cathedral strongly influence its structural behaviour. Indeed, the model, which considers the soil-structure interaction, is able to provide with more accuracy a state stress congruent with the cracks pattern detected.

Moreover, from the static analyses it can be recognized that the main vulnerabilities are:

- the tendency of the longitudinal perimeter walls to develop out-of-plane movements, as revealed by the 3D laser scanner, probably due to the unconstrained thrusts of the arches and differential settlements;
- the overall rotation movement towards the Ghirlandina Tower, caused by the strong interaction between the Cathedral and the Tower, that promotes differential soil settlements (note that the portion of the apses is significantly heavier than the other portions);
- the concentration of cracks and peaks of the tensile stresses in the portion coinciding with the location of the old Cathedrals.

The results of the seismic analyses reveal vulnerabilities of the perimeter walls with respect to out-of-plane overturning. These numerical results have been confirmed by the experimental evidences of the damages observed after the recent 2012 Emilia Romagna earthquake sequence.

3 Local structural analyses

3.1 Introduction

The seismic performances of historical masonry buildings are closely related to the behaviour of each substructure. In general, the horizontal seismic forces cause damages and/or collapses mainly in the following specific elements: large space without structural walls, arches, vaults, domes, ... , which are common in the historical churches. The analysis of the main damages suffered by Italian churches due to the recent earthquakes (L'Aquila 2009, Emilia 2012, Umbria-Marche 2016) has shown a number of common collapse mechanisms, which may involve the local response of single structural elements [32], [30]. In particular, the information on damage location and extent, collected after these violent earthquakes, highlighted that, among all structural elements, the most vulnerable one are masonry vaults.

In this chapter, the local collapse mechanisms of the main substructures of the Cathedral have been studied. In addition, 3D Finite element models of the most damaged vaults, after the 2012 Emilia Romagna earthquake, have been developed in order to provide information on the stress and deformation state.

3.2 The models and the simulation

The local collapse mechanisms which aim at providing the value of the load that activates the failure mechanisms of each elements through kinematics models (both in-plane and out-of-plane mechanisms) have been evaluated for the single sub-elements of the cathedral. Then, the stress levels of vaults under dynamic excitation and displacement imposed at their springings have been investigated making use of 3D linear Finite element models. The analyses developed are summarized in Table 9.

Table 9- The different analyses developed

Model-Element	Analysis
Sub-elements: façade, nave, vaults, aisles...	local collapse mechanisms
3D FEM models of the vaults	Static analyses
3D FEM models of the vaults	Seismic analyses

3.3 Local collapse mechanisms

The local collapse mechanisms are strongly dependent on the construction techniques and on the connection details between orthogonal masonry walls and between the masonry walls and the possible

restraining horizontal elements, such as tie-beams, well connected floors, The cathedral has been divided into sub-elements, i.e. structural elements characterized by an autonomous structural behaviour: the façade, the nave, the aisles, the vaults, the longitudinal perimeter walls, the columns, the transept, the triumphal arch and the apses. For each one of these sub-elements, when applicable, out-of-plane mechanisms and in-plane mechanisms have been considered. As far as the out-of-plane mechanisms are concerned, the limit analysis approach has been applied. Each sub-element is assumed to be composed by a number of stiff, incompressible and infinitely-resistant blocks, and the limit load multiplication coefficient (λ) is calculated by means of equilibrium equations. Limit load is the maximum seismic horizontal load that the structure can safely carry. In general, the limit analysis of masonry structures involves the following assumptions [33]: (i) masonry has no tensile strength, (ii) stresses are so low that masonry has effectively an unlimited compressive strength, (iii) sliding failure does not occur. Here, only the calculations related to the evaluation of the limit load multiplication coefficient of the façade are entirely presented. The crack pattern shows lesions in the orthogonal longitudinal walls next to the facade Figure 39a) that suggest a good connection between these elements. However, three different hypotheses of connections are here considered : (1) good connection between orthogonal masonry walls , (ii) bad connection (negligible connection between orthogonal masonry walls) and (III) reasonable estimation of the connection. The following mechanisms have been taken into account:

- overturning of the whole façade (Figure 39b and Figure 40– mechanism 1);
- overturning of the left portion of the façade (Figure 40– mechanism 2);
- overturning of the central portion of the façade (Figure 40-mechanism 3);
- overturning of the right portion of the façade Figure 40– mechanism 4-5).

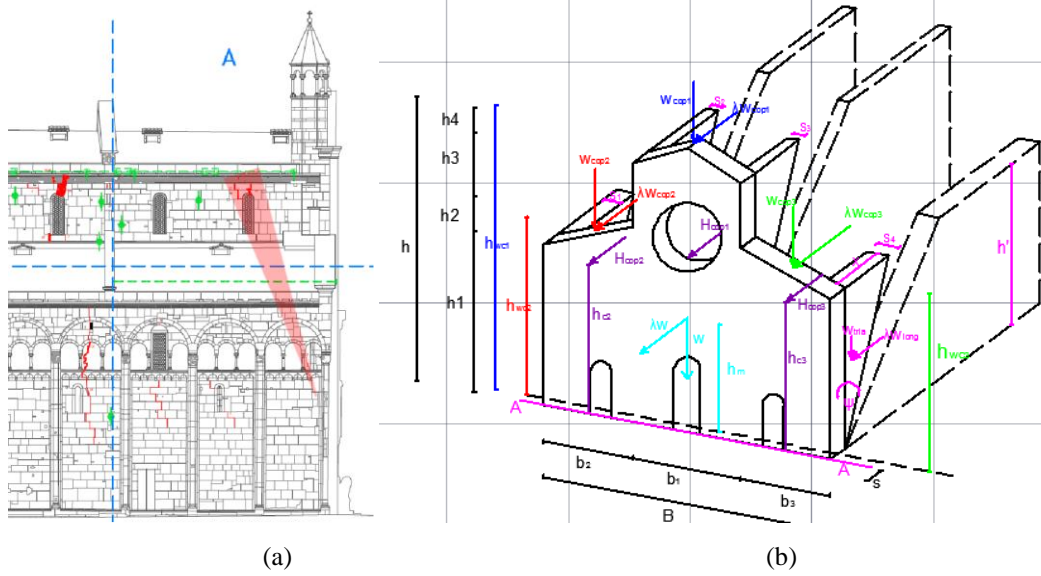


Figure 39: (a) Cracks in longitudinal walls of Cathedral, (b) Overturning of global facade around the base dashed straight line.

The behaviour of the wall in limit equilibrium conditions has been simulated by applying the principle of virtual works, i.e. equating the overturning moment (due to horizontal loads) and the stabilizing moment (due to self-weight):

$$M_{overturning} = M_{stabilizing}$$

$$\left[\left((W - W_{holes}) \cdot \frac{s}{2} + W_{cop} \cdot d_c - H_{cop1} \cdot h_c + W_{tria} \cdot \left(s + \frac{1}{3} x_i \right) \right) \right] -$$

$$-\lambda \cdot \left[W_{wall} \cdot h_m - W_{holes} \cdot h_f + W_{cop1} \cdot h_{wc1} + W_{long} \cdot \left(\frac{2}{3} \cdot h_i' \right) \right] = 0 \quad (3.1)$$

The limit load corresponding to the spectral acceleration that activates the local mechanism of collapse has been obtained from Equation 12.1.

$$\lambda = \frac{\left[(W - W_{holes}) \cdot \frac{s}{2} + W_{cop1} \cdot d_{c1} + W_{cop2} \cdot d_{c2} + W_{cop3} \cdot d_{c3} - H_{cop1} \cdot h_{c1} - H_{cop2} \cdot h_{c2} - H_{cop3} \cdot h_{c3} \right]}{\left[W_{wall} \cdot h_m - W_{holes} \cdot h_f + W_{cop1} \cdot h_{wc1} + W_{cop2} \cdot h_{wc2} + W_{cop3} \cdot h_{wc3} \right]} = 0,22 \quad (12.2)$$

$$a_0 = \lambda \cdot g = 0,22g \quad (12.3)$$

Figure 40 shows the acceleration values that activate overturning mechanisms of the different portions of the façade for the different connection considered. These values, also considering the good

connection, are higher than the acceleration reference values for the past earthquakes obtained from HDSHA §1.2.1 (0.15-0.20 g), but lower than the acceleration estimates for the possible future earthquakes obtained from MHEA §1.2.2 (0.50 g).

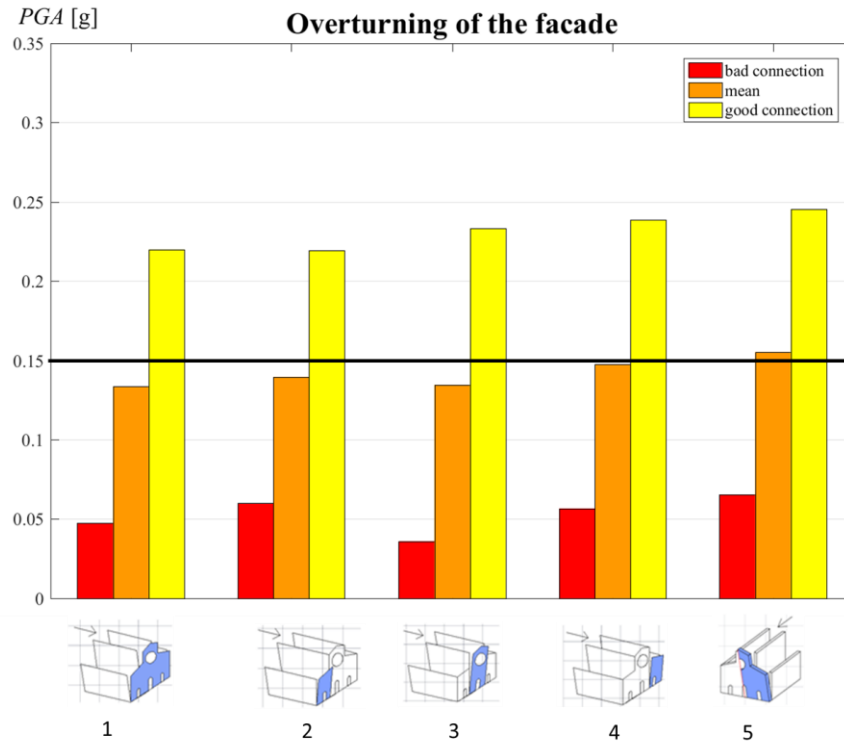
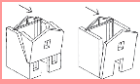




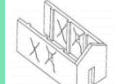
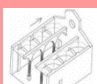
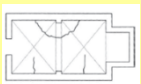
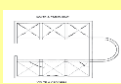


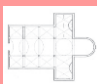

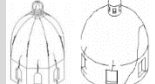
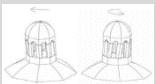








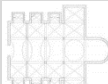






Figure 40: Comparison between the accelerations that activate the 4 mechanisms of collapse for the façade

The results obtained for the other substructures are summarized in Table 10. The acceleration that activates the failure mechanisms reported in Table 10 are referred to the most unfavourable condition of each elements (bad connections, more susceptible element).

In general, the study of the local mechanism of other sub-elements reveal that the main local vulnerabilities are relevant to the façade (as described above), the top façade (with trigger accelerations around 0.06 g), the cross vaults (with trigger accelerations around 0.12 g), the triumphal arch (0.07 g), the transversal response of the columns (0.14 g) and the out-of-plane behaviour of the apse walls (0.13 g).

Table 10-The acceleration that activates the failure mechanisms for each sub structures

<p>1. OVERTURNING OF THE FACADE</p>  <p>0.13 g</p>	<p>2.OVERTURNING TOP OF THR FACADE</p>  <p>0.06 g</p>	<p>3. IN OLANE MECHANISMS OF THE FACADE</p>  <p>0.33 g</p>	<p>4. PROTHYRUM</p> 	<p>5. TRANSVERSAL RESPONSE OF THE AULA</p>  <p>0.17 g</p>	<p>6. SHEAR IN THE LATERAL WALLS</p>  <p>0.31 g</p>	<p>7. LONGITUDINAL RESPONSE OF THE COLUMNS</p>  <p>0.14 g</p>
<p>8.VAULTS OF THE CENTRAL NAVE</p>  <p>0.19 g</p>	<p>9. VAULTS OF THE AISLES</p>  <p>0.21 g</p>	<p>10. OVERTURNING TRANPSET WALLS</p>  <p>0.13 g</p>	<p>11. SHEAR IN THE TRANSEPT</p>  <p>0.24 g</p>	<p>12. VAULTS OF THE TRANSEPT</p>  <p>0.12 g</p>	<p>13. TRIUMPHAL ARCHES</p>  <p>0.07 g</p>	<p>14. DOME</p> 
<p>15. LANTERNA</p> 	<p>16. OVERTURNING OF THE APSE</p>  <p>0.15 g</p>	<p>17. SHEAR MECHANISMS ON THE APSE</p>  <p>0.37 g</p>	<p>18. VAULTS OF THE APSE</p>  <p>0.34 g</p>	<p>19. ROOF SYSTEM</p> 	<p>20. ROOF OF THE TRANSEPT</p> 	<p>21. ROOF OF THE APSE</p> 
<p>22. OVERTURNING OF THE CHAPEL</p> 	<p>23. SHEAR MECHANISMS ON THE CHAPEL</p> 	<p>24. VAULTS OF THE CHAPEL</p> 	<p>25. PLAN AND HEIGHT IRREGULARITIES</p> 	<p>26. AGGETTI (PINNACLES)</p>  <p>0.21 g</p>	<p>27. BELL TOWER</p> 	<p>28. CELL BELL</p> 

a < 0.15 g
0.15g < a < 0.25 g
a > 0.25 g
<i>Not present, or static patterns insufficiently representative of reality</i>

3.4 The vault

The investigation of the structural behavior of the cross vaults under earthquake excitation is a fundamental issue in order to plan effective structural interventions. However, the evaluation of their seismic response is severely complex and depends on several factors, such as the three-dimensional geometry, the mechanical properties of the constituent materials and the behavior of the underneath vertical elements (lateral walls and piers) [34]. A vault under earthquake excitation is mainly subjected to two different phenomena (Figure 41):

- pseudo-static response of the vault to the relative displacements imposed at its springings, due to the horizontal movements of the underneath structures (walls and piers).
- dynamic response of the vault to the acceleration imposed at its springings due to the seismic vibration of the underneath structures (walls and piers);

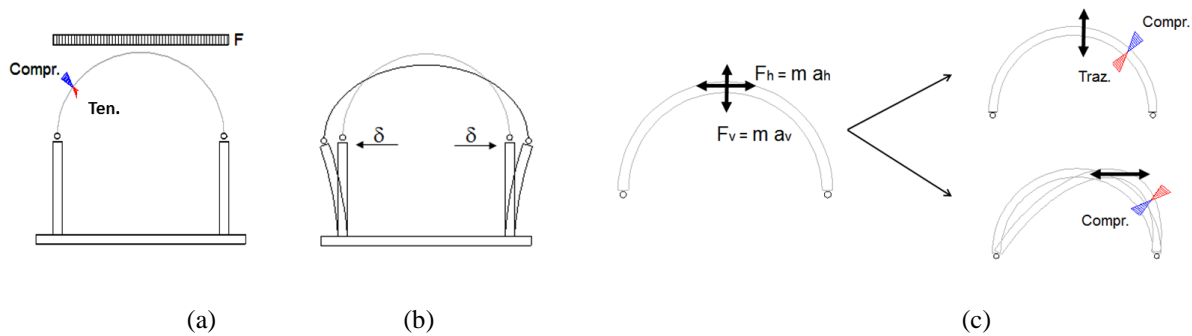


Figure 41: Schematization of the effects used for the assessment of the seismic response of the vaults: (a) vault undergo to vertical loads, (b) vault subject to imposed displacement at the springings and (c) vault under earthquake excitation

In this section the structural behavior of the vaults of the cathedral has been investigated. First, static analyses have been developed in order to identify the stress level due to the self-weight and displacement imposed at their springings (as obtained in §2.4.3). Then, linear time history analyses, using the acceleration recorded by the MDN station §1.3, have been performed.

3.4.1 3D FE models of the vaults

Static and dynamic analyses have been developed on the 3D FE models of the two most damaged vaults (VNC1 and VNS7) after the 2012 earthquake of the cathedral. The FE models reproduce the actual geometry of the groin vaults, which has been determined by means of laser scanning surveys, paying particular attention to the restraining given by the support and contrast elements (Figure 42). The information regarding the geometry of the two vaults are reported in Table 11. In the FE modelling the masonry is modelled as homogeneous continuum. For this reason, the FE models are not suitable to capture the expected failure modes but may give indications on the level of stress on

the vaults. High tensile stress resulting from static and dynamic loads are assumed to indicate cracking due to material failure.

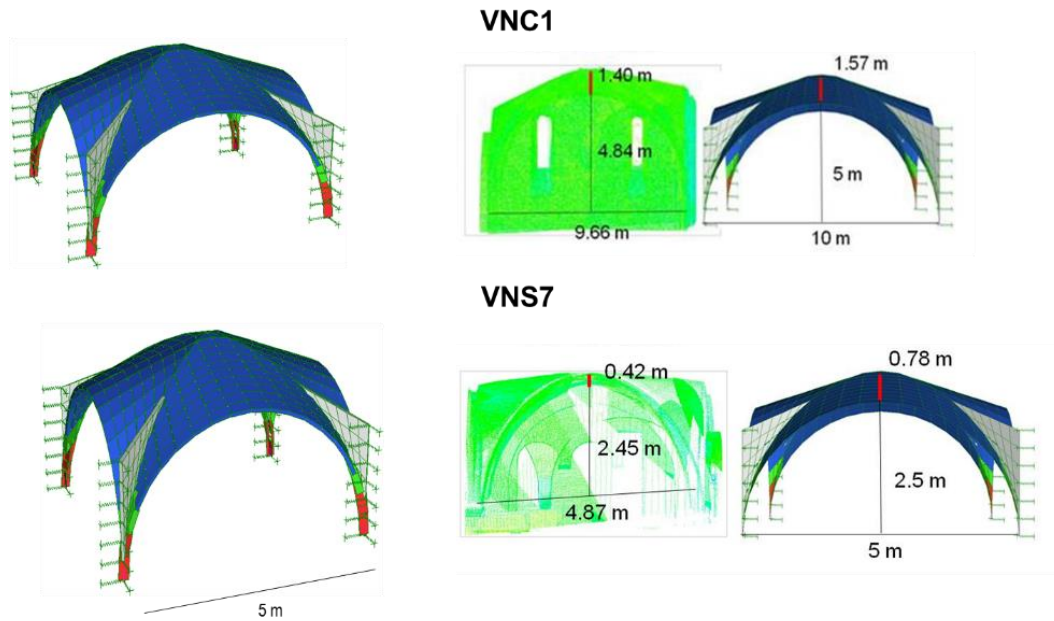


Figure 42: The actual geometry of the central and lateral vaults (VNC1 and VNS7) and the corresponding 3D FE models

Table 11: The geometry of the central and lateral vault of the cathedral

CENTRAL VAULT (VNC1)						
Base [m]	High [m]	Area [m ²]	Thickness [m]	γ [kg/m ³]	Weight [kN]	E [KPa]
9.1	10.2	211	0.12	1800	7.9	4144000
LATERAL VAULT (VNS7)						
Base [m]	High [m]	Area [m ²]	Thickness [m]	γ [kg/m ³]	Weight [kN]	E [KPa]
5.2	5.6	70	0.12	1800	150	4144000

Static analyses considering also imposed displacements at the springings of the vaults, as obtained by the time history analyses on the global model of the cathedral, have been conducted. The increment of the level of stress (both compression and tensile stress) due to the widening and closing displacements imposed at the springings are substantially irrelevant. On the other hand, however, the shear displacements imposed causes a not negligible increment of the tensile stress at the extrados of the vaults (it can reach $2/3 \text{ kg/cm}^2$), with particular concentrations along the diagonals. The maximum compressive stresses remain instead contained within limits compatible with the resistance of the materials characteristics (below 10 kg/cm^2) (Figure 43 and Figure 44).

VNC1: SELF-WEIGHT AND SHEAR DISPLACEMENT

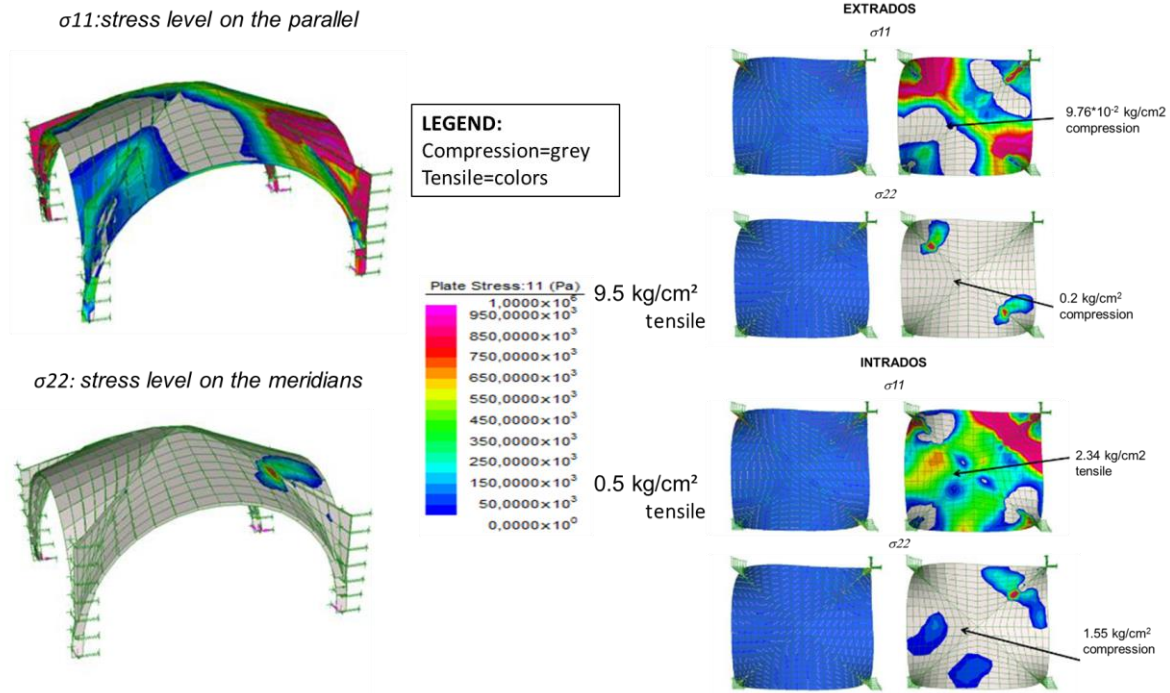


Figure 43: Stress levels of the vault VNC1 obtained from the static analyses considering the considering self- weight and the shear imposed displacements

VNN7: SELF-WEIGHT AND SHEAR DISPLACEMENT

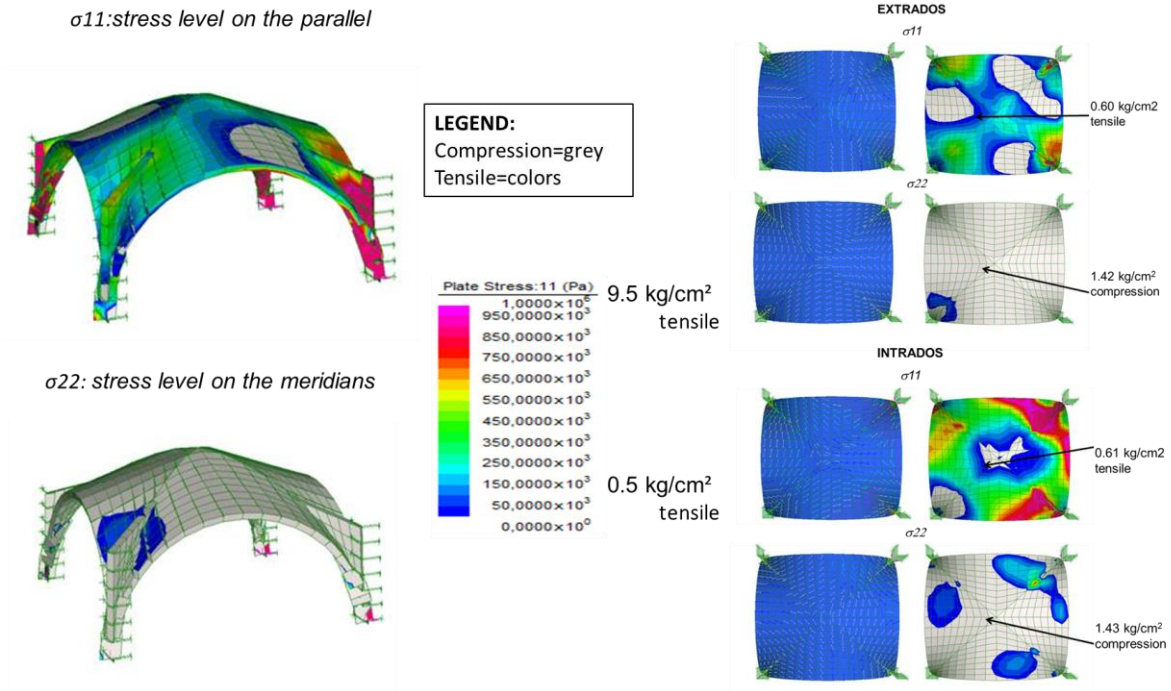


Figure 44: Stress levels of the vault VNN7 obtained from the static analyses considering the considering self- weight and the shear imposed displacements

Linear time history analyses on the 3D FE models of the vaults have been also developed applying as input the acceleration recorded by the station close to Modena during the 2012 earthquake. Figure 45 and Figure 46 display the stress level on the vault VNC1 and the vault VNN7 obtained from the dynamic analyses considering the self-weight and the seismic load. These analyses show that the effect of the dynamic response of the vaults is substantially comparable in terms of maximum tensile stresses to that induced by the shear displacements imposed at the springings.

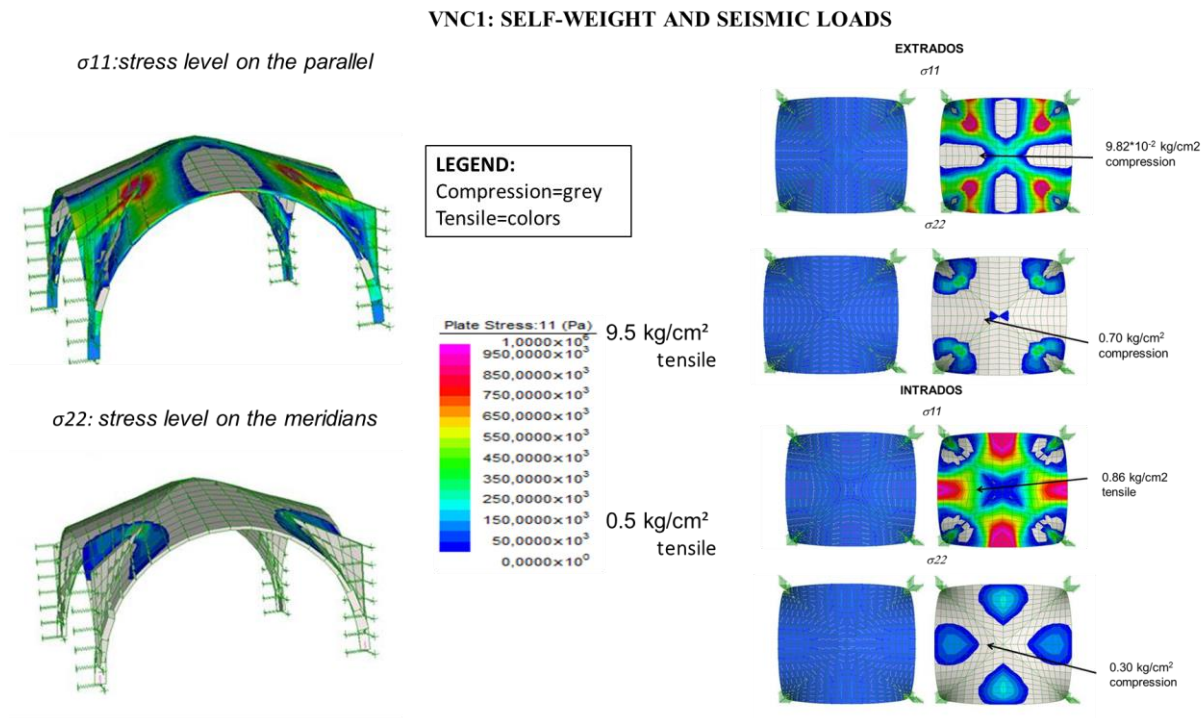


Figure 45: Stress levels of the vault VNC1 obtained from the dynamic analyses considering the considering self- weight and the seismic loads

VNN7: SELF-WEIGHT AND SEISMIC LOADS

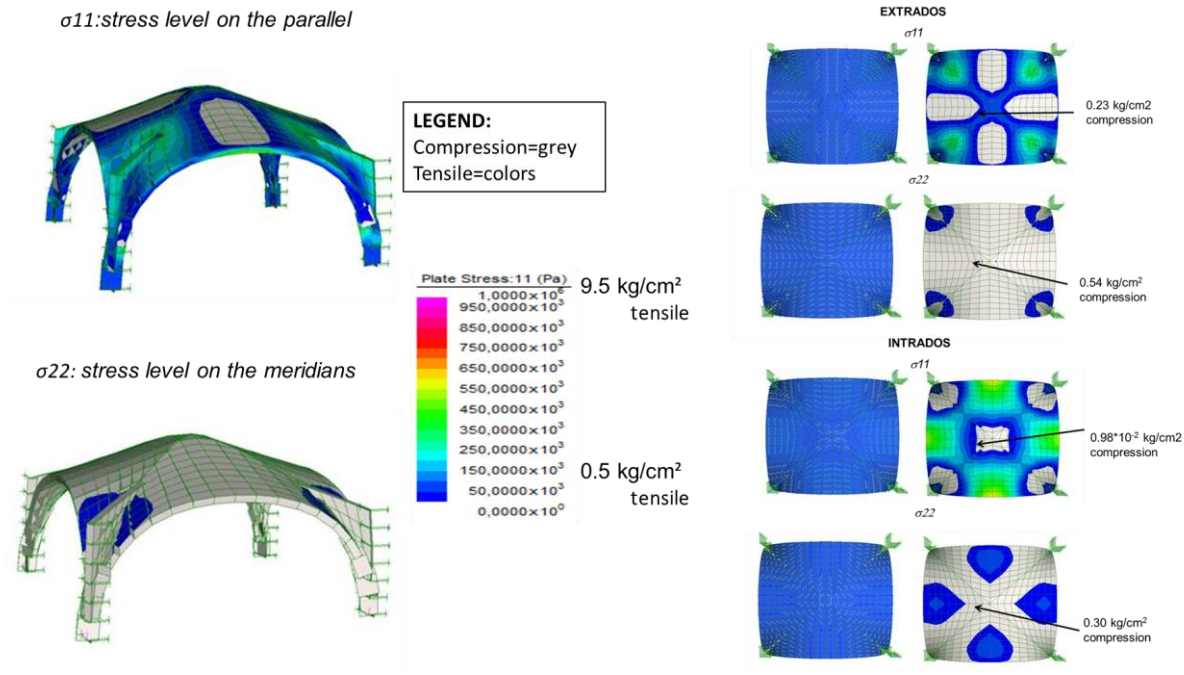


Figure 46: Stress levels of the vault VNN7 obtained from the dynamic analyses considering the considering self- weight and the seismic loads

3.5 Conclusions

The local collapse mechanisms allowed to identify the most vulnerable sub-structures of the cathedral of Modena. In detail, these analyses reveals that, considering a negligible connection between orthogonal masonry walls and between the masonry walls and the possible restraining horizontal elements (“bad connection”) the most vulnerable elements are:

- the top of the façade: the overturning could be occur for acceleration around 0.06g;
- the triumphal arch: the collapse could be occur for acceleration around 0.07g;
- cross vaults: the collapse could be occur for acceleration around 0.12g;
- the apse walls: the out-of-plane behaviour could be occur for acceleration around 0.13g;
- the façade: the overturning could be occur for acceleration around 0.13g;
- longitudinal response of the columns: the mechanism could be occur for acceleration around 0.14g;

It is noted that, considering a good connection, the local mechanisms of collapse for the elements analysed could be activated for highest acceleration values. For this reason, it seems essential to ensure good connection between the orthogonal walls through appropriate interventions.

The static and dynamic analyses developed on the 3D model of the two most damaged vaults, after the 2012 earthquake, reveal that:

- the increment of the stress level (both compression and tensile stress) because of the widening and closing displacements imposed at the springings due to the horizontal movements of the underneath structures (walls and piers). are substantially irrelevant;
- the increment of the stress level because of the shear displacements imposed at the springings due to the horizontal movements of the underneath structures are not negligible. The increment of the tensile stress at the extrados of the vaults can reach $2/3 \text{ kg/cm}^2$, with particular concentrations along the diagonals. The maximum compressive stresses remain instead contained within limits compatible with the resistance of the materials characteristics (below 10 kg / cm^2);

The increment of the stress level because of the acceleration imposed at the springings due to the seismic vibration of the underneath structures (walls and piers) are substantially comparable in terms of maximum tensile stresses to that induced by the shear displacements imposed.

4 Structural analyses via Discrete Element Method

In the light of the results obtained in the previous section, the cross section located in the fourth span from the west and characterized by different soil stiffness and absence of tie-rods appears the most vulnerable portion of the cathedral (Figure 47). This cross section has been investigated in order to evaluate the interactions between the vaults and the longitudinal walls under seismic loads.

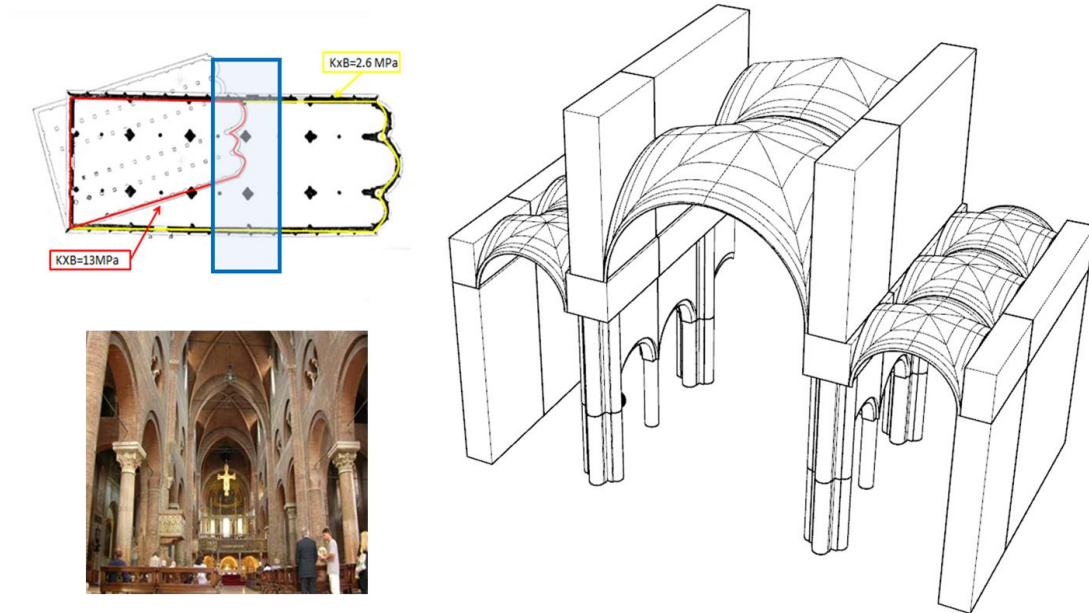


Figure 47: Position of the cross section studied

4.1.1 The model and the analyses

The cross section has been investigated through 2D models (where the density of the blocks and the stiffness at the interfaces takes into account the depth of 10 meters of the walls and of the vaults and the weight of the overlying non-structural elements) in order to evaluate the dynamic response of this portion of the Cathedral and the interaction between the vaults and the longitudinal walls. Figure 48 schematizes the structural elements of the portion of the Cathedral investigated. Two-limit schematizations have been considered in the analyses:

- (i) 2D cross section modelling the longitudinal walls, the vaults and also the transversal walls (hereinafter called “COMPLETE DEM” and represented in Figure 48b) and
- (ii) 2D cross section schematizing only the longitudinal walls and the vaults (hereinafter called “SIMPLIFIED DEM” and represented in Figure 48c). The transversal walls are here considered only as weight applied.

The COMPLETE DEM model is analyzed under static loads only, given the onerous computational time required to develop an earthquake time-history analysis. The main issue is to evaluate the detachment of the blocks (corresponding to the cracks openings) and compare them with the observed crack patterns. The SIMPLIFIED DEM model is analyzed under both static gravity loads and earthquake ground motion.

It has to be noted that the complete model is able to account for the lateral thrust exerted by the lower arches, which is not considered in the simplified model. Such a discrepancy may affect the lateral displacement induced by both vertical and horizontal loads.

In the case of dynamic analyses, after the application of the gravity loads, the ground motion recorded in Modena during the 2012 Emilia's earthquake is applied to blocks 9,10,11. The analyses developed are summarized in Table 12.

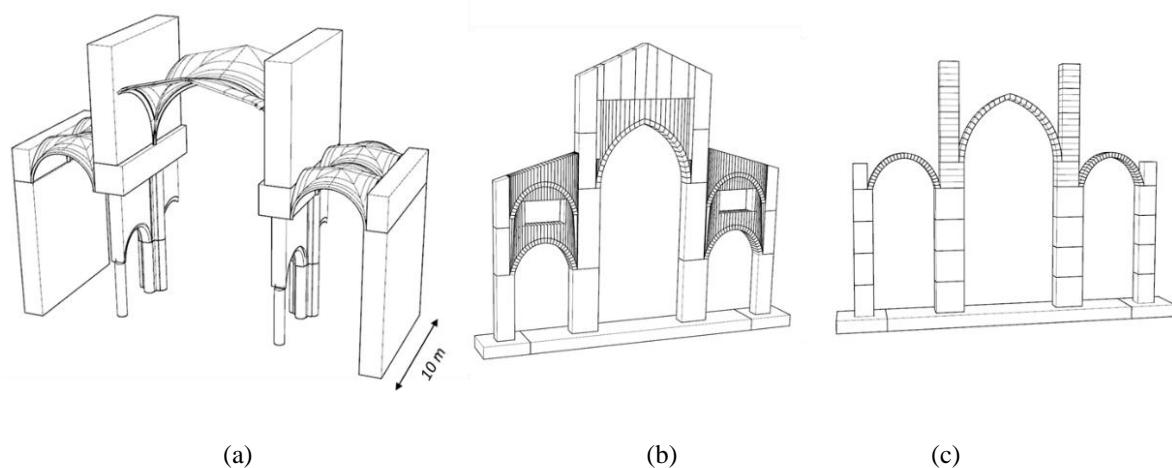


Figure 48: (a) The investigated cross-section of the Cathedral of Modena: representation of the structural elements, (b) the "COMPLETE DEM", (c) the "SIMPLIFIED DEM"

Table 12- The different analyses developed

Model	Static analysis	Dynamic analysis (Acceleration recorded in Modena)
COMPLETE DEM	x	
SIMPLIFIED DEM	X	X

4.1.2 The modelling parameters of the three numerical models

In the next sections, the modelling parameters used in the analyses are only synthetically shown.

4.1.2.1 Complete DEM model

Figure 49a shows the “COMPLETE DEM” model analysed and the names of the elements used in the calculation of the properties of the blocks and interfaces. In particular, Figure 49a displays the rendering made with the software Rhinoceros 5 and imported in 3DEC. The specific number of blocks in which the elements have been subdivided is shown in Figure 49b (that represents the 3DEC model). It can be noticed that the arches were schematized with six blocks. The modelling parameters used are reported in the Table 13, Table 14 and Table 15.

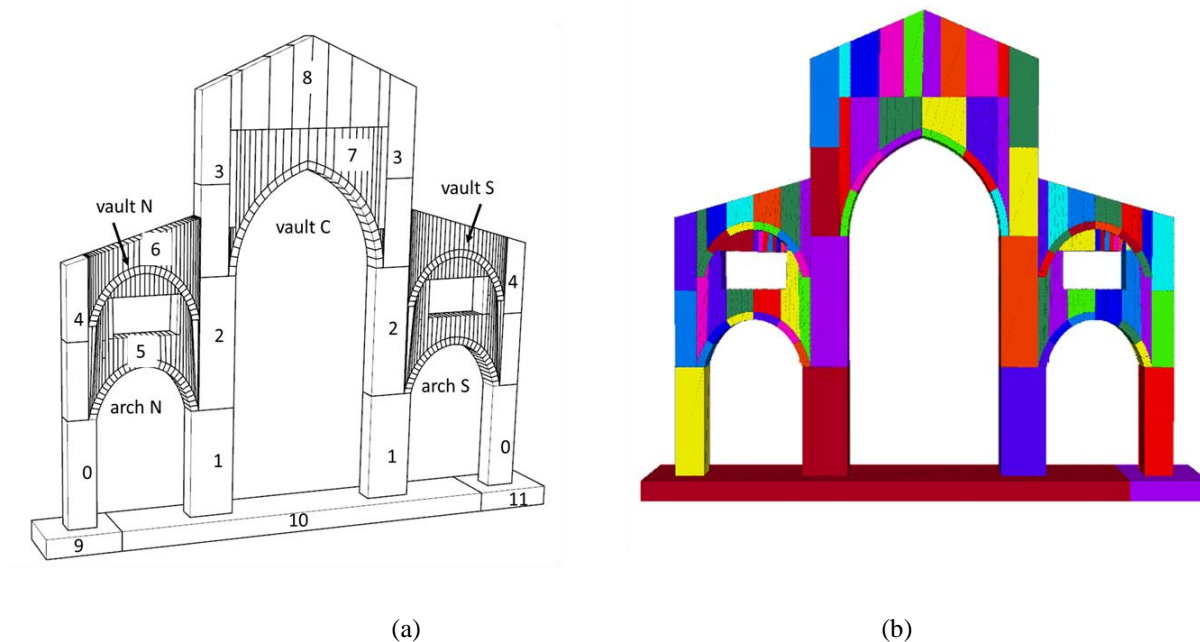


Figure 49: The “COMPLETE DEM” model analysed: (a) The Rhinoceros rendering and the name of the element used in the following calculation, and (b) the 3DEC model

Properties of the blocks:

Table 13- The properties of the blocks used in the analyses of the “complete cross-section”

Element	Weight per unit volume [KN/m ³]	*Elastic Modulus [KPa]	Dimension of the blocks [m]	Density [10 ³ Kg/m ³]
Wall ₀	119	4144000	1.5·1·5.05 m	11.9
Wall ₁	39	1727000	2.3·1·5.05 m	3.9
Wall ₂	80	1727000	1.9·1·1.08	8.0
Wall ₃	105	1727000	1.5·1·4.0	10.5

Wall ₄	144	4144000	1.1·1·2	14.4
Wall ₅	17	4144000		1.7
Wall ₆	19	4144000		1.9
Wall ₇	24	4144000		2.4
Wall ₈	17	4144000		1.7
Vault N-S	141	4144000	0.4·1·0.27 m	2.44
Vault C	159	4144000	0.4·1·0.27	4.07
arch N-S	17	4144000		1.7

*Elastic modulus used in the calculation of the interfaces stiffness (the blocks are here considered rigid)

Joint stiffness of the interfaces

Table 14- The properties of the interfaces in the vertical direction used in the analyses

Interface	Joint Kn [KPa/m]	Joint Ks [Kpa/m]
Wall ₀ –Wall ₄	4.4 10 ⁶	1.9 10 ⁶
Wall ₁ -Wall ₂	6.5 10 ⁵	2.8 10 ⁵
Wall ₂ -Wall ₃	2.7 10 ⁶	1.9 10 ⁶
Wall ₄	9.7 10 ⁶	4.1 10 ⁶
Wall ₇ -Wall ₈	9.98 10 ⁵	4.2 10 ⁵
Vault N-S	3.0 10 ⁷	1.3 10 ⁷
Vault C	1.8 10 ⁷	7.5 10 ⁶
Wall ₇ -Vault C	1.5 10 ⁶	6.3 10 ⁵
Wall ₆ -Vault N-S	1.8 10 ⁶	7.6 10 ⁵
Wall ₅ -Vault N_S	1.97 10 ⁶	8.3 10 ⁵
Arch N-S	1.99 10 ⁷	8.4 10 ⁶
Wall ₀ –9	5.1 10 ⁴	1.3 10 ⁶
Wall ₁ –10	1.1 10 ⁴	3.0 10 ⁶
Wall ₀ –11	2.0 10 ⁴	1.3 10 ⁶

The equivalent normal stiffness at the base of walls of the cross-section have been used in the analysis and are calculated in the Equation 4.1-4.3:

$$k_{ntot_wall_{0-9}} = k_n + \Delta k_n = 5.1 \cdot 10^4 + 2.6 \cdot 10^6 = 2.7 \cdot 10^6 \frac{kPa}{m} \quad (4.1)$$

$$k_{ntot_wall_{1-10}} = k_n + \Delta k_n = 1.1 \cdot 10^4 + 6.0 \cdot 10^6 = 6.0 \cdot 10^6 \frac{kPa}{m} \quad (4.2)$$

$$k_{ntot_wall_{0-11}} = k_n + \Delta k_n = 2.0 \cdot 10^4 + 2.6 \cdot 10^6 = 2.6 \cdot 10^6 \frac{kPa}{m} \quad (4.3)$$

Table 15- The properties of the interfaces in the horizontal direction used in the analyses

Interface	Joint Kn [KPa/m]	Joint Ks [Kpa/m]
Wall ₃ –Wall ₇	4.2 10 ⁶	1.810 ⁶
Wall ₇	1.8 10 ⁶	8 10 ⁵
Wall ₃ -Wall ₆	5.5 10 ⁶	2.310 ⁶
Wall ₆	3.2 10 ⁶	1.4 10 ⁶
Wall ₄ -Wall ₅	5.5 10 ⁶	2.3 10 ⁶
Wall ₂ -Wall ₅	5.5 10 ⁶	2.3 10 ⁶
Wall ₅	3.2 10 ⁶	1.4 10 ⁶
Wall ₃ –Wall ₈	1.5 10 ⁶	6.2 10 ⁵

4.1.2.2 Simplified DEM model

Figure 50 shows the “SIMPLIFIED DEM” model analysed and the names of the elements used in the calculation of the properties of the blocks and interfaces. Also in this case the Figure 50b displays the 3DEC model with the respective subdivision in blocks of the elements used in the analyses. The modelling parameters used are reported in the Table 16 and Table 17.

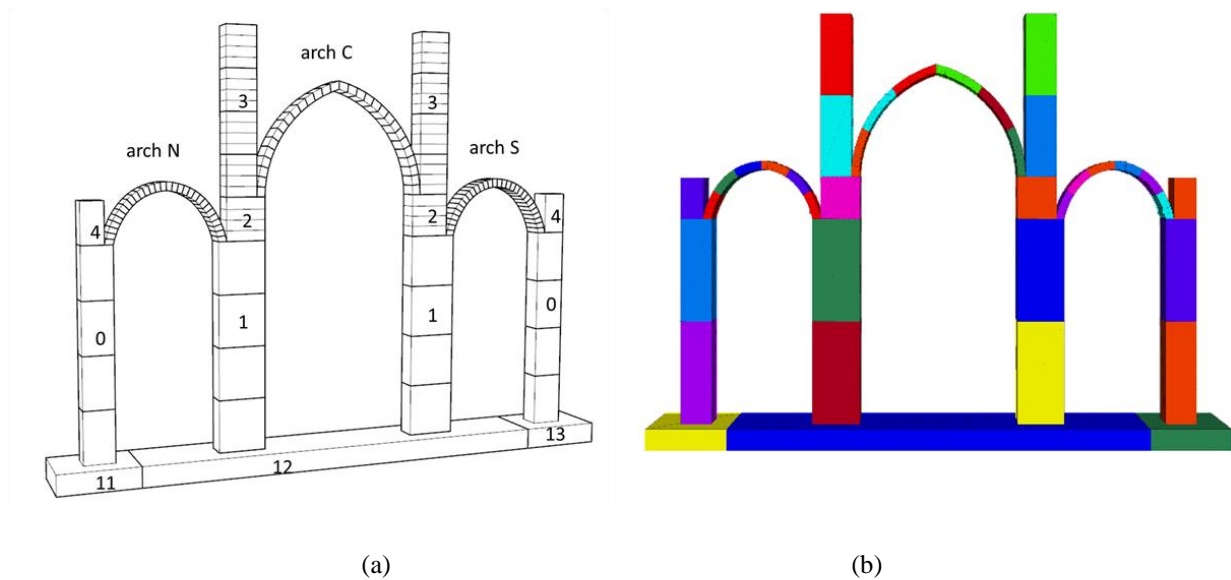


Figure 50: The “SIMPLIFIED DEM” model analysed: (a) The Rhinoceros rendering and the name of the element used in the following calculation, and (b) the 3DEC model

Properties of the blocks:

Table 16- The properties of the blocks used in the analyses of the “simple cross section”

Element	Weight per unit volume [KN/m ³]	*Elastic Modulus [KPa]	Dimension of the blocks [m]	Density [10 ³ Kg/m ³]
Wall ₀	125	4144000	1.5·1·5.05 m	12.5
Wall ₁	50	1727000	2.3·1·5.05 m	5.0
Wall ₂	127	1727000	1.9·1·1.08	12.7
Wall ₃	140	1727000	1.5·1·4.0	14.0
Wall ₄	213	4144000	1.1·1·2	21.3
ArchN-S	141	4144000	0.4·1·0.27 m	14.1
Arch C	159	4144000	0.4·1·0.27	15.9

*Elastic modulus used in the calculation of the interfaces stiffness (the blocks are here considered rigid)

Joint stiffness of the interfaces:

Table 17- The properties of the interfaces used in the analyses of the “simple cross-section”

Interface	Joint Kn [KPa/m]	Joint Ks [Kpa/m]
Wall ₀	8.2 10 ⁶	3.5 10 ⁶
Wall ₀ -Wall ₄	1.2 10 ⁷	5.0 10 ⁶
Wall ₁	7.8 10 ⁵	3.3 10 ⁵
Wall ₁ -Wall ₂	1.1 10 ⁶	4.7 10 ⁵
Wall ₂ -Wall ₃	1.3 10 ⁶	5.5 10 ⁵
Wall ₃	1.2 10 ⁶	4.2 10 ⁵
Arch N-S	3.0 10 ⁷	1.3 10 ⁷
ArchN-S-Wall ₀	1.3 10 ⁷	5.5 10 ⁷
Arch C	1.8 10 ⁷	7.5 10 ⁶
Arch C-Wall ₁	1.9 10 ⁷	7.9 10 ⁶
Wall ₀ -11	2.7 10⁶	1.3 10⁶
Wall ₁ -12	6.0 10⁶	3.0 10⁶
Wall ₀ -13	2.6 10⁶	1.3 10⁶

Damping

$$f_{crit} = \frac{\omega_e \sqrt{2}}{2\pi} = \frac{1391\sqrt{2}}{2\pi} = 222 \text{ cycles / second}$$

4.1.3 The results

4.1.3.1 Static analyses

Contour maps of the lateral displacements along x direction are reported in Figure 51. The maximum displacement in the x direction of the longitudinal walls obtained from the static analyses of the COMPLETE DEM model is around 0.012 m (Figure 51a). Instead, the SIMPLIFIED DEM model provides a maximum displacement by around 0.004m (Figure 51b). As expected, the COMPLETE DEM model gives larger lateral displacements probably due to the lateral thrust exerted by the lower arches (not modelled in the SIMPLIFIED DEM model).

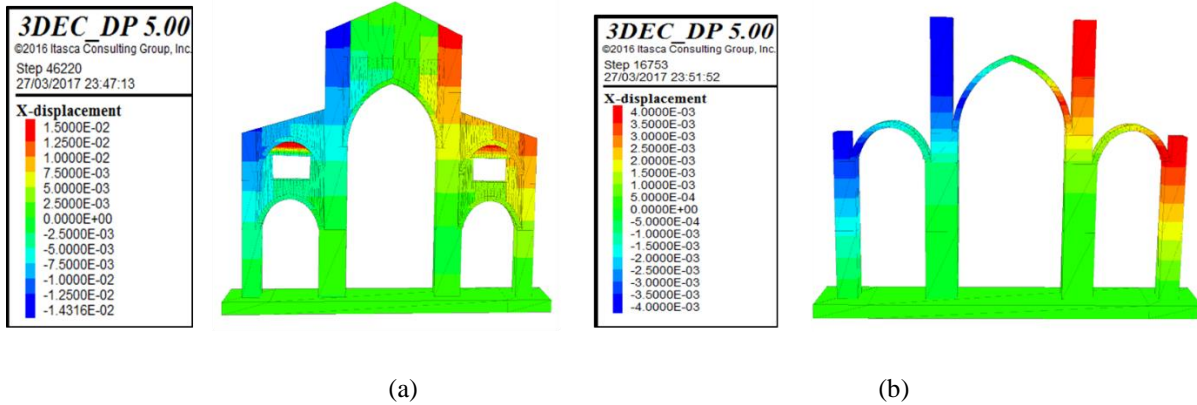


Figure 51: Contour maps of the lateral displacements along x direction obtained by : (a) COMPLETE DEM model and (b) SIMPLIFIED DEM model

Figure 52 displays the contour plot of the interfaces, relative block-to-block, displacement (blue indicate an opening between the blocks). The contour plot is qualitatively compared with the crack patterns as observed before the 2012 Emilia Earthquake (see §1.1.3). It can be noted that the block openings agrees with the location of the main cracks. It reminds that the model takes into account of the different soil stiffness at the base of the walls that are probably the first cause of the crack patterns detected before the 2012.

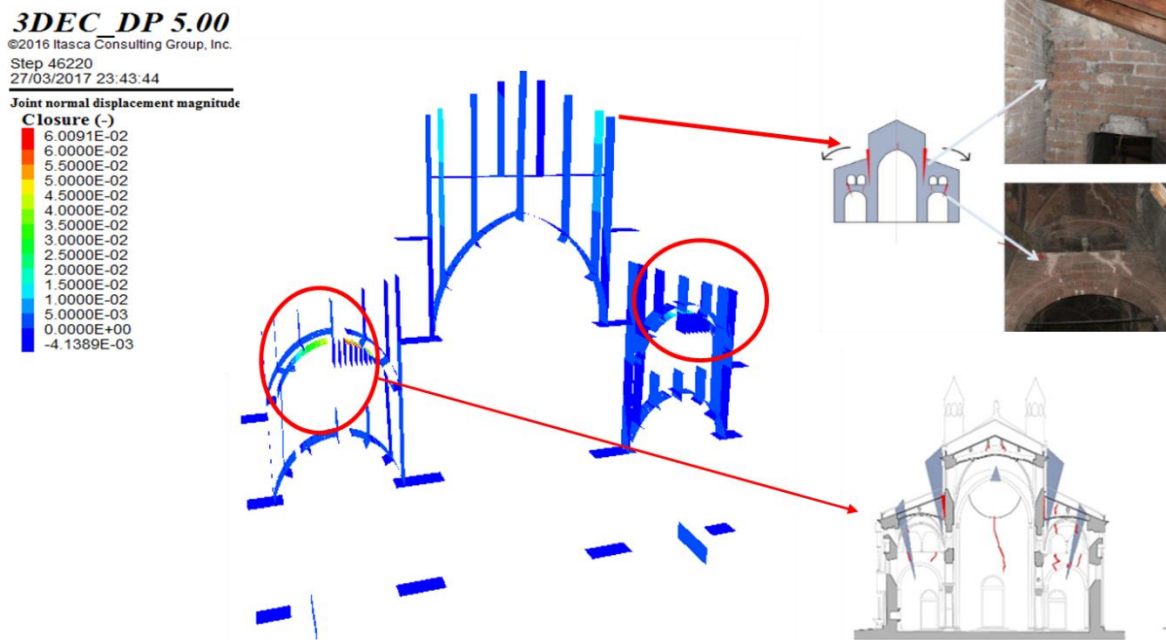


Figure 52: Contour plot of the interfaces of the COMPLETE DEM model and the crack pattern detected in the 2010

4.1.3.2 Dynamic analyses

As expected the dynamic analyses performed on the SIMPLIFIED DEM model considering the ground motion recorded in Modena during the 2012 Emilia's earthquake (§1.3) do not lead to the collapse of the structure. Figure 53 displays the contour plot of the interfaces, relative block-to-block, displacement (orange and red colors indicate an opening between the blocks) obtained by the SIMPLIFIED DEM model. It can be noticed that under the seismic loads several new openings appear mainly concentrated on the arches (that schematized the vaults). These openings are in good agreement with the cracks observed after the Emilia Earthquake (own concentrated predominantly in the vaults §1.1.3).

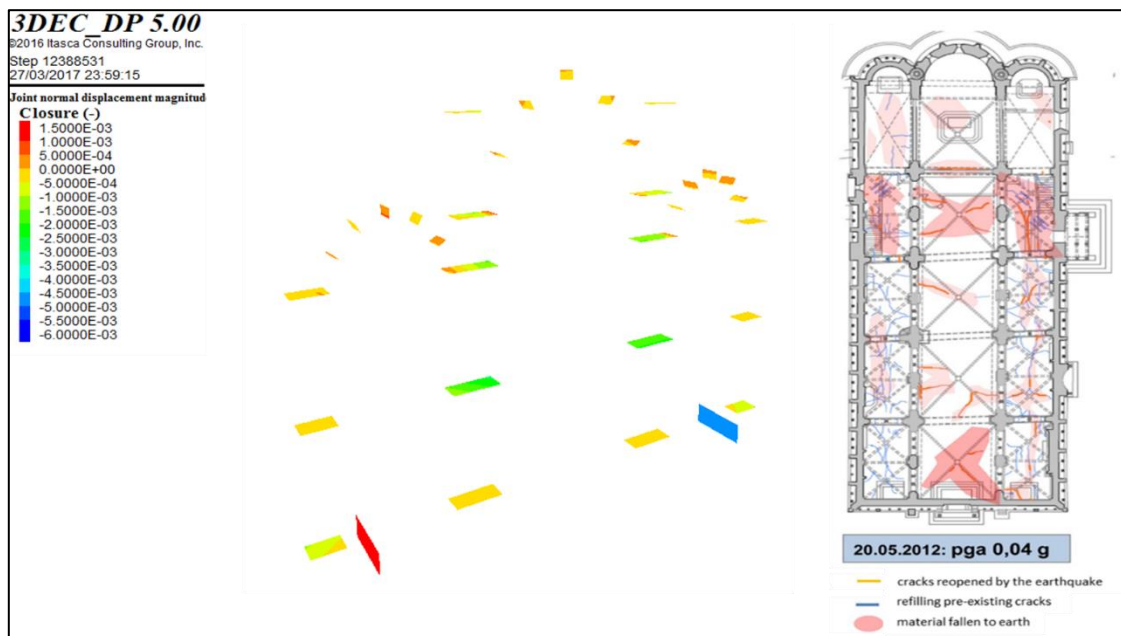


Figure 53: Contour plot of the interfaces of the SIMPLIFIED DEM model and the crack pattern detected in after the 2012 Emilia earthquake

4.2 Conclusion

The DEM models of the cross section of the Cathedral of Modena allow to identify the cracks due to the gravity loads and the different stiffness of the soil at the base and those due to the seismic loads. The results obtained seem to be in agreement with the crack patterns detect (before and after the 2012 earthquake).

5 Results obtained from the Static Structural Health Monitoring of the Cathedral of Modena

5.1 Introduction

In the 2003, a static SHM system has been installed on the Cathedral of Modena, whose construction began in 1099 and finished in 1184.

The large amount of data recorded by the monitoring system has been analyzed, using an approach that will be presented in next section

5.2 Approach for a critical interpretation of the data acquired by a Static SHM system

SSHM systems return discrete time series which can be generally referred to as $x(t_i)$, where x represents the monitored quantity (e.g. displacement, strain, angle inclination, crack width, temperature, ...) and t_i represents a specific instant of time t [35]. Each monitored quantity is here assumed to be a function of two main factors:

$$x(t) = f[F(t), S(t)] \quad (5.1)$$

$F(t)$ represents the (time-dependent) external forces acting on the structure, and $S(t)$ represents the time evolution of the “state” of the structure, i.e. the condition of the structure due to its geometrical configuration, the materials mechanical properties, its boundary conditions, etc. In general, the state of the structure can be assumed stationary if it does not change significantly from year to year or not stationary if it changes with time. The variation of the state may be due to different factors such as material degradation, soil-structure interaction, etc.

The external actions $F(t)$ on the building can be classified into three main groups [36]:

- Dead loads $D(t)$: the permanent forces acting on a structure such as the self-weight of the structure;
- Live loads $L(t)$: the non-permanent forces acting on the structure. In detail, these encompass the forces that depend on the weather effects, which are herein referred to as natural forces, $N(t)$, such as wind, temperature, precipitations, etc.
- Accidental loads $A(t)$: the forces depending on rare events, such as earthquakes, hurricanes, explosions, etc.

Therefore, the external actions $F(t)$ can be decomposed into:

$$F(t) = D(t) + L(t) + A(t) \quad (5.2)$$

while the state $S(t)$ may be seen as:

$$S(t) = S(t_0) + \Delta S(t_0, t) = S_0 + \Delta S(t_0, t) \quad (5.3)$$

where S_0 is the state of the structure at time t_0 (which is assumed as known), and $\Delta S(t_0, t)$ represents the variation of the state over the time. In the case of $\Delta S(t_0, t)$ is approximately null over a certain time period, it follows that the state can be assumed as stationary (i.e. $S(t) = S(t_0)$). On the contrary, in the case of $\Delta S(t_0, t)$ differs from zero on a certain time period (on average), it follows that the state is not stationary and some potential damage evolution is in act.

The main problem for data interpretation is that the components of the records due to the external forces are generally larger (order of magnitudes) than the components relegated to the eventual change in the state, a direct analysis of the time-history recorded often does not allow to detect the evolution of the state. On the other hand, in the case of dead and loads are within their usual ranges, we expect that the recorded data should be characterized by predominant components due to seasonal and daily temperature excursions (assuming the temperature as the predominant external factor). In the absence of extreme events inducing accidental actions $A(t) = 0$, and assuming that the live loads are predominately due to the natural forces $L(t) = N(t)$, $F(t)$ can be expressed as the sum of the two components $D(t)$ and $N(t)$. Moreover, assuming constant dead loads, $D(t) = \bar{D}$ Equation (5.2) specifies as follows:

$$F(t) = \bar{D} + N(t) \quad (5.4)$$

Substituting Equations (5.2), (5.3) and (5.4) in Equation (5.1) leads to:

$$x(t) = f[\bar{D}, N(t), S_0, \Delta S(t_0, t)] \quad (5.5)$$

For historic buildings, generally composed of massive masonry walls, the temperature is typically the external factor which mainly affects the structural response (in usual operational condition). It is here assumed that the natural forces are periodic functions with two fundamental components:

$$N(t) = N_1(t) + N_2(t) \quad (5.6)$$

N_1 has period T equal to 365 days (due to the motion of revolution of the earth around the sun) leading to the annual oscillations and a contribution N_2 with a period T equal to 1 day (due to the motion of rotation of the earth around its axis) leading to the daily oscillations. Based on all the above assumptions and considerations, the time series $x(t)$ can be decomposed into two main components:

$$x(t) = x_1(t) + x_2(t) \quad (5.7)$$

$x_1(t)$ is the periodic component of $x(t)$ depending on $N(t)$ and \bar{D} , while $x_2(t)$ is the component of $x(t)$ depending on the state $S(t)$.

5.2.1 Reference quantities

In the light of all the above consideration, it appears that a useful analysis of the data from a SHM system have to focus on the identification of the potential evolutionary trends of response, which typically oscillates following the daily and seasonal thermal excursions. To do that, it is first necessary to characterize these seasonal and daily effects by introducing appropriate descriptors, hereafter referred to as “reference quantities”

The collection of these “reference quantities” constitute a specific nomenclature for an interpretation of the data obtained from a structural monitoring that also allow to collect data in a systematic fashion and thus compare them with those of similar structural typologies. The systematic identification of the “reference quantities” from the recorded data allows to identify the presence of potential evolutionary trends of the monitored state by the specific sensor. In effect, the "reference quantities", extracting useful information of the data recorded in a daily and annual span of time, allow to compare these values over all the period of monitoring.

With reference to the j -th generic day, the quantities of interest are:

- the *Daily Amplitude* ($\delta_{day,j}$), that represents the difference between the maximum and minimum of the discrete time series recorded $x(t_i)$ in the specific j -th day

$$\delta_{day,j} = [\max x(t_i) - \min x(t_i)] \quad \forall t_i \in j\text{-th day} \quad (5.8)$$

- the *Mean Daily Value* ($\mu_{day,j}$), that represents the mean value of the discrete time series recorded $x(t_i)$ in the specific j -th day

$$\mu_{day,j} = \frac{1}{n_j} \sum_{i=1}^{n_j} x(t_i) \quad \forall t_i \in j\text{-th day} \quad (5.9)$$

- the *Absolute Daily Residuals of the Mean Value* ($r_{\mu day,j(k-k_0)}$), that represents the difference between the mean value, recorded in the j -th day, of the k -th year and the k_0 -th year (reference year, generally corresponding to the first year of monitoring)

$$r_{\mu day,j(k-k_0)} = \mu_{\mu day,j(k)} - \mu_{\mu day,j(k_0)} \quad (5.10)$$

- the *Progressive Daily Residuals of the Mean Value* ($\text{rp}_{\mu\text{day},j(k+1-k)}$), that represents the difference between the mean value, recorded in the j-th day, of the $k+1$ -th year and the k-th year

$$\text{rp}_{\mu\text{day},j(k+1-k)} = \mu_{\text{day},j(k+1)} - \mu_{\text{day},j(k)} \quad (5.11)$$

With reference to the y-th year, the quantities of interest are:

- the *Annual Amplitude* ($\Sigma_{\text{year},y}$), that represents the difference between the maximum and minimum of the discrete time series recorded $x(t_i)$ in the specific y-th year

$$\Sigma_{\text{year},y} = [\max x(t_i) - \min x(t_i)] \quad \forall t_i \in \text{y-th year} \quad (5.12)$$

- the *Mean Annual Value* ($M_{\text{year},y}$), that represents the mean value of the discrete time series recorded $x(t_i)$ in the specific y-th year

$$M_{\text{year},y} = \frac{1}{n_y} \sum_{i=1}^{n_y} x(t_i) \quad \forall t_i \in \text{y-th year} \quad (5.13)$$

- the *Absolute Annual Residuals of the Mean Value* ($R_{M\text{year},(k-k_0)}$), that represents the difference between the mean annual value recorded in the k-th year and the k_0 -th year (reference year, generally corresponding to the first year of monitoring)

$$R_{M\text{year},(k-k_0)} = M_{\text{year},k} - M_{\text{year},k_0} \quad (5.14)$$

- the *Progressive Annual Residuals of the Mean Value* ($\text{Rp}_{M\text{year},(k+1-k)}$), that represents the difference between the mean annual value recorded on the $k+1$ -th year and the k-th year

$$\text{Rp}_{M\text{year},(k+1-k)} = M_{\text{year},k+1} - M_{\text{year},k} \quad (5.15)$$

In addition also sudden drops may be present in the recorded time series $x(t_i)$. These sudden drops may be related either to an instrument malfunctioning, either to external factors, or to extreme events (such as earthquakes, hurricanes, ...) and are here identified through the letter Δ . Table 18 collects the “reference quantities” defined. For the sake of clarity, in order to describe the “reference quantities” a fictitious signal is displayed in Figure 54 and some of its corresponding reference quantities are presented in Figure 55.

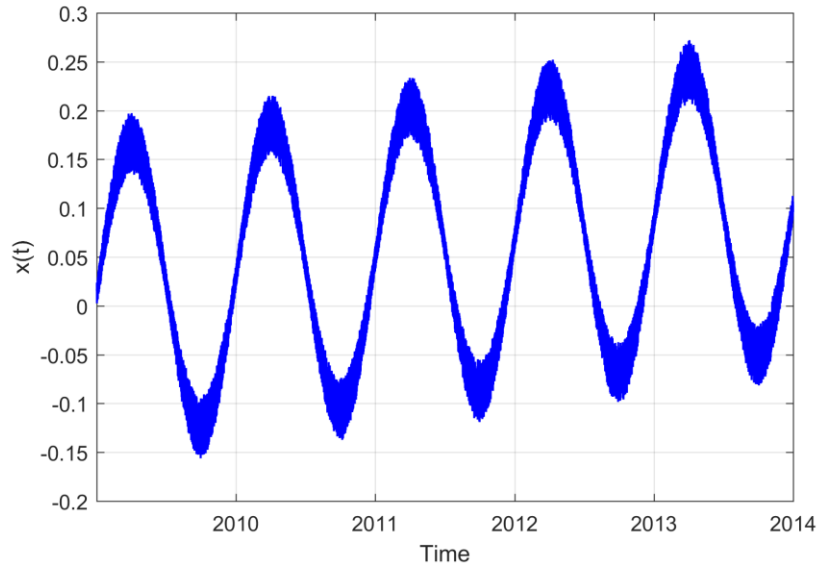


Figure 54- Time series $x(t)$

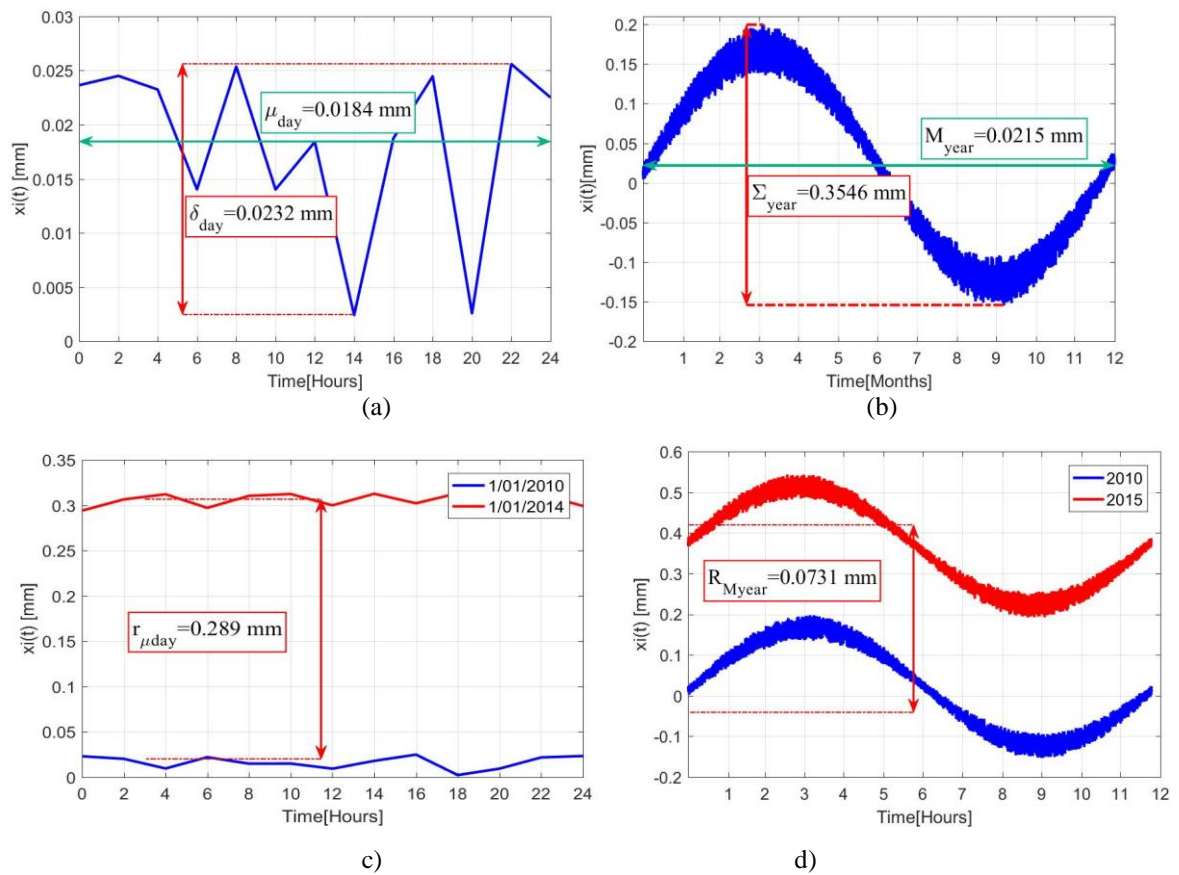


Figure 55: Reference quantities of the fictitious signal: (a) Daily amplitude and Mean Daily Value, (b) Annual amplitude and Mean Annual Value, (c) Absolute Daily Residuals of the Mean Value and (d) Absolute Annual Residuals of the Mean Value

Table 18- The introduced “reference quantities” for the analysis of the recorded data.

Reference quantity	Definition	Mean value within the observation period Δt
Daily Amplitude	$\delta_{day,j} = [\max x(t_i) - \min x(t_i)] \quad \forall t_i \in j\text{-th day}$	$\bar{\delta} = \frac{1}{N_{\Delta t}} \sum_{j=1}^{N_{\Delta t}} \delta_{day,j}$
Mean Daily Value	$\mu_{day,j} = \frac{1}{n_j} \sum_{i=1}^{n_j} x(t_i) \quad \forall t_i \in j\text{-th day}$	$\bar{\mu} = \frac{1}{N_{\Delta t}} \sum_{j=1}^{N_{\Delta t}} \mu_{day,j}$
Absolute Daily Residuals of the Mean Value	$r_{\mu day,j(k-k_0)} = \mu_{day,j(k)} - \mu_{day,j(k_0)}$	$\bar{r}_{\mu} = \frac{1}{N_{\Delta t}} \sum_{j=1}^{N_{\Delta t}} r_{\mu day,j(k-k_0)}$
Progressive Daily Residuals of the Mean Value	$rp_{\mu day,j(k_{+1}-k)} = \mu_{day,j(k_{+1})} - \mu_{day,j(k)}$	$\overline{rp}_{\mu} = \frac{1}{N_{\Delta t}} \sum_{j=1}^{N_{\Delta t}} rp_{\mu day,j(k_{+1}-k)}$
Annual Amplitude	$\Sigma_{year,y} = [\max x(t_i) - \min x(t_i)] \quad \forall t_i \in y\text{-th year}$	$\bar{\Sigma} = \frac{1}{N_{\Delta t}} \sum_{y=1}^{N_{\Delta t}} \Sigma_{year,y}$
Mean Annual Value	$M_{year,y} = \frac{1}{n_y} \sum_{i=1}^{n_y} x(t_i) \quad \forall t_i \in y\text{-th year}$	$\bar{M} = \frac{1}{N_{\Delta t}} \sum_{y=1}^{N_{\Delta t}} M_{year,y}$
Absolute Annual Residuals of the Mean Value	$R_{Myear,(k-k_0)} = M_{year,k} - M_{year,k_0}$	$\bar{R}_M = \frac{1}{N_{\Delta t}} \sum_{y=1}^{N_{\Delta t}} R_{Myear,(k-k_0),y}$
Progressive Annual Residuals of the Mean Value	$Rp_{Myear,(k_{+1}-k)} = M_{year,k_{+1}} - M_{year,k}$	$\overline{Rp}_M = \frac{1}{N_{\Delta t}} \sum_{y=1}^{N_{\Delta t}} Rp_{Myear,(k_{+1}-k),y}$
Drop	Δ	

5.3 Types and location of instruments

The monitoring system allows monitoring the main cracks across the walls and vaults, the relative displacements between the cathedral and the Ghirlandina tower, the inclination of the external longitudinal walls, and the temperature. Most of the instruments were installed in 2003, while others (such as the deformaters and inclinometers) were installed at the end of 2010. Data are acquired at time intervals of 30 minutes. The following symbols have been used to indicate the type of instrument: **D**=deformeter, **MGB**=biaxial joint meter, **MGT**= triaxial joint meter, **FP**=inclinometer, **T**= thermometer.

The different instruments installed on the Cathedral are displayed in Figure 56.

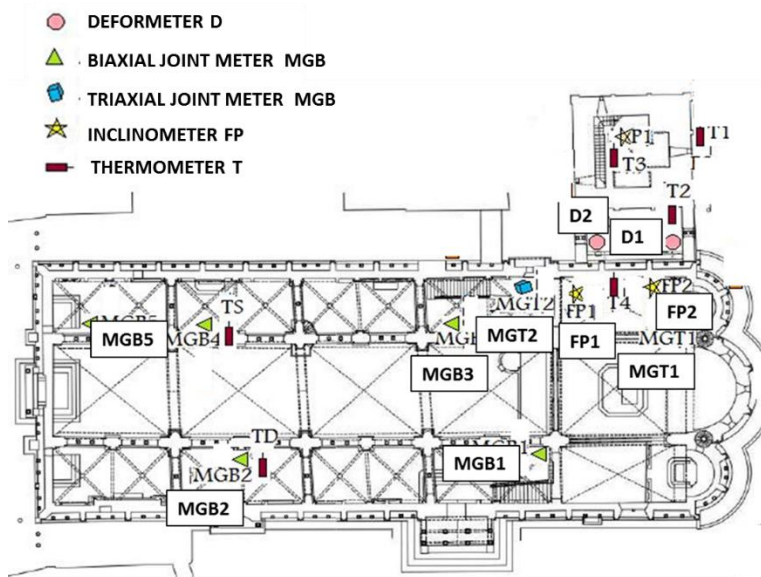


Figure 56: Location of the sensors.

The instruments installed on the Cathedral are briefly described below.

Invar Deformeter

The deformaters were placed on the buttresses between the Cathedral and the Ghirlandina Tower (Figure 57). They are designed to perform the deflection measurements of a structure of a substantial amount (in this case have an overall length of 5 meters). They consist of Invar rods having a low coefficient of thermal expansion. On the wall of the Ghirlandina tower was put the anchor support, while on the Cathedral wall is anchored to a non-contact sensor of the inductive type with 8 mm theoretical measurement range with a resolution of 0.01 mm. They are fed to a continuous voltage of 24 Vdc and the analog output signal is between 4 and 20 mA proportional to the distance between the transducer and the target. Conventionally the positive values on the graphs, which will be explained later, correspond to an estrangement between the Tower and the Cathedral, while negative values

correspond to a rapprochement of the two. Table 19 collects some technical specification of these Invar Deformeters.

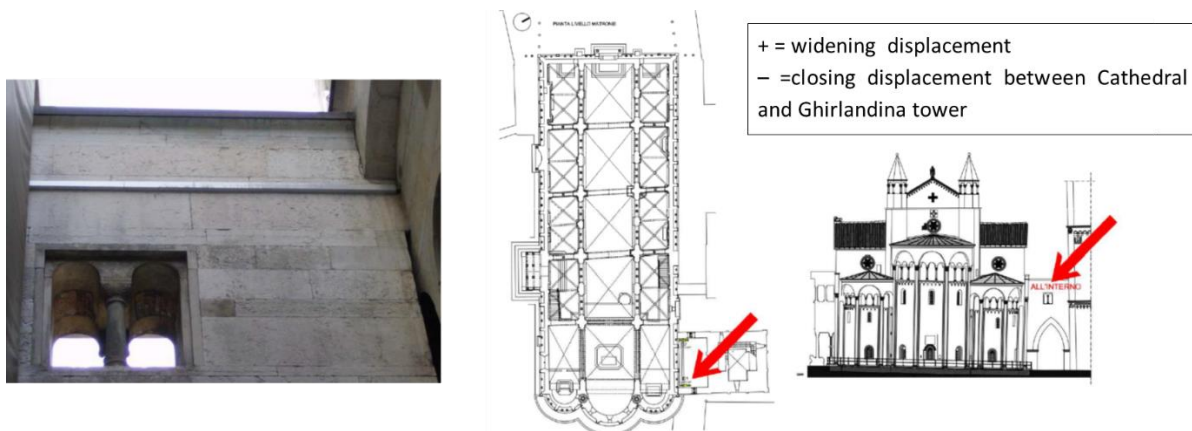


Figure 57: Deformometer installed on the buttress of the Cathedral (D1)
Table 19- Technical specification of the Invar Deformeters

TECHNICAL SPECIFICATIONS	
Full scale	8 mm
Resolution	0,4 μm
Accuracy	< 0.01mm
Dimension	5 m
Temperature Range	(-10/+80)°C

Biaxial joint meter- Triaxial joint meter

The variation in the opening of cracks in the bearing elements, due in most cases to the interaction with the ground and / or to an intrinsic degradation of materials is carried out by means of measuring instruments such as joint meters or deformeters. The joint meters are bound rigidly to the wall using anchors at the turn of the crack to be monitored. They may be biaxial, in this case the measure movements detected are in a plane (for example, a wall surface) (Figure 58) or triaxial if are able to detect also the displacements orthogonal to the plane (Figure 59). Seven main cracks of the Cathedral have been monitored through these sensors. In particular, in 2003, four biaxial joint meters were installed in the central nave and a triaxial joint meter were installed in the wall close to the two buttresses that link the Cathedral and the Tower. In December 2010, other two joint meters were installed. Table 20 collects some technical specification of the biaxial and triaxial joint meters.

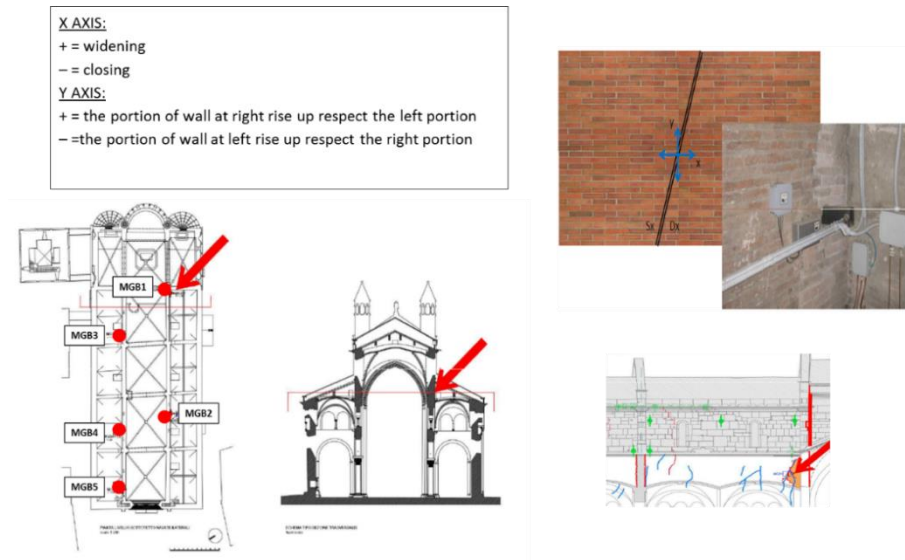


Figure 58: Biaxial joint meter installed in the central nave of the Cathedral (MGB1)

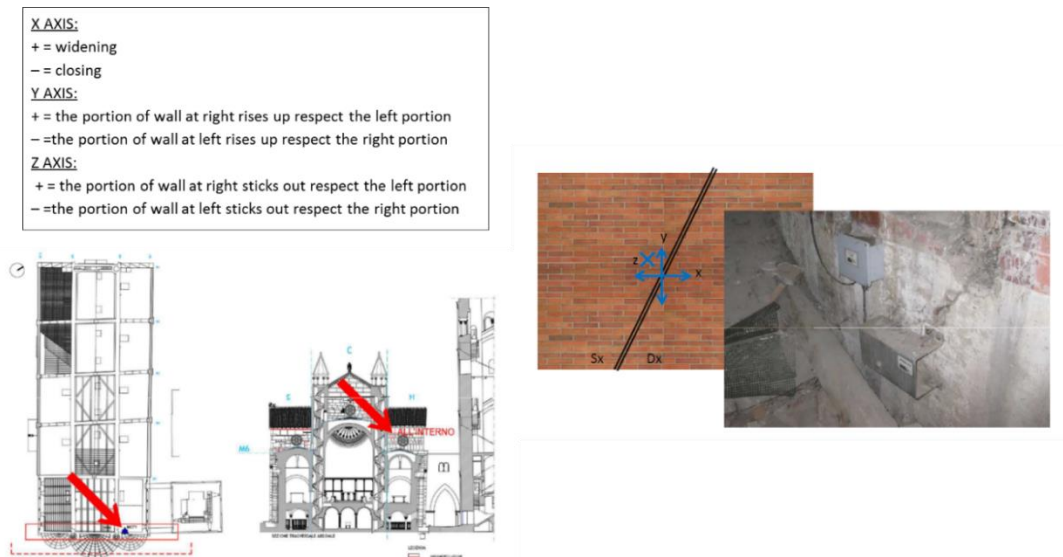


Figure 59: Triaxial joint meter installed in the longitudinal wall of the Cathedral (MGT1)
 Table 20- Technical specification of the biaxial-triaxial joint meters

TECHNICAL SPECIFICATIONS	
Full scale	8 mm
Resolution	0.01 mm
Accuracy	0.01 mm
Dimension	300x 200x150 mm

Inclinometer

The inclinometers (or pendulums) installed on the cathedral are designed for the control of the stability of the buildings, and their operation is based on the principle of a plumb line (Figure 60). It consists of: an upper berth, to the plumb bob (consists of Invar alloy to contain the thermal expansions), and the measuring instrument (that allows to perform the automatic measurement of the plumb line portion). This data allow analysing the slope changes of the Cathedral, both periodic (due to temperature variations) and permanent ones due to real structural behaviour. **Errore. L'origine iferimento non è stata trovata.** collects some technical specification of the inclinometers.

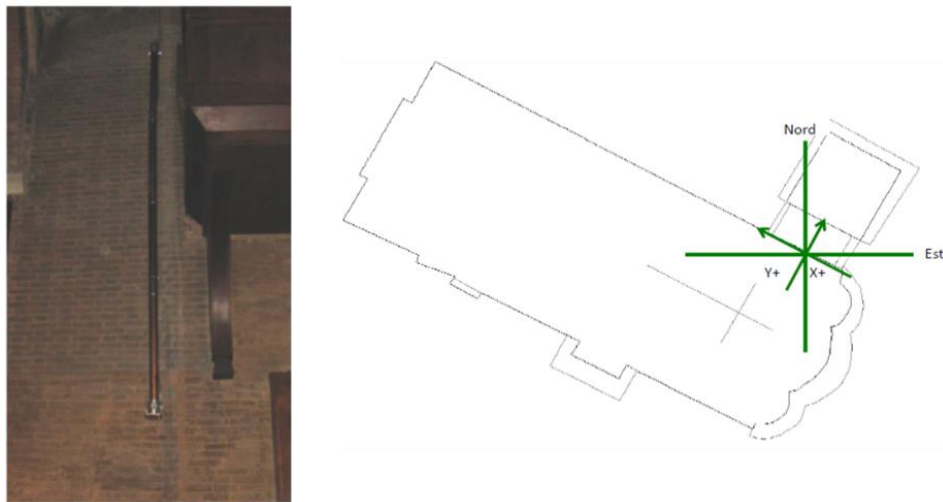


Figure 60: Inclinometer installed on the longitudinal wall of the cathedral (close to the buttress) FP1 and the conventional signs used.

Table 21- Technical specification of the inclinometers

TECHNICAL SPECIFICATIONS	
Full scale	8 mm
Resolution	0.4 μm
Accuracy	0.01 mm
Dimension	ϕ 80 mm, H=4 m

5.4 Reference quantities

The reference quantities defined in § 5.2.1 have been identified for all the data recorded by sensor of the monitoring system installed on the Cathedral of Modena.. In the next section, the salient results, obtained from the interpretation of the static monitoring data through the proposed procedure, are illustrated.

5.4.1 Invar deformer

The deformers D1 and D2, placed on the buttresses between the Cathedral and the Ghirlandina Tower in order to monitor the movements between the two structures, recorded significant drops during the seismic event that hit the Emilia Romagna in May 2012. In particular, the drops corresponding to the two days where the tremors of greatest intensity were recorded (20th and 29th May 2012). As mentioned above, positive values on the graph correspond to an estrangement between the Tower and the Cathedral, while negative values correspond to a rapprochement of the two.

Deformers D1

From 1th January 2011 until 20th May 2012, D1 records a slight estrangement between the Cathedral and the tower. After the 2012 earthquake, the trend recorded by this device changes considerably. On days 20th and 29th May it has recorded two drops of $\Delta_{20\text{may}} = 0.53\text{mm}$ and $\Delta_{29\text{may}} = 0.3 \text{ mm}$, respectively, that indicate an approaching of the two structures (Figure 61). After the seismic event, the recorded data are negative, indicating a progressive approach between Ghirlandina and Cathedral. This sensor is characterized by several missing data; therefore, the systematic identification of the reference quantities does not lead to significant results. However, it is interesting to note that the mean value of the daily amplitude, not considering the data recorded in the 2012, is around of 0.03 mm. The daily amplitudes recorded on 20th and 29th May are, thus, around 20 times more than the mean value of the daily amplitude recorded in the other years.

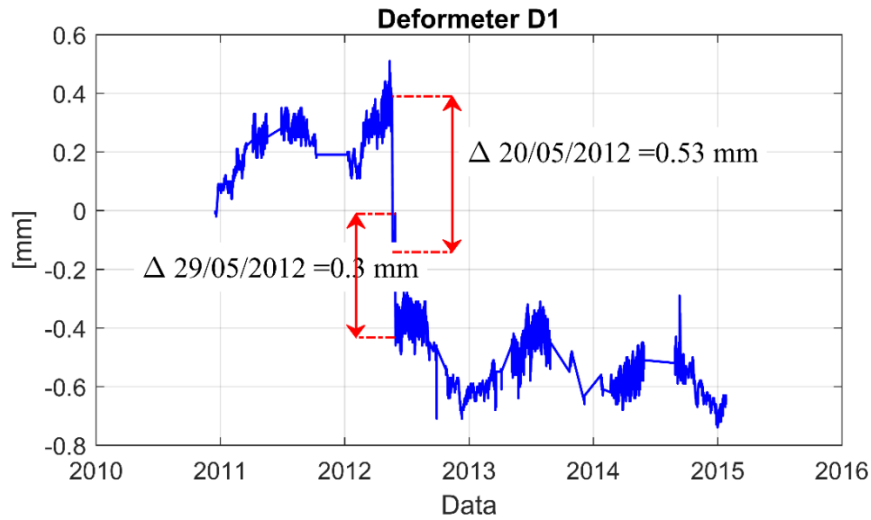


Figure 61: Data recorded by the deformer D1 installed on the buttresses between the Cathedral and the Ghirlandina Tower

Deformers D2

The deformer D2 does not record specific anomalies during the main shocks of the 2012 Emilia earthquake. However, a drop was recorded in 27th August 2012 (August $\Delta 27 = 0.4$ mm). On that date it is detected a earthquake of much lower intensity compared to those of May during which the device did not show significant changes. It excludes, therefore, that the cause of this drop is due to slight earthquake but it's probably due to interference. Before and after the drop, the device has recorded a cyclical trend. The negative values on the graph correspond to a rapprochement between the cathedral and the tower (Figure 62).

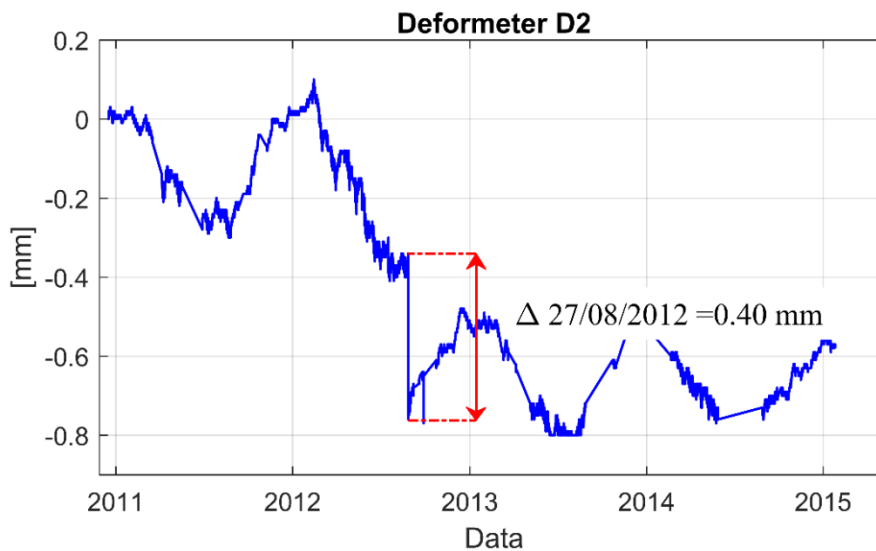


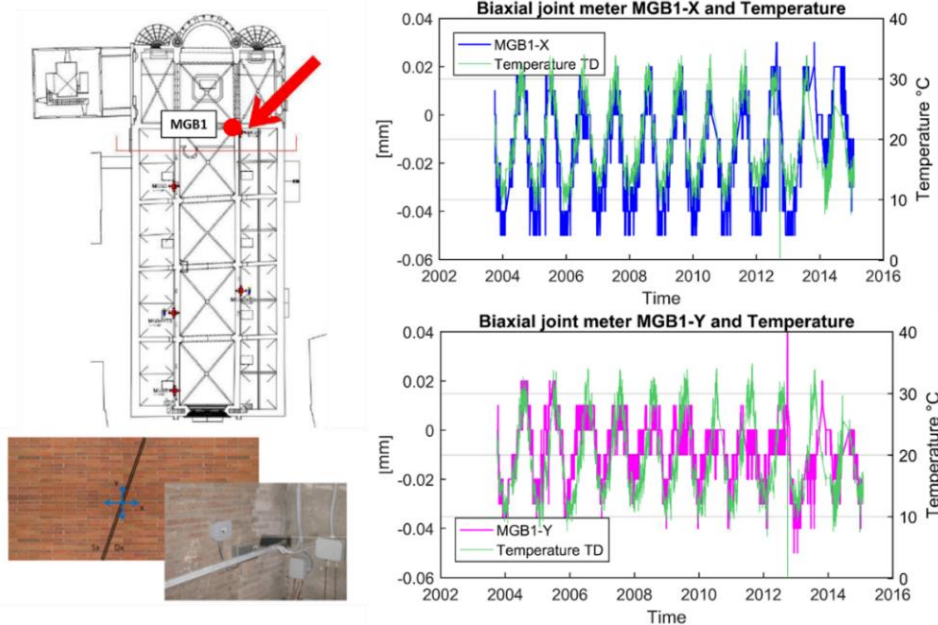
Figure 62: Data recorded by the deformer D2 installed on the buttresses between the Cathedral and the Ghirlandina Tower

5.4.2 Joint meter

The biaxial joint meters MGB1, MGB2, MGB3, MGB4 and the triaxial joint meter MGT1 were installed in October 2003 while MGB5 and MGT2 was added later in 2010. It is noted that MGT2 is characterized by many missing data. For this reason its data are not reliable in order to perform evaluations on the structural health and their will not considered in the following analyses.

Biaxial joint meter MGB1

The sensor MGB1 monitors the movements of a crack located in the South aisle, apse side in correspondence with the cracks area which transversely crosses the fourth nave. The temperature effect is significant and the recorded data evidence a high direct correlation with respect to the temperature data (Figure 63 a). When the temperature increases, in fact, the wall tends to expand with consequent closure of the crack and, vice versa, with the decrease of the temperature, the masonry walls tends to compresses with a widening of the crack. The absolute daily residuals reveal that the crack under observation has opened of 0.02 mm and the portion of wall at right of the crack rise up of 0.03 mm respect the left portion, during all years of monitoring (Figure 63 b, c).



(a)

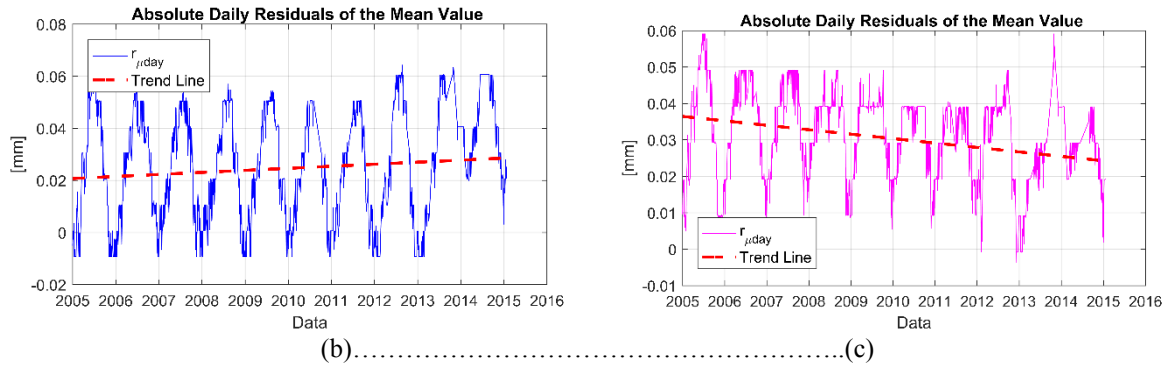
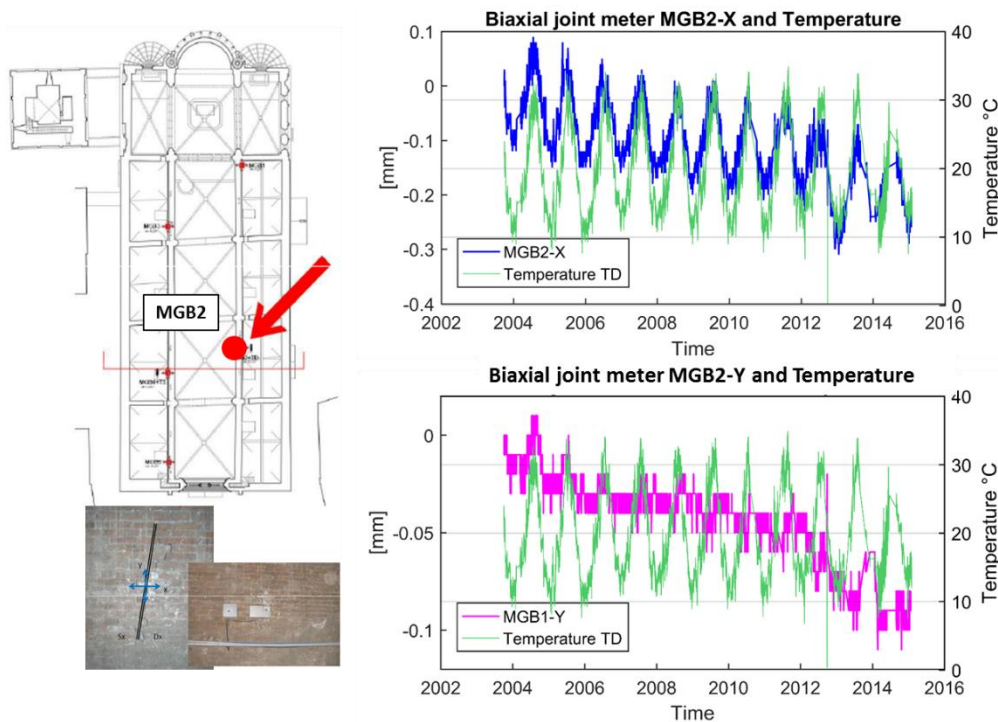


Figure 63: Biaxial joint meter MGB1: row-data recorded by MGB1 considering also the temperature variation, as recorded by the thermometer TD, and (b),(c) the absolute daily residuals evaluated for both X and Y direction

Biaxial joint meter MGB2

The sensor MGB2 monitors the movements of a crack located in the South aisle in correspondence with the cracks area, which transversely crosses the second nave (see §10.3.4). The data recorded are in phase with respect to temperature data (Figure 64 a). MGB2 records a cyclical trend that is repeated for all the years and, as already seen for MGB1, probably due to the correlation with the thermal variations. The trend of the daily amplitudes is, in fact, regular. Unlike what was seen for the previous device, MGB2 shows a decreasing trend over the years for both the X component that Y. This indicates that the lesion tends progressively to open up and the portion of wall at left of the crack rises up compared to the wall at the right. However, the absolute daily residuals reveal that the movements are small: a cumulative trend of -0.04 mm in both the directions is recorded (Figure 64 b, c).



(a)

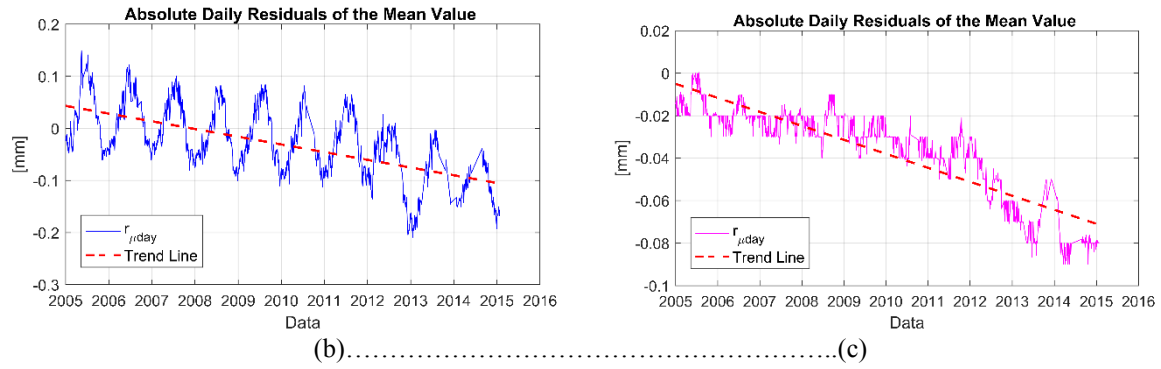
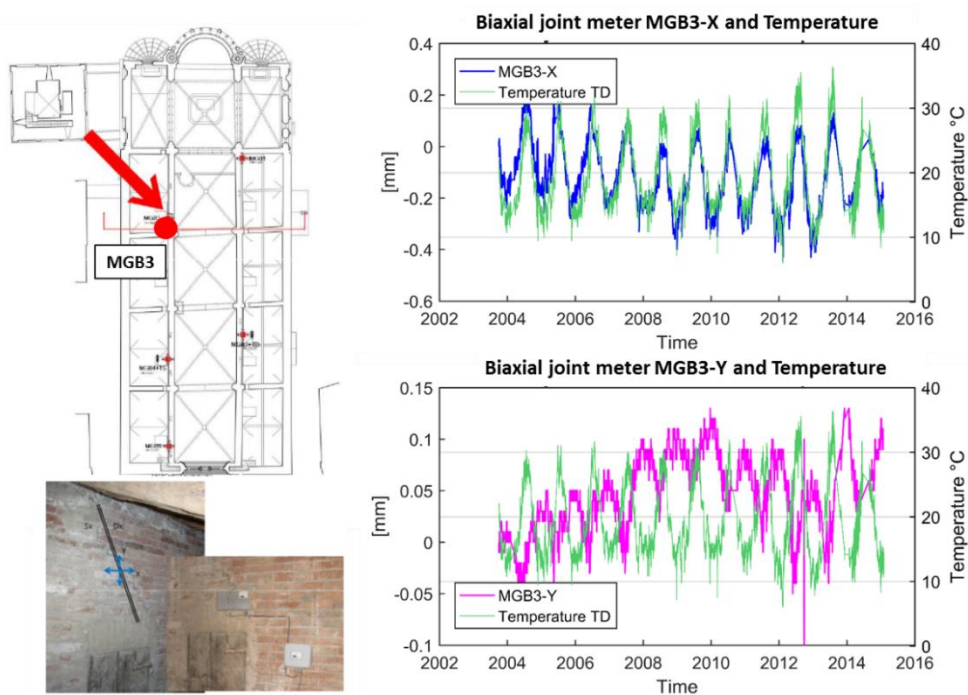


Figure 64: Biaxial joint meter MGB2: row-data recorded by MGB2 considering also the temperature variation, as recorded by the thermometer TS, and (b),(c) the absolute daily residuals evaluated for both X and Y direction

Biaxial joint meter MGB3

The sensor MGB3 monitors the movements of a crack located in the North aisle, apse side in correspondence with the cracks area, which transversely crosses the second nave (see §1.1.4). The recorded data for the x component evidence a high direct correlation with respect to the temperature data. The data recorded for the y component appears to be out of phase with the temperature data (Figure 65a). The x component recorded a decreasing trend throughout the observation period, and then a gradual opening of the crack (with a cumulative trend of -0.03 mm), (Figure 65b). The y component, instead, recorded an increasing trend that indicates that the portion of the wall at the left of the crack rise up with respect to that of the right. Then until 2014, a decreasing trend has been recorded. The absolute daily residuals reveal for the y component a cumulative trend of +0.05mm (Errore. L'origine riferimento non è stata trovata.c)



(a)

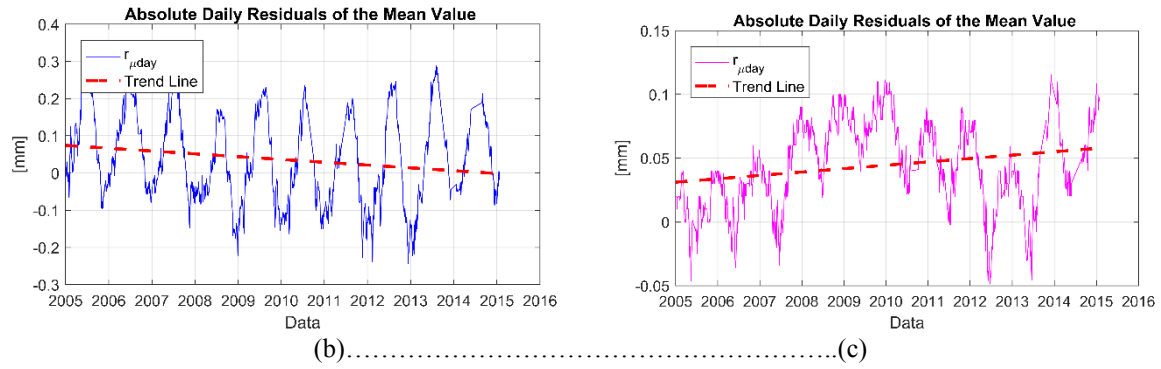
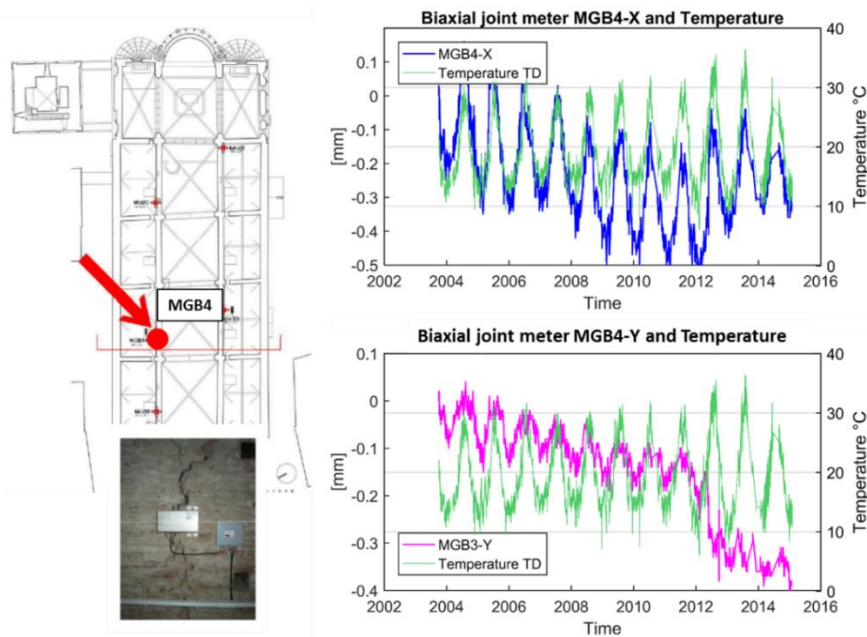


Figure 65: Biaxial joint meter MGB3: row-data recorded by MGB3 considering also the temperature variation, as recorded by the thermometer TS, and (b),(c) the absolute daily residuals evaluated for both X and Y direction

Biaxial joint meter MGB4

The sensor MGB4 monitors the movements of a crack located in the North aisle. The recorded data are in phase with respect to the temperature data recorded by the thermometer TS (Figure 66 a). The x component shows a decreasing trend, which indicates a slight opening of the crack. The absolute daily residuals reveal for the x component a cumulative trend of -0.1 mm (Figure 66 b). Even the y component registers a decreasing trend (the portion of wall at left of the crack tends to rise compared to the wall at the right). Moreover, three drops are recorded in 20th, 29th May and 28th September 2012, respectively of $\Delta_{20\text{May}} = 0.05$ mm, $\Delta_{29\text{May}} = 0,08$ mm and $\Delta_{28\text{September}} = 0.10$ mm. The first two drops correspond with the tremors of greatest intensity of the seismic event of May 2012. The list of earthquakes recorded in Modena does not present significant earthquakes in September. The absolute daily residuals reveal for the y component a cumulative trend of -0.13 mm (Figure 66 c).



(a)

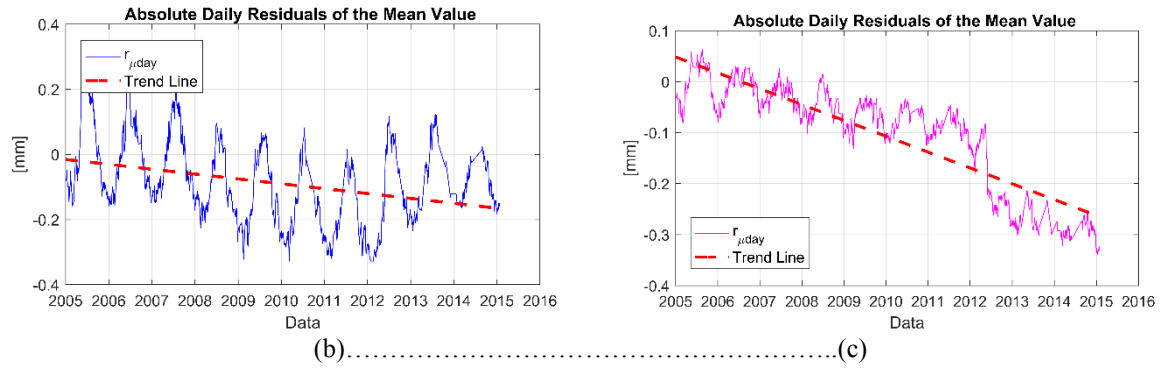
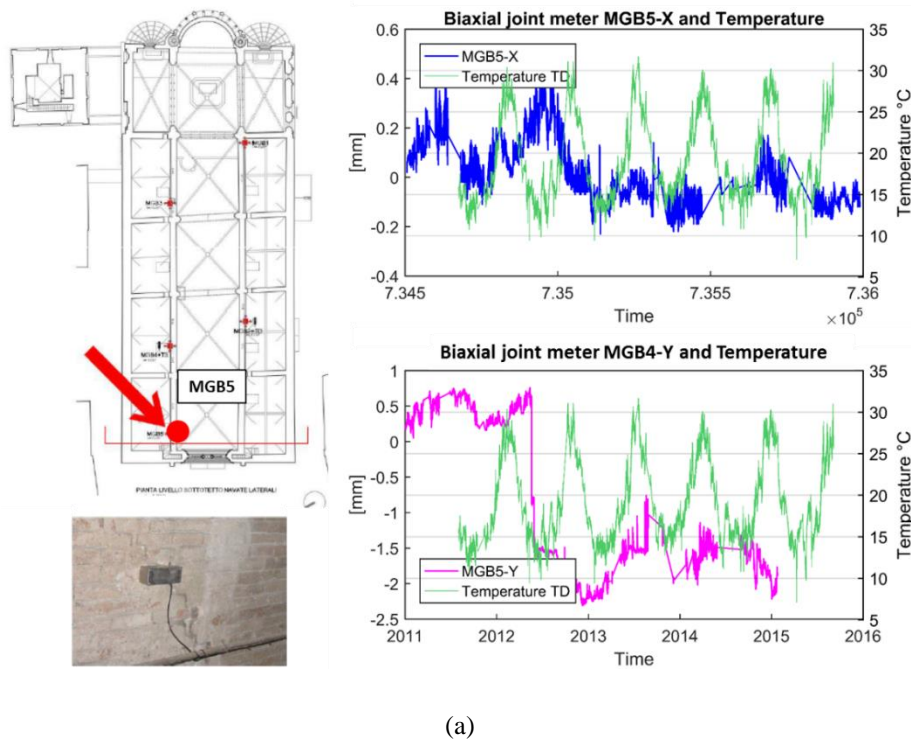
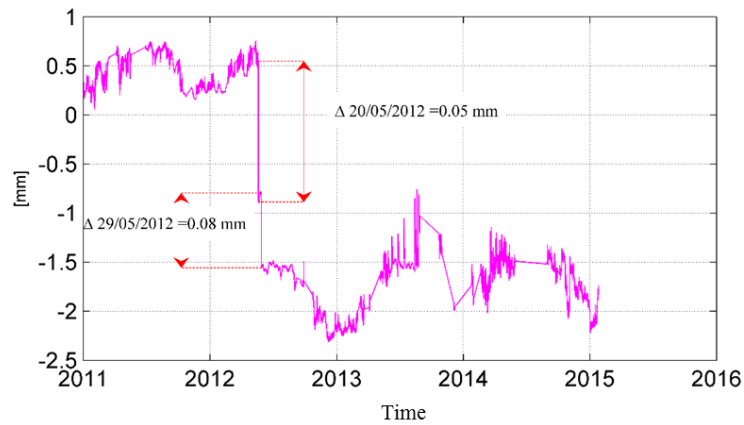


Figure 66: Biaxial joint meter MGB4: row-data recorded by MGB4 considering also the temperature variation, as recorded by the thermometer TS, and (b),(c) the absolute daily residuals evaluated for both X and Y direction

Biaxial joint meter MGB5

The sensor MGB5 was installed in 2010 to monitor a crack present in North aisle. The recorded data indicate that the opening of the crack (x-direction) has followed a cyclical pattern substantially due to thermal variations (Figure 67 a). The y component instead shows, in addition to cyclical trends relate to the temperature, two significant drops in correspondence of 20 and 29 May 2012 (Figure 67b). These drops indicate that seismic events in May 2012 have led to an, albeit slight, changes in the relative quota between the two walls close to the crack, with the portion of the wall to the left of the crack that is rise up of approximately 1.5 mm with respect to the right.





(b)

Figure 67: Biaxial joint meter MGB5: row-data recorded by MGB5 considering also the temperature variation, as recorded by the thermometer TS and (b) the drops recorded in the y direction during the seismic events of May 2012

Triaxial joint meter MGT1

The sensor MGT1 monitors the movements of a crack located in the transversal wall close to the apses. The recorded data are in phase with respect to the temperature data recorded by the thermometer TS (Figure 68a). In the x direction, MGT1 records a cyclical trend substantially related to the effects of temperature variations. However, a slight increasing trend concentrated in the last years is recorded indicating the tendency of the crack to close over the time. The absolute daily residuals reveal a cumulative trend of -0.5 mm (**Errore. L'origine riferimento non è stata trovata.** b). The y component shows a decreasing trend until 2008 (the portion of the wall to the left of the crack rise up compared to that of the right). From 2008 until 2012, the device recorded a recovery indicated by the increasing trend. During seismic events, a total drop of $\Delta = 0.13$ mm has been recorded indicating a further lifting of the left wall compared to that of the right. The absolute daily residuals reveal a cumulative trend of -0.1 mm in the thirteen years of monitoring (Figure 68c). The recordings detected in the Z direction (perpendicular to the plane) show an increasing trend, indicating, therefore, an increase in the protrusion of the right wall compared to that of the left with a cumulative residua of 0.14 mm (Figure 68a, d).

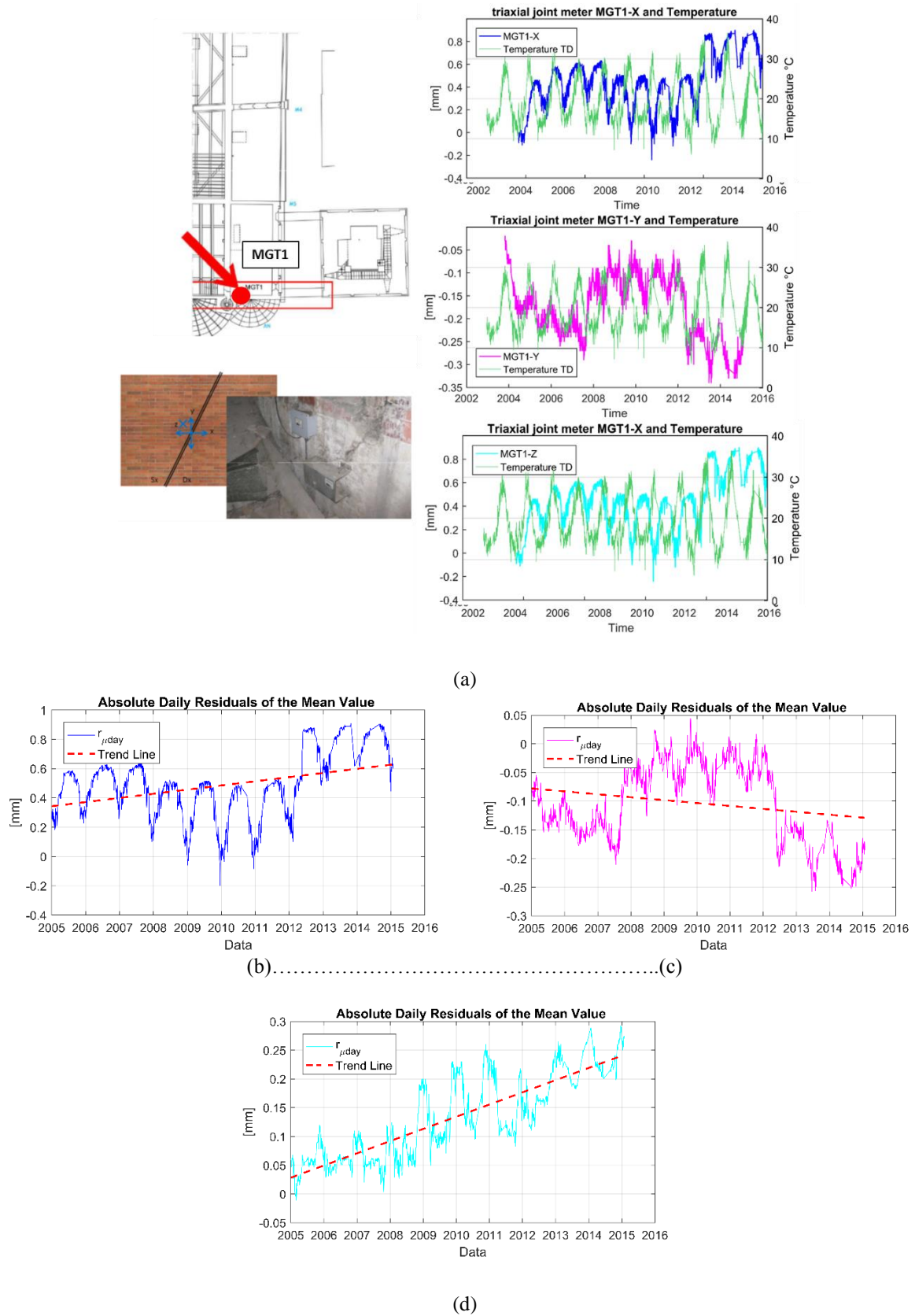


Figure 68: Triaxial joint meter MGT1: row-data recorded by MGT1 considering also the temperature variation, as recorded by the thermometer TS, and (b),(c), (d) the absolute daily residuals evaluated for both X , Y and Z direction

The mean values over the entire observation period of the reference quantities are collected in Table 5-22 for all the joint meters.

Table 5-22- Mean values of the reference quantities over the thirteen years of monitoring for the joint meters

Sensor	Year	$\delta_{day,j}$ [mm]	$rp_{\mu day}$ [mm]	$r_{\mu day}$ [mm]	M_{year} [mm]	Σ_{year} [mm]	$Rp_{My year}$ [mm]	$R_{My year}$ [mm]
MGB1-X	mean	0.006	0.000	0.024	-0.016	0.078	0.001	0.013
MGB1-Y	mean	0.005	-0.001	0.029	-0.010	0.053	0.000	0.013
MGB2-X	mean	0.020	-0.014	-0.043	-0.124	0.200	-0.016	-0.061
MGB2-Y	mean	0.005	-0.006	-0.042	-0.049	0.038	-0.007	-0.037
MGB3-X	mean	0.022	-0.009	0.033	-0.129	0.408	-0.006	-0.005
MGB3-Y	mean	0.007	0.005	0.048	0.053	0.098	0.009	0.048
MGB4-X	mean	0.018	-0.015	-0.095	-0.250	0.376	-0.017	-0.114
MGB4-Y	mean	0.007	-0.024	-0.129	-0.174	0.108	-0.030	-0.142
MGB5-X	mean	0.059	-0.041	-0.104	0.011	0.333	-0.051	-0.198
MGB5-Y	mean	0.085	-0.457	-	-0.954	0.707	-0.239	-
MGT1-X	mean	0.035	0.035	0.501	0.462	0.536	0.050	0.484
MGT1-Y	mean	0.012	-0.008	-0.113	-0.184	0.398	-0.017	-0.140
MGT1-Z	mean	0.011	0.016	0.146	0.179	0.125	0.024	0.159

5.4.3 Inclinator

Inclinometer FP1

The sensor FP1, located in the longitudinal wall close to the buttressed, measures the variation of the inclination of the wall. FP1 pendulum recorded a constant trend, in both the directions, up to 20 May 2012. During the 2012 earthquake, and particularly in the two days where the most significant tremors are recorded, two drops in both directions were recorded (Figure 69). The drops recorded on 20 and 29 May indicate a movement of the top of the wall of about 1.0 mm in the South-West direction, and equal to about 1.3 mm in the southeast. It is noted that in the months following the earthquake sequence have been recorded jumps probably due to interference in the instrument recording because there have been no significant seismic events on those dates. In particular, the 24th October 2014 the device records a drop that allows to recover most of the overhangs recorded during the earthquake of May 2012.

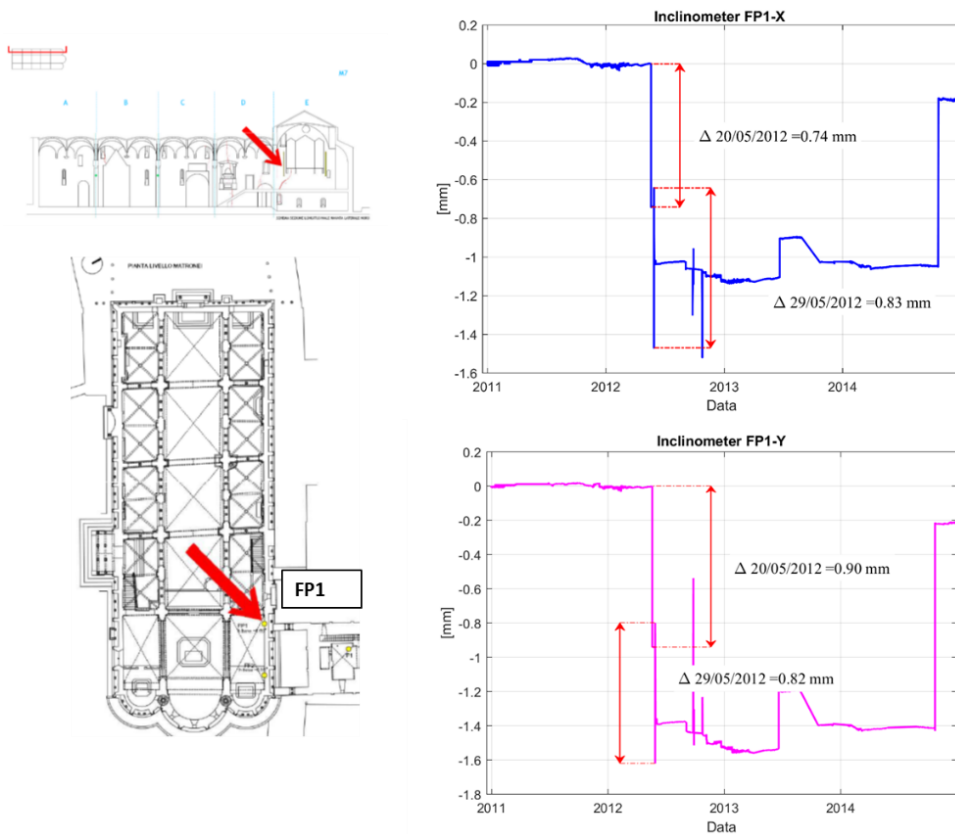


Figure 69: Inclinator FP1: row-data recorded by FP1 highlighted the drops recorded during the 2012 earthquake

Inclinometer FP2

The sensor FP2 is located in the some longitudinal wall of FP1, close to the buttressed. FP2 has recorded a similar behaviour to that recorded by FP1. Before the 2012 earthquake, FP2 recorded a regular trend with very small daily amplitudes oscillations. On 20th and 29th May 2012, drops in both the directions were recorded. The drops recorded indicate movements of the top of the wall to the South-West direction (towards the inside of the Cathedral) of about 1.68 mm. On 28th September 2012 was registered another drop probably due to interference, given that it has been fully recovered on the same day, while the 21 June 2013 is recorded a drop in both the directions, indicating a further movements of the top of the wall toward the inside of the Cathedral (Figure 70)

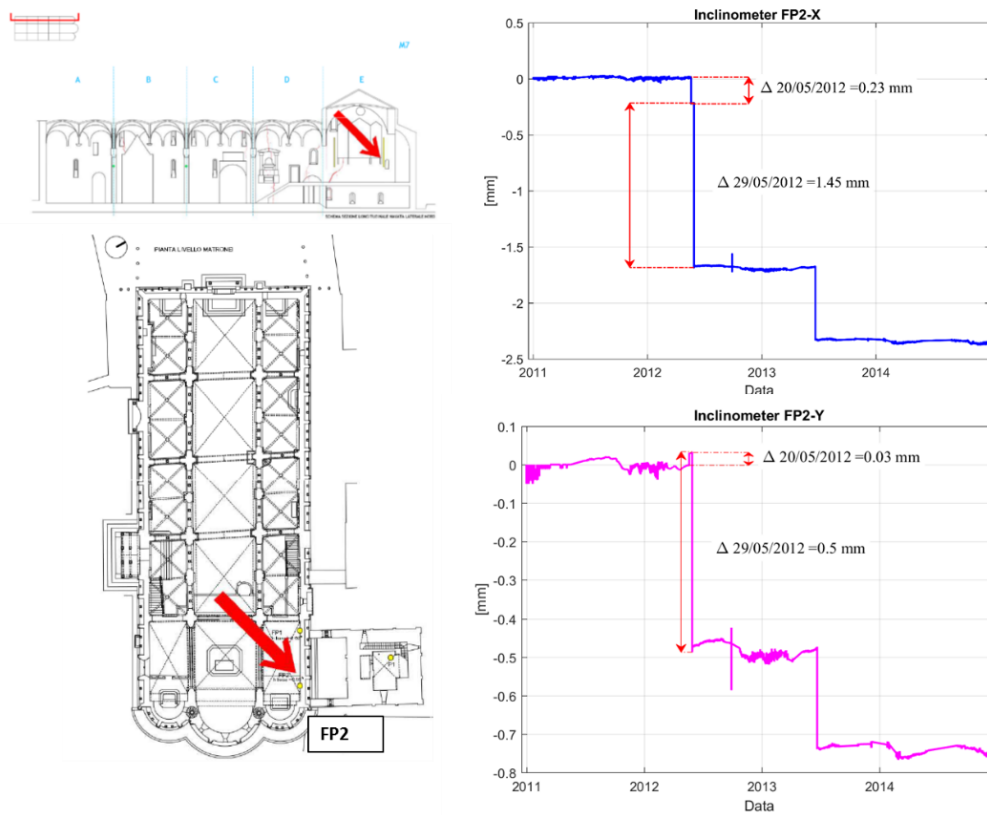


Figure 70: Inclinometer FP2: row-data recorded by FP2 highlighted the drops recorded during the 2012 earthquake

5.4.4 Conclusions

The interpretation of the data recorded (from 2004 to 2015) by the static monitoring system installed on the Cathedral of Modena has been performed making use of the reference quantities presented in § 5.2.

More specifically, the following conclusions are drawn:

- the data recorded by the devices installed on the Cathedral have allowed to control the condition of the structure after the 2012 Emilia earthquake. In particular, the analyses of the data made it possible to understand their possible evolutionary trends triggered by the seismic load.
- The invar deformeters and the inclinometers, while not recording data continuously, have caught some movements caused by the 2012 earthquake. In more detail, the invar deformeters have recorded a rapprochement between the cathedral and the Ghirlandina tower during the earthquake. These movements are not recovered later, but the devices, after the earthquake, record again a cyclical trend meaning that the movements triggered by the earthquake are not evolving. A similar condition has been recorded by the inclinometers.
- The joint meters, which measure the movements of some cracks, display a high direct correlation with the temperature. It should be noted that some of the joint meters record an evolutionary trend (MGB2, MGB3 and MGB4). The "evolutionary" phenomenon noted suggests the need for a precise control of the specific cracks in order to exclude dangerous amplification of the phenomenon under observation. At the moment, however, the situation appears substantially "not alarming". The order of magnitude of the cumulative residues reveals in fact small movements in the thirteen years of monitoring. Moreover, these trends showing an analogy with the main movements identified through the integrated knowledge and the structural analyses performed on the Cathedral.

The main periodicity of the recorded data by the joint meters have been investigated through the signal frequency analyses and reveal the predominant component with period close to $T = 365$ days. Other important amplitudes are observed for periods equal to 170 days and 500 days

Strengthening interventions performed on the Cathedral

This part will be integrated based on the results of ongoing research and studies.

6 The main vulnerability

Starting from the knowledge acquired by the multi-disciplinary approach, the structural behaviour of the Cathedral has been investigated in order to identify the more vulnerable elements of the building. The results of the static analyses have been used to interpret the cracking patterns as obtained from in situ surveys and the deformations related to changes in the geometrical configuration.

The static analysis has been developed through simple limit schematizations and finite element models with increasing complexity (2D models, 3D models, models with fixed base, models accounting for the soil-structure interaction).

The different finite element models, validated through simple patterns, are then compared with the “survey” of the actual state of the building. The most representative one of the structural behaviour of the Cathedral is the model considering the soil-structure interaction.

On this model, various analyses have been carried out in order to identify the seismic behaviour of the monument. The local collapse mechanisms and the global seismic response of the structure have been studied.

From the static analyses and the knowledge, it can be recognized that the main vulnerabilities are:

- the tendency of the longitudinal perimeter walls to develop out-of-plane movements, as revealed by the 3D laser scanner, probably due to the unconstrained thrusts of the arches and differential settlements, Fig.4a;
- the overall rotation movement towards the Ghirlandina Tower, caused by the strong interaction between the Cathedral and the Tower, that promotes differential soil settlements (note that the portion of the apses is significantly heavier than the other portions), Fig.4b;
- the concentration of cracks in the portion coinciding with the location of the old Cathedrals;

Instead, the masonry arches, that link the Cathedral and the Tower, contrast the rotation movement of the Cathedral creating a critical point on the longitudinal wall.

Regarding the seismic behaviour, the results of the local analyses reveal that the main local vulnerabilities are the facade mechanisms, the failures of the cross vaults (as confirmed by the damages observed after the seismic sequence that hit Modena in the May 2012), the out-of-plane behaviour of the apse walls and the pinnacles

Moreover, the results of the global analyses reveal vulnerabilities of the perimeter walls with respect to out-of-plane overturning.

7 Solution strategies to reduce the main vulnerabilities

The structural analyses have allowed identifying the main vulnerabilities of the Cathedral of Modena and thus the elements, which need a priority of strengthening. As well known, for the restoration of the historical monuments the intervention techniques and the used materials merit special care on account of their individual historical and architectural importance, or their significance as surviving representatives of an earlier tradition.

Beyond being the basis for a robust structural analysis, the importance of the integrated knowledge rises also from the possibility of identifying compatible materials and intervention techniques able to preserve the aesthetic and historical value of the monument.

In light of this, a strengthening design aimed at increase the safety level of the Cathedral preserving its integrity has been developed and will be effected in the next years. In particular, regarding the vaults several interventions have been planned.

The extrados of the vaults will be consolidated by a removal of the existing layer and re-filling through injections of lime. At their intrados, there is a decorated plaster dating back to the beginning of the XX century, with false paintings bricks. The project includes the fill of the cracks with a compatible lime and the consolidation of the plaster with the use of pigments of the same colors (Figure 71). Furthermore, the reinforcement of the vaults will be also achieved by attenuating the discontinuities (through the extension of the “frenelli” and the insertion of “diatoni” bricks, Figure 72a) and/or putting a 5cm-thick layer of lime added with eco-pozzolana and reinforced with carbon-fiber mesh. (Figure 72b).



Figure 71: Consolidation of the decorated plaster with using compatible pigments

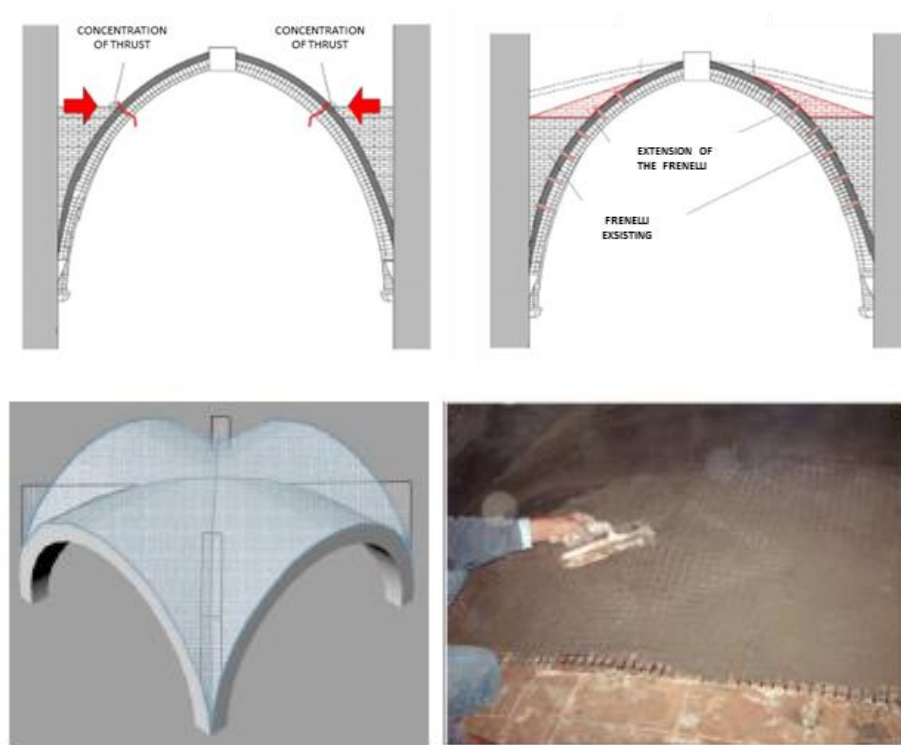


Figure 72: Interventions for strengthening the vaults: a) extension of the “frenelli”; b) layer of lime added with eco-pozzolana and reinforced with carbon-fiber mesh

The out-of-plane overturning of the perimeter walls and the façade can be contrasted with the insertion/ add of adequately dimensioned transversal and longitudinal tie rods. In particular, the strengthening design includes 36-millimeter tie rods at two different level: at 5.86 meter and at 13.28 meter. Figure 73 shows the cross section of the Cathedral and the blue lines represent the existing tie-rods while the red lines indicates the tie-rods planned at 5.86 meters height in order to contrast the thrust due to the arches. Similarly, the Figure 74 shows in red lines the added tie-rods at 13.28 meters height in order to avoid the out-of-plane overturning of the perimeter walls and of the façade.

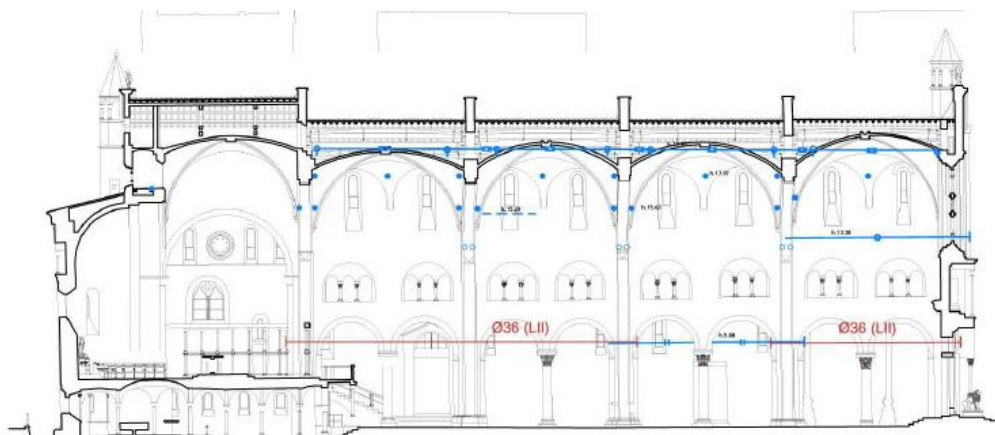


Figure 73: Tie-rods to contrast the thrust due to the arches

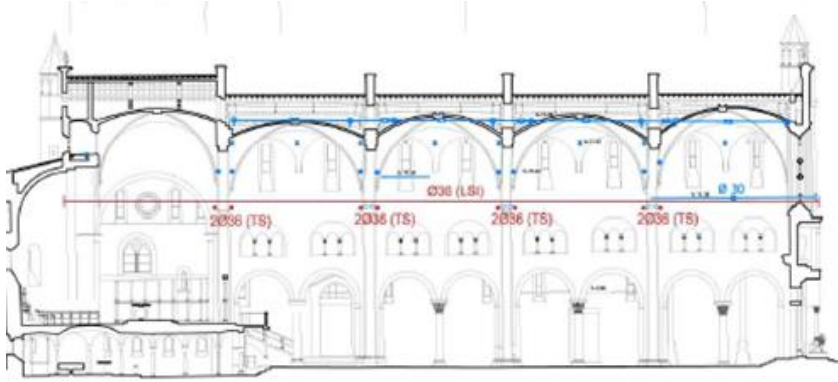


Figure 74: Tie-rods for avoiding the overturning mechanisms of the facade and of the perimeter walls

In order to ensure a box behaviour, an important concept to increase the seismic behaviour of the Cathedral, the connections between the orthogonal walls will be improved through insertions of new diatons and injections of compatible lime.

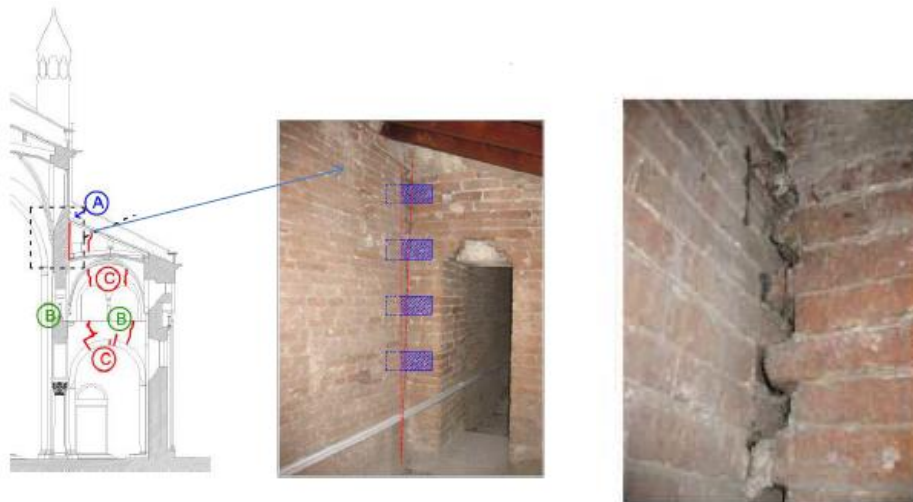


Figure 75: Connection of the orthogonal walls

The effectiveness of the existing tie-rods and end-plate anchors will be re-established in order to ensure a suitable safety against the overturning of the façade and of its top part (Figure 76). Moreover, a steel mesh grid has been placed internally and externally around the rose window to prevent the eventual out of plane mechanisms.

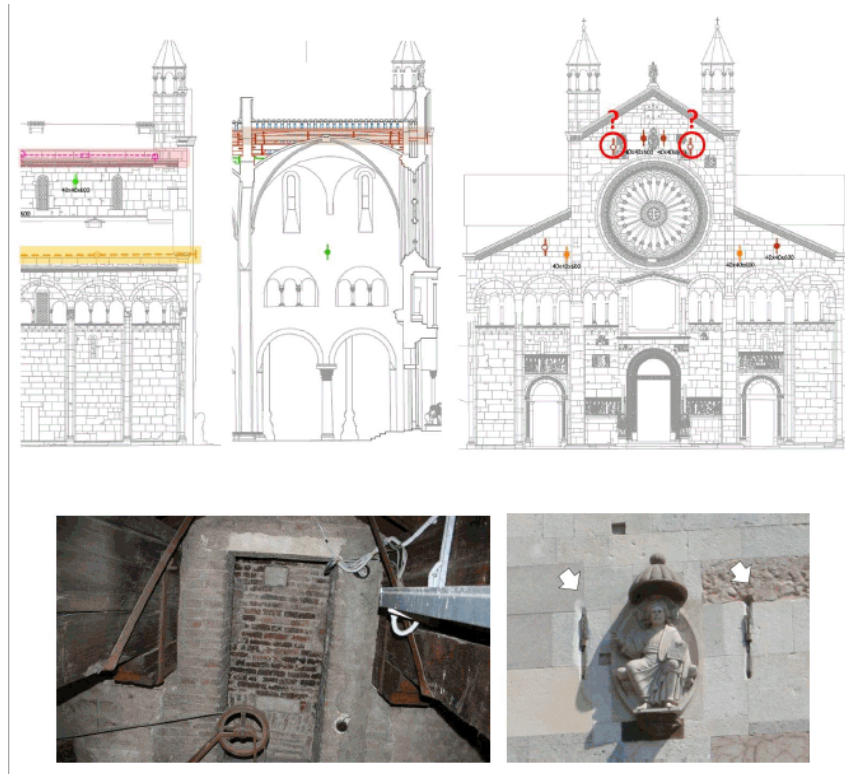


Figure 76: Reactivation of the existing tie-rod and plate anchors to contrast the overturning of the facade

Finally, the strengthening of the slender pinnacles will be carried out by inserting into the internal cavity a steel core, Figure 77.

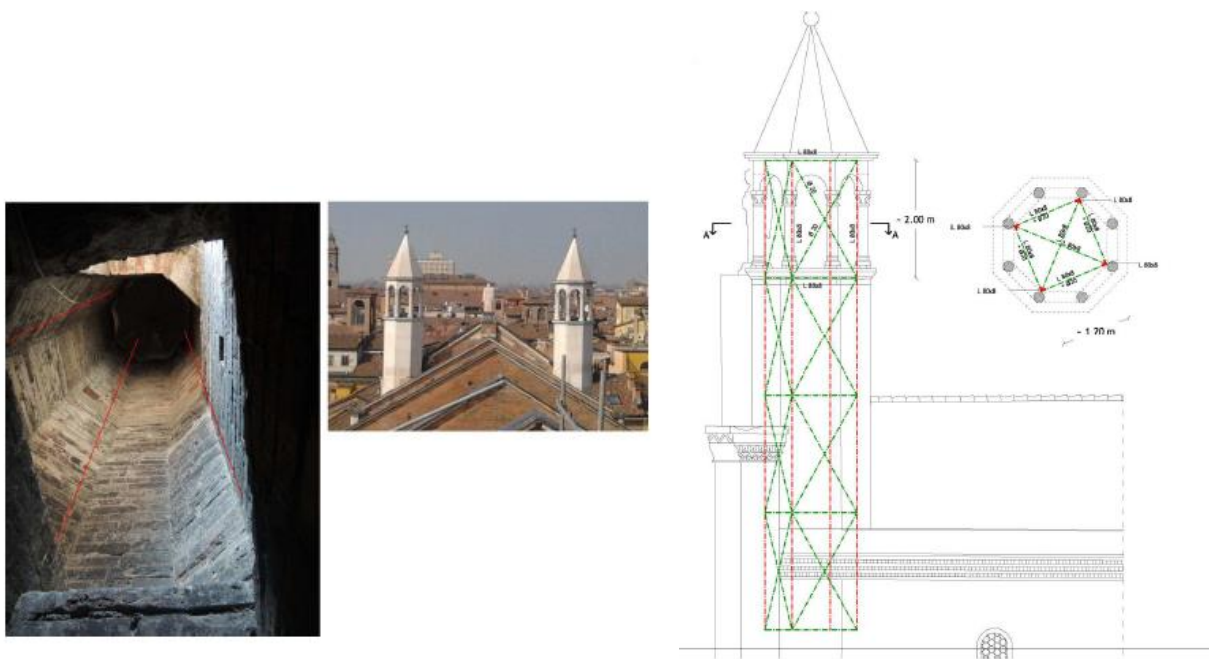


Figure 77: Strengthening of the slender pinnacles

1. CONCLUSIONS

Combining a deep knowledge of the history, geometry, material properties, interaction soil-structure, and construction technique of the Cathedral of Modena with the results obtained from robust structural analyses, the main criticalities of this monument have been identified.

A strengthening design has been performed with the purpose of reducing the main vulnerabilities located in vaults, connection between orthogonal walls, cracks, pinnacles, façade overturning. The proposed intervention techniques have been evaluated in the light of respecting the architectural and cultural integrity of the monument.

PART 3: PRELIMINARY FLOOD RISK ASSESSMENT

The European Directive 2007/60/EC establishes a “framework for the assessment and management of flood risks, aiming at the reduction of the adverse consequences for human health, the environment, cultural heritage and economic activity associated with floods in the Community” (Art 1).

According to this Directive, floods are defined as the “temporary covering by water of land not normally covered by water. This shall include floods from rivers, mountain torrents, Mediterranean ephemeral water courses, and floods from the sea in coastal areas, and may exclude floods from sewerage systems” (Art. 2).

A preliminary flood risk assessment is to be undertaken by considering each river basin district. In the context of the case study of Modena Dome, the results provided in the Flood Risk Assessment Plan for the Po River Basin are hereby considered (<http://pianoalluvioni.adbpo.it/il-piano/>). The Flood Risk Assessment Plan for the Po River Basin was compiled by the Po River Basin Authority. This plan defines flood hazard maps and flood risk maps.

FLOOD HAZARD MAPS

As stated in the European Directive 2007/60/EC, flood hazard maps cover the geographical areas which could be flooded according to the following 3 scenarios:

- a) floods with a low probability, or extreme event scenarios;
- b) floods with a medium probability (likely return period ≥ 100 years);
- c) floods with a high probability, where appropriate.

In the context of the Flood Risk Assessment Plan for the Po River Basin, flood hazard maps consider different methodological approaches based on the following territorial classes:

- Main river reaches (RP, from the Italian *Reticolo idrografico principale*): it comprises the Po river and its main tributaries (total length of approximately 5000 km).
- Secondary river reaches across hills and mountains (RSCM, from the Italian *Reticolo secondario collinare e montano*): it comprises smaller stream and rivers across hills and mountains, but also mountain reaches of main rivers
- Secondary river reaches across plains (RSP, from the Italian *Reticolo secondario di pianura*): it comprises artificial channels for irrigation purposes in the Po Plain, managed by Land Reclamation Bureaus.

- Coastal areas (ACM, from the Italian *Aree costiere marine*): areas close to the Po river delta in the Adriatic Sea.
- Lake areas (ACL, from the Italian *Aree costiere lacuali*): areas close to Maggiore Lake, Como Lake, Garda Lake etc.

Flood hazard maps identify the maximum extension of flooded areas associated with flood events with low, medium and high probability, as provided in Table 24 and 25.

Table 23 – Summary of territorial classes and responsibility

TERRITORIAL CLASS	RESPONSIBILITY
Main river reaches (RP)	Po River Basin Authority
Secondary river reaches across hills and mountains (RSCM)	Administrative regions
Secondary river reaches across plains (RSP)	Administrative regions and Land Reclamation Bureaus
Coastal areas (ACM)	Administrative regions
Lake areas (ACL)	Administrative regions, Regional agencies for Environmental Protection, Lake regulation consortia

Table 24 – Summary of flood scenarios: comparison between the European Directive 2007/60/EC and the Flood Risk Assessment Plan for the Po River Basin.

Flood Directive		Flood Risk Assessment Plan	
Scenario	Return Period (years)	Hazard class	Return period (years) for Main river reaches (RP)
High flood probability	20-50 (frequent)	P3 High	10-20
Medium flood probability	100-200 (less frequent)	P2 Medium	100-200
Low flood probability	> 500 (rare)	P1 Low	500

Flood hazard maps for the city of Modena are available in the Flood Risk Assessment Plan for the Po River Basin in panel “RP_RSCM_Tavola_201SE”. An extract is reported in Figure 82, which shows that the city of Modena and particularly the Dome area presents a low probability to be flooded (i.e. return period equal to 500 years).

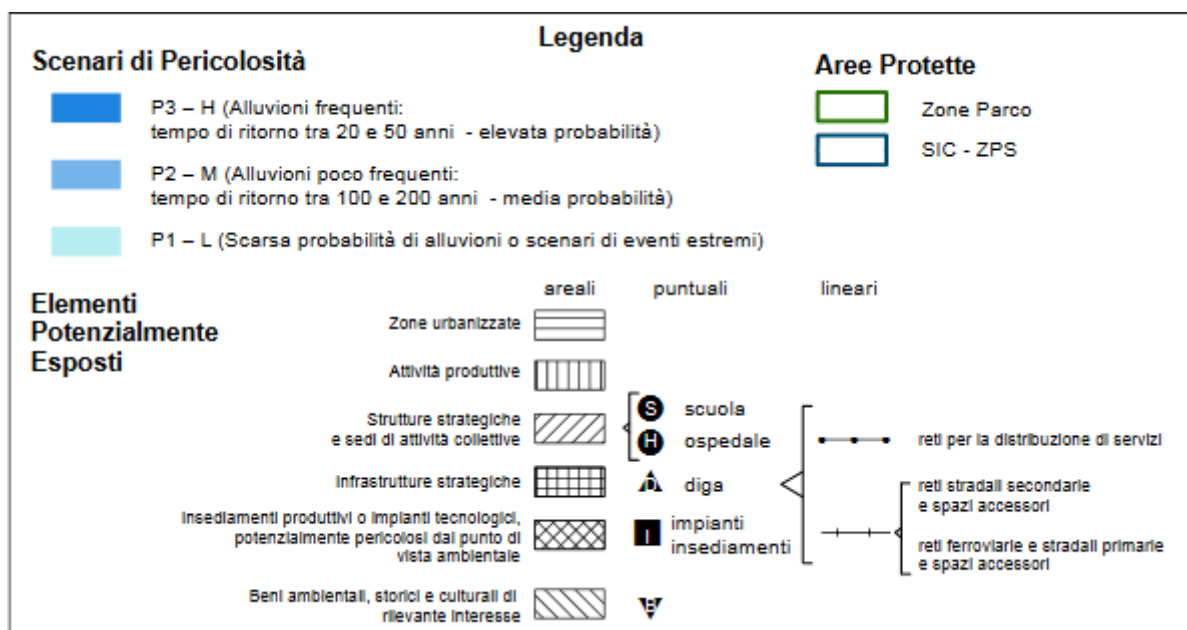
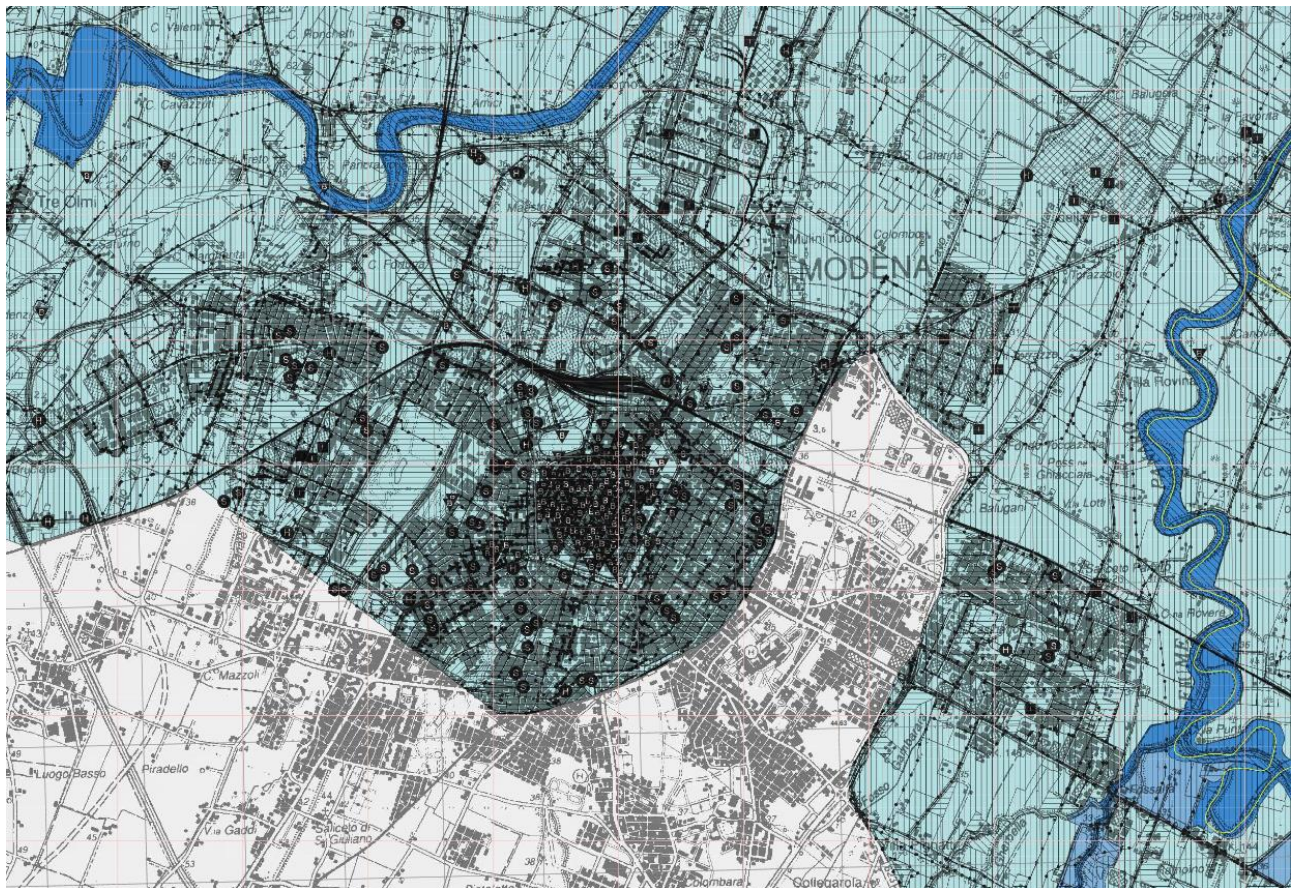


Figure 78 – Flood hazard map for the city of Modena.

FLOOD RISK MAPS

As stated in the European Directive 2007/60/EC, flood risk maps show the potential adverse consequences associated with flood scenarios (i.e. flood hazard) and also embed information about the indicative number of inhabitants potentially affected as well as the type of economic activity of the area potentially affected.

In the context of the Flood Risk Assessment Plan for the Po River Basin, flood risk maps identify 4 different classes of risk, by following Italian regulations (i.e. D.P.C.M. 29.09.98 and D.Lgs. 49/2010):

- R4 (very high risk): potential human losses, severe human injuries, severe damages to buildings, infrastructures and the environment, severe damages to socio-economic activities.
- R3 (high risk): potential injuries to people, damages to buildings and infrastructures, socio-economic activities brake-offs, damages to the environment.
- R2 (average risk): potential minor damages to buildings, infrastructures and the environment without affecting people safety.
- R1 (low or negligible risk): social, economic and environmental damages are negligible or null.

Flood risk (R) is defined by employing the following formula:

$$R = P \times E \times V = P \times D$$

where:

P (hazard): probability of occurrence, within a certain study area and time interval, of a flood with a given magnitude

E (exposure): elements at risk, i.e. economic and intrinsic values that are present at the location involved. Population density, capital investment, and land or property value can be indicators of flood exposure. More specifically, the following categories are considered: (i) inhabitants (data gathered from Italian Statistical Analysis – ISTAT), (ii) economic activities (data gathered from land use maps available from the EU CORINE LCL), (iii) Highly Pollutant Industrial Plants, as defined by the Industrial Emissions Directive (data gathered from the Italian Institute for Environmental Protection, ISPRA), (iv) protected areas (data gathered from Po River Basin Authority).

V (vulnerability): capacity of the society to deal with the flood event, namely, the state of susceptibility to harm from exposure to an undesired event, floods in this study, associated with environmental and social change, and lack of capacity to adapt. Lack of flood defenses or protection of economic values and human lives susceptible to floods are indicators of vulnerability.

$D = E \times V$ (Potential damage): integrated measure of the environmental and socio-economic consequences of floods.

Estimates of potential damage D is not always easy to derive without any specific data concerning vulnerability, this variable V is assumed to be constant and equal to 1. Furthermore, potential damage assessment is performed by following a qualitative approach, also based on expert opinions, providing a value from D1 to D4, for less and more important land use classes, respectively. Higher values are assigned to residential classes, showing a constant human presence, whereas lower values are assigned to different kinds of economic activities, from industrial to agricultural ones. Higher values are also assigned to cultural heritage sites.

Flood risk analysis is then performed in a GIS environment by overlaying the following thematic maps: flood hazard and potential damages. This algorithm employs a matrix, which associates hazard classes P1, P2, P3 to damages classes D1, D2, D3, D4. Then, moving from the 3 hazard levels (P1, P2, P3) and the 4 damage levels (D1, D2, D3, D4), 4 risk levels are established (R1, R2, R3, R4) and flood risk maps are outlined. Figure 83 shows flood risk levels. The flood risk map for the city of Modena is shown in Figure 84 (extract from the Flood Risk Assessment Plan in the Po River Basin, panel “RP_RSCM_Tavola_201SE”).

CLASSI DI RISCHIO		CLASSI DI PERICOLOSITA'		
		P3	P2	P1
CLASSI DI DANNO	D4	R4	R4	R2
	D3	R4	R3	R2
	D2	R3	R2	R1
	D1	R1	R1	R1

Matrice 1

- Reticolo principale (RP)
- Reticolo secondario collinare e montano (RSCM alpino)

CLASSI DI RISCHIO		CLASSI DI PERICOLOSITA'		
		P3	P2	P1
CLASSI DI DANNO	D4	R4	R3	R2
	D3	R3	R3	R1
	D2	R2	R2	R1
	D1	R1	R1	R1

Matrice 2

- Aree costiere lacuali (ACL)
- Aree costiere marine (ACM), Reticolo secondario collinare e montano (RSCM appenninico)

CLASSI DI RISCHIO		CLASSI DI PERICOLOSITA'	
		P3	P2
CLASSI DI DANNO	D4	R3	R2
	D3	R3	R1
	D2	R2	R1
	D1	R1	R1

Matrice 3

- Reticolo secondario di pianura (RSP)

Figure 79 – Definition of flood risk levels, based on hazard levels (P1, P2, P3) and economic damages levels (D1, D2, D3, D4) for main river reaches (RP), secondary river reaches (RSCM and RSP).

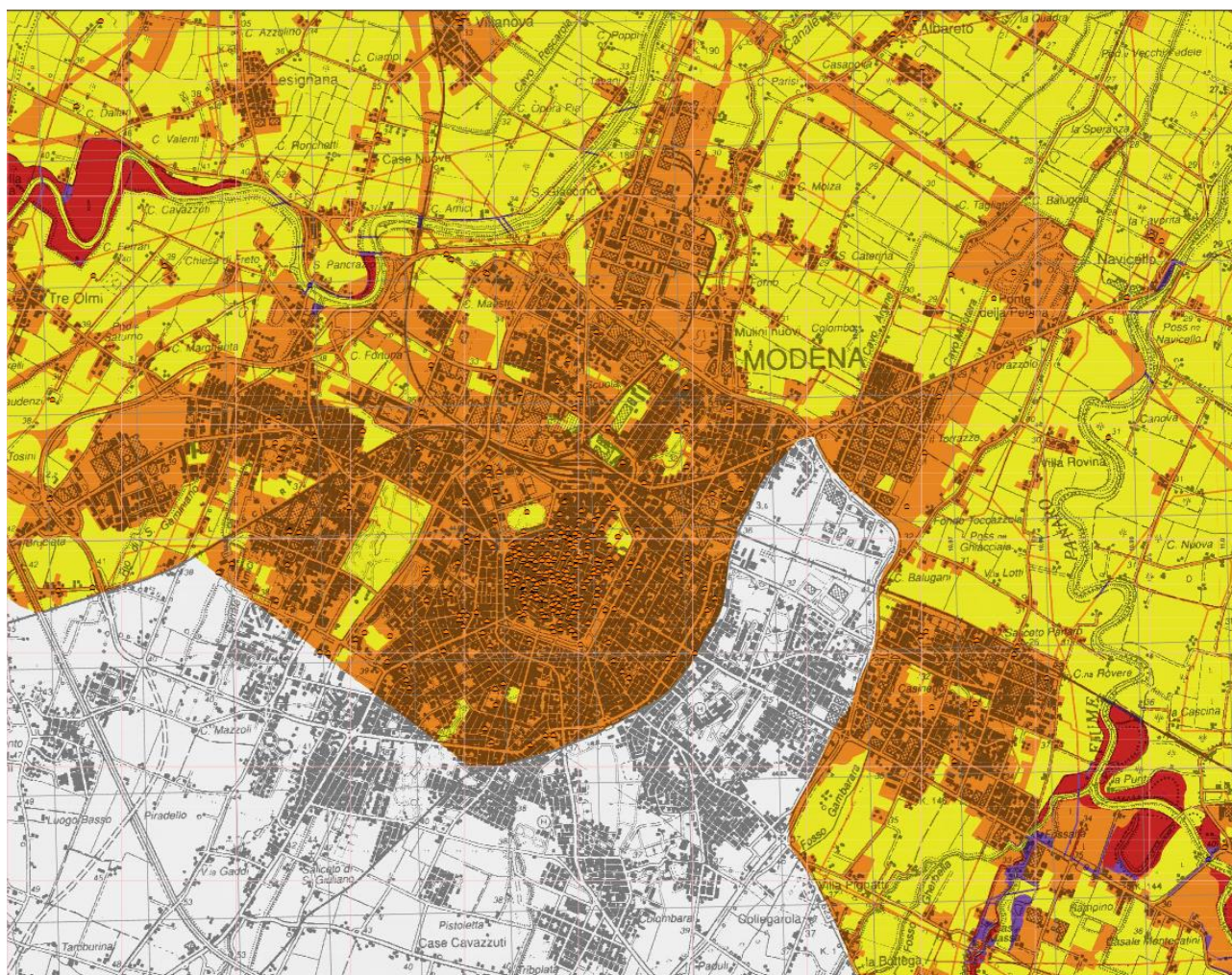


Figure 80 - Flood risk map for the city of Modena.

Figures 82 and 84 clearly shows the hazard and risk levels linked to flood events close to Modena Dome. Concerning flood hazard, Modena Dome is located in an area quite far from the river network: Secchia river is on the Western side of the city center, while Panaro river is on the Eastern side. As a consequence, the Modena city center shows a relatively low probability to be flooded (return period approximately equal to 500 years). Despite this situation, flood risk is classified as moderate due to the presence of cultural heritage sites such as Modena Dome.

Bibliography

- [1] ISCARSAH (International Scientific Committee for Analysis and Restoration of Structures of Architectural Heritage), “Recommendations for the analysis, conservation and structural restoration of Architectural Heritage,” *Icomos*, no. June, pp. 3–6, 2003.
- [2] P. Lourenço, “Computations of historic masonry structures,” *Struct. Eng. Mater.*, 2002.
- [3] Guidelines for Evaluation and Mitigation of Seismic Risk to Cultural Heritage, “Guidelines for Evaluation and Mitigation of Seismic Risk to Cultural Heritage,” *Gazz. Uff.*, vol. 47, 2011.
- [4] ISCARSAH, “Recommendations for the analysis, conservation and structural restoration of Architectural Heritage,” *Icomos*, no. June. pp. 3–6, 2003.
- [5] C. Blasi and E. Coïsson, “The importance of historical documents for the study of stability in ancient buildings: The french Panthéon case study,” *Asian J. Civ. Eng. (Building Housing)* 7, 2006.
- [6] D. Labate, “Il contributo dell’archeologia alla lettura di un monumento, in La torre Ghirlandina. Un progetto per la Conservazione,” L. Sossella, Ed. 2009.
- [7] Cadigiani, R., *La torre Ghirlandina. Un progetto per la Conservazione*. 2009.
- [8] G. Bertoni, “La cattedrale modenese preesistente all’attuale: Primo ragguaglio sugli scavi del Duomo, agosto-settembre 1913/Giulio Bertoni.,” Orlandini, Ed. 1914.
- [9] P. Frankl, “Der Dom in Modena, in ‘Jahrbuch fur Kunstwissenschaft,’” SIFET., 1927.
- [10] A. Peroni, “Architettura e scultura: Aggiornamenti, in Wiligelmo e Lanfranco nell’Europa romanica,” 1989.
- [11] A. Peroni, “Il Duomo di Modena. L’architettura, in Il Duomo di Modena,” F. C. Panini, Ed. *Mirabilia Italiae* 9., 1999.
- [12] S. Lomartire, “Paramenti murari del Duomo di Modena. Materiali per un ‘edizione critica, in Wiligelmo e Lanfranco nell’Europa romanica,” 1989.
- [13] M. Armandi, “Copie e originali. Il repertorio di mensole figurate del Duomo di Modena,” in *Il Duomo di Modena*, C.FRUGONI, Ed. Franco Cosimo Panini., 1999.
- [14] E. Silvestri, “Una rilettura delle fasi costruttive del Duomo di Modena,” 2013.
- [15] A. K. Porter, “Lombard Architecture,” H. and Milford, Eds. Yale University Press, 1917.
- [16] A. Dondi, “Il Duomo di Modena, notizie storiche ed artistiche,” 1896.
- [17] and M. D. Castagnetti, C., E. Bertacchini, A. Capra, “Il laser scanning terrestre per l’analisi di edifici di interesse storico ed artistico,” in *Geomatica - le radici del futuro*, 2011.
- [18] R. Lancellotta, “Geotechnical Engineering,” T. and Francis, Ed. 2009.
- [19] R. Lancellotta, “Aspetti geotecnici nella salvaguardia della torre Ghirlandina.,” in *La Torre*

Ghirlandina. Un progetto per la conservazione, 2009.

- [20] R. Lancellotta, “La torre Ghirlandina: Una storia di interazione strutturaterreno,” *Riv. Ital. di Geotec.*, 2013.
- [21] S. Lugli, “La Pietra Ringadora in Piazza Grande a Modena: Caratterizzazione geologica, provenienza, fenomeni di degrado e valorizzazione didattico-divulgativa,” 2011.
- [22] M. Palermo, S. Silvestri, G. Gasparini, S. Baraccani, and T. Trombetti, “An approach for the mechanical characterisation of the Asinelli Tower (Bologna) in presence of insufficient experimental data,” *J. Cult. Herit.*, vol. 16, no. 4, pp. 536–543, 2015.
- [23] T. P. Tassios, “Meccanica delle murature,” Liguori, Ed. 1988.
- [24] A. W. Hendry, “Structural masonry,” 1990.
- [25] Istruzioni CNR-DT 206, “Istruzioni CNR-DT 206/2007. Istruzioni per la Progettazione, l'Esecuzione ed il Controllo di Strutture di Legno, Cons. Nazionale delle Ricerch.” 2007.
- [26] Cornell C.A, “Engineering seismic risk analysis,” *Bull. Seismol. Soc. Am.*, 1968.
- [27] Krinitzsky E.L., “Deterministic versus probabilistic seismic hazard analysis for critical structures,” *Eng. Geol.*, 1995.
- [28] F. Sabetta and A. Pugliese, “Attenuation of Peak Horizontal Acceleration and Velocity from Italian Strong - motion Records,” *Bull. Seismol. Soc. Am.*, 1987.
- [29] B. Gutenberg and Richter ,C. F., “Seismicity of the Earth,” 1949.
- [30] M. Dolce *et al.*, “The Emilia Thrust Earthquake of 20 May 2012 (Northern Italy): Strong Motion and Geological Observations - Report 1 -,” vol. 2012, pp. 1–12, 2012.
- [31] D. M. Norme Tecniche per le Costruzioni, “Italian Ministerial Decree of 14 January 2008,” *Gazzetta Ufficiale* n. 29 of 04 Feb 2008, 2008.
- [32] F. Parisi, F. De Luca, F. Petruzzelli, R. De Risi, and E. Chioccarelli, “Field inspection after the May 20th and 29th 2012 Emilia-Romagna earthquakes,” 2012.
- [33] J. Heyman, *The stone skeleton: structural engineering of masonry architecture*. Cambridge University Press, 1995.
- [34] J. McInerney and M. DeJong, “Discrete Element Modeling of Groin Vault Displacement Capacity,” *Int. J. Archit. Herit.*, vol. 9, no. 8, pp. 1037–1049, 2015.
- [35] P. J. Brockwell and R. A. Davis, “Time series: theory and methods,” 2009.
- [36] ASCE7-98, “Minimum Design Loads for Buildings and Other Structures,” American Society of Civil Engineers, 1998.